U.S. Department of Transportation
Federal Highway Administration

SD2014-14-F

Connecting South Dakota and the Nation

South Dakota

Department of Transportation
Office of Research

Development of Alternative Bridge Superstructures for South Dakota Local Roads

Study SD2014-14

Final Report

Prepared by

South Dakota State University

Brookings, SD 57007

January 2019

DISCLAIMER

The contents of this report, funded in part through grant(s) from the Federal Highway Administration, reflect the views of the authors who are responsible for the facts and accuracy of the data presented herein. The contents do not necessarily reflect the official views or policies of the South Dakota Department of Transportation, the State Transportation Commission, or the Federal Highway Administration. This report does not constitute a standard, specification, or regulation.

The South Dakota Department of Transportation provides services without regard to race, color, gender, religion, national origin, age or disability, according to the provisions contained in SDCL 20-13, Title VI of the Civil Rights Act of 1964, the Rehabilitation Act of 1973, as amended, the Americans With Disabilities Act of 1990 and Executive Order 12898, Federal Actions to Address Environmental Justice in Minority Populations and Low-Income Populations, 1994. Any person who has questions concerning this policy or who believes he or she has been discriminated against should contact the Department's Civil Rights Office at 605.773.3540.

ACKNOWLEDGEMENTS

This work was performed under the direction of the SD2014-14 Technical Panel:

Cody Axlund ..... Local Government Assistance
Ron Bren ..... Local Government Assistance
Aaron Breyfogle ..... Research
Mark Clausen .... Federal Highway Administration
Justin Cook ..... Research
Hadly Eisenbeisz ..... Bridge Design
Harvey Fitzgerald ..... Research
Kevin Heiman ..... Yankton Office
Thomas Herman ..... Road Design
Marc Hoelscher . Federal Highway Administration
Tom Kallemeyn ..... Bridge Design
Aaron Litka ..... Research
Gregory Vavra ..... SDLTAP

This study was jointly funded by the South Dakota Department of Transportation (SDDOT) and the US Department of Transportation (USDOT) through the Mountain Plains Consortium (MPC) - University Transportation Center (UTC). Their support and guidance are greatly appreciated. The authors would like to thank Gage Brothers Concrete Products, Gruen-Wald Engineered Laminates, Inc., and Headed Reinforcement Corporation for their support and contributions throughout the project. The authors acknowledge the assistance and valuable feedback of Aaron Breyfogle of the Research Office at the South Dakota Department of Transportation, Jared Gusso of Journey Construction, and Zachary Gutzmer of South Dakota State University (SDSU).

TECHNICAL REPORT STANDARD TITLE PAGE

1. Report No.	2. Government Accession No.	3. Recipient's Catalog No.
SD2014-14-F		

4. Title and Subtitle	5. Report Date
Development of Alternative Superstructure Bridges for South Dakota Local Roads	01/31/2019
	6. Performing Organization Code

7. Author(s)	8. Performing Organization Report No.
Zach Carnahan, Michael Mingo, Mostafa Tazarv, and Nadim Wehbe	

9. Performing Organization Name and Address	10. Work Unit No.
South Dakota State University	HRY414
Crothers Engineering Hall/Box 2219	11. Contract or Grant No.
Brookings, SD 57007	311231

12. Sponsoring Agency Name and Address	13. Type of Report and Period Covered
South Dakota Department of Transportation	Final Report
Office of Research	April 2015 – January 2019
700 East Broadway Avenue	14. Sponsoring Agency Code
Pierre, SD 57501-2586	

15. Supplementary Notes

16. Abstract

The South Dakota Department of Transportation (SDDOT) allows the use of precast double-tee bridges in counties because they are economical and fast in construction. Alternative durable prefabricated bridge systems are needed to provide more options to local governments. This study was carried out to investigate the feasibility of alternative prefabricated bridge systems that can be incorporated in South Dakota. The project technical panel approved testing of two superstructure bridge systems: (1) precast full-depth deck panels on prestressed inverted tee girders and (2) glulam timber bridges. This report includes the design, construction, testing methods, and the recommendations for the selected bridge alternatives.

Three full-scale bridges, one fully precast and two glulam timber, were tested under fatigue and ultimate loading. The precast bridge specimen was 50 ft long by 9.5 ft wide. No significant damage beyond the prior-to-testing shrinkage cracks was observed throughout the fatigue test, and the overall bridge stiffness did not deteriorate. The ultimate load testing showed that the load at the first crack was higher than the AASHTO Service and Strength I limit state loads, indicating sufficient performance. Based on the construction, testing, and cost analysis, it was concluded that that the

precast full-depth deck panels on prestressed inverted tee girder bridge is a viable alternative to the double-tee girder bridge. The full-scale glulam girder bridge test model was 50 ft long and 9.25 ft wide. The full-scale glulam slab bridge was 16.5 ft long and 8 ft wide. Both timber bridge types showed minimal damage during fatigue testing. The only damage of the girder timber bridge was cracking of tongue-and-groove deck-to-deck connections, which can be eliminated using flat-end panels. Ultimate testing of the two bridge systems confirmed that the AASHTO design method for timber bridges is adequate. Girders of glulam bridges should be designed as fully non-composite members. Based on the construction, testing, and cost analysis, it was concluded that both types of glulam timber bridges are viable alternatives to the double-tee girder bridges.

17. Keywords	18. Distribution Statement		
Superstructure Bridges, Precast Bridges, Timber Bridges, ABC.	No restrictions. This document is available to the public from the sponsoring agency.		
19. Security Classification (of this report)	20. Security Classification (of this page)	21. No. of Pages	22. Price
Unclassified	Unclassified	156	

TABLE OF CONTENTS

LIST OF TABLES

LIST OF FIGURES

TABLE OF ACRONYMS

Acronym	Definition
AASHTO	American Association of State Highway and Transportation Officials
ABC	Accelerated Bridge Construction
ACM	Advanced Composite Material
ADT	Average Daily Traffic
ADTT	Average Daily Truck Traffic
AFRP	Aramid Fiber Reinforced Polymer
AITC	American Institute of Timber Construction
ANSI	American National Standards Institute
ASD	Allowable Stress Design
AWC	American Wood Council
CFCC	Carbon Fiber Composite Cable
CFRP	Carbon Fiber Reinforced Polymer
CIP	Cast-in-place
COF	Coefficient of Friction
DOT	Department of Transportation
FE	Finite element
FHWA	Federal Highway Administration
ft	Foot or feet
FDDP	Full-Depth Deck Panels
HSS	Hollow Structural Steel
in.	Inch or inches
kip	Kilo pound = 1000 pounds
klf	Kip per linear foot
ksi	Kip per square inch
lbs	Pounds
LMC	Latex Modified Concrete
LRFD	Load and Resistance Factor Design

Acronym	Definition
LTAP	Local Transportation Assistance Program
LVDT	Linear Variable Differential Transformer
m	Meter
mm	Millimeter
NBI	National Bridge Inventory
NCHRP	National Cooperative Highway Research Program
NDS	National Design Specification for Wood Construction
PCI	Precast/Prestressed Concrete Institute
psi	Pound per square inch
SD	South Dakota
SDDOT	South Dakota Department of Transportation
SDSU	South Dakota State University
SLT	Stress-Laminated Timber
UHPC	Ultra-High Performance Concrete
VDOT	Virginia Department of Transportation
VHPC	Very-High Performance Concrete

1 EXECUTIVE SUMMARY

1.1 Introduction

The precast prestressed double-tee girder bridge system is commonly used on South Dakota local roads due to its economical and rapid construction. However, many double-tee bridges have been deteriorating faster than the 75-year design life. Furthermore, the double-tee bridge system only has one supplier in South Dakota. Alternative durable precast or prefabricated bridge systems are needed to provide more options to local governments when designing a new bridge. Different alternatives will also give local governments more flexibility to select the best system by comparing performance, availability, durability, and cost of various options. This study was carried out to investigate the feasibility and structural performance of three alternative prefabricated bridge systems that could be incorporated in South Dakota.

1.2 Problem Description

Many bridges across the United States of America are in need of replacement. Of the 5,870 bridges in SD, 1,208 are structurally deficient and 237 are functionally obsolete according to the Federal Highway Administration (FHWA, 2012). The South Dakota Department of Transportation (SDDOT) owns approximately 30% of South Dakota bridges and the others are owned by local governments. Although 90% of state-owned bridges are not deficient, a large portion of bridges owned by local governments are either structurally deficient or functionally obsolete mainly due to inadequate maintenance. Local governments rely on SDDOT to help replace them, but, with limited resources, SDDOT can only help replace about 30 bridges statewide each year, causing a backlog of local bridges in need of replacement.

The most common bridge type on South Dakota local roads is the double-tee girder bridge with more than 700 currently in service in the state. Bridges are often designed for a service life of 75 years, but many of current double-tee bridges in South Dakota are deteriorating or need replacement after only 40 years in service.

Double tee bridges are used because of their ease of construction, reduced construction time, and relatively low cost. With only one supplier of double-tee bridges in the state, new alternative systems are needed to provide local governments more options when designing a new bridge or replacing a deteriorated one. Alternative systems and suppliers allow local governments to select the best system by comparing performance, availability, durability, and cost of different options. Feasibility and performance of three full-scale prefabricated bridge systems, one precast concrete and two glued laminated (glulam) timber, were investigated in this study.

1.3 Research Work

Three full-scale prefabricated bridge superstructure specimens were tested at the Lohr Structures Laboratory at South Dakota State University (SDSU): (1) a fully precast bridge consisting of two precast prestressed inverted tee girders supporting five precast full-depth deck panels, (2) a glulam timber bridge consisting of three glulam girders and 13 glulam deck panels connected using epoxy, and (3) a glulam timber bridge consisting of two glulam deck panels placed in the longitudinal direction of the

bridge connected together incorporating three glulam stiffeners. Each specimen represented approximately one lane of traffic. The main objective of the laboratory tests was to evaluate the structural performance of the proposed systems under fatigue and ultimate loading.

Each specimen was subjected to cyclic loading representative of the American Association of State Highway and Transportation Officials (AASHTO) Fatigue II limit state, then tested to failure under increasing monotonic loads. Fatigue II loading was included in this study to investigate the effect of the maximum stress ranges that could result from an Average Daily Truck Traffic (ADTT) of 15 for 75 years of service. Stiffness tests were performed after every 10,000 or 50,000 fatigue load cycles to investigate bridge deterioration. Finally, a strength test was carried out for each specimen to study the bridge performance under AASHTO Service and Strength limit states, and to understand the bridge failure mode.

1.4 Research Findings

Following is a summary of the experimental findings, constructability, and cost estimate for the three bridge systems considered in this study.

1.4.1 Fully Precast Bridge (Full-Depth Deck Panels on Inverted Tee Girders)

- The design of the proposed bridge system was simple, and the bridge assembly was easy and fast without the need for advanced technologies or skilled labor.
- The proposed bridge system did not exhibit any sign of deterioration or water leakage through 500,000 Fatigue II load cycles (equivalent to 91 years of service) and an additional 150,000 Fatigue II load cycles adjacent to the middle panel transverse joints (equivalent to 27 years of service). The overall stiffness of the proposed bridge system essentially remained the same throughout fatigue testing.
- Shrinkage cracks were observed at 125,000 load cycles in almost all of the full-depth shear pockets, all of the transverse joints, and the grouted haunch. These cracks were shallow since there was no water seepage when the deck was tested for water leaks.
- The first horizontal shear cracks in the grouted haunch region were observed at an actuator load of 200 kips, which was higher than the equivalent AASHTO Strength I limit state load of 131 kips.
- Both inverted U-shape shear studs and double headed shear studs performed adequately through the entire fatigue testing and the ultimate test.
- The hidden pocket detail was found to be a better alternative than the full-depth pockets since they provided a better durability. Shrinkage cracks were observed in almost all full-depth pockets, but none in hidden pockets.
- The bridge girders did not crack until the applied load exceeded the equivalent Strength I limit state load, indicating adequate design and performance.

- The superstructure materials and fabrication cost for the proposed system for a bridge 50 ft long by 34.5 ft wide is estimated to be 11% higher than that for a double-tee bridge with the same geometry.

Overall, it was concluded from the design, construction, testing, and cost estimate that the proposed bridge system, full-depth deck panels supported on inverted tee girders, is a viable alternative to precast double-tee girder bridges.

1.4.2 Glulam Timber Girder Bridge

- Construction of the glulam girder bridge was fast and did not require any advanced technology or skilled labor.
- The girder bridge did not exhibit any signs of deterioration throughout the 500,000 AASHTO Fatigue II load cycles (equivalent to 91 years of service), and the bridge overall stiffness essentially remained constant throughout fatigue testing.
- Damage of tongue-and-groove deck-to-deck connections was observed at 250,000 load cycles (equivalent to 45 years of service). The damage can be eliminated by connecting flat deck panels with epoxy, instead of using a tongue-and-groove connection.
- Although there was partial composite action between the glulam girders and the glulam deck panels, it was not sufficient to warrant composite design. Glulam timber girders should be designed as fully non-composite sections.
- The epoxy connection between the glulam deck and the glulam girder performed adequately throughout fatigue and strength testing.
- The girder bridge did not meet the AASHTO service and strength limit state requirements under ultimate testing because, by mistake, a wrong grade of wood was used in the fabrication. Furthermore, the girders were designed assuming a partial composite action. A calculation of the bridge capacity assuming non-composite behavior and as-built material properties and bridge geometry led to accurate estimation of the bridge test model capacities. Therefore, the current AASHTO method of design for this type of bridge is valid.
- The superstructure cost for a glulam timber girder bridge 50 ft long by 34.5 ft wide designed according to the proposed guidelines is estimated to be 70% of that for a double-tee bridge with the same geometry.

1.4.3 Glulam Timber Slab Bridge

- Construction of the glulam slab bridge was fast and did not require any advanced technology or skilled labor.
- The slab bridge did not exhibit any signs of deterioration through the 550,000 AASHTO Fatigue II load cycles (equivalent to 50 years of service) and the bridge overall stiffness essentially remained constant throughout the fatigue testing.

- No damage was observed during the ultimate testing at an actuator load of 270 kips, which was three times higher than the AASHTO Strength I limit state load of 85.7 kips. The test was stopped due to setup limitations.
- The current AASHTO method of design for this type of bridge is valid.
- The superstructure cost per square foot for a glulam slab bridge 16.5 ft long by 34.5 ft wide is estimated to be only 50% of that for a typical double-tee bridge.

Overall, it was concluded from the design, construction, testing, and cost estimate that both types of the glulam timber bridges are viable alternatives to the precast double-tee girder bridges. The AASHTO method of design for timber bridges can be used for the design of these types of bridges.

1.5 Recommendations

Based on the findings of this study, the research team offers the following recommendations.

1.5.1 Recommendation 1: Precast Full-Depth Deck Panel Bridges

The guidelines as detailed in Section A.1 of Appendix A should be adopted for the construction of "precast full-depth deck panel bridges". A span length of 40 ft to 70 ft is recommended for this bridge type.

Precast full-depth deck panel bridges generally consist of precast inverted tee girders and precast full-depth deck panels. The test results of a full-scale 50-ft long precast full-depth deck panel bridge showed that this bridge type is a viable alternative to double-tee girder bridges, which are common in South Dakota. To minimize durability issues due to cold joints: (1) only hidden pocket detailing was allowed, (2) all bridge deck reinforcement was recommended to be epoxy coated, and (3) hollow structural steel sections, which are used to reduce the splice length, was recommended to be galvanized. These precast bridges with the recommended span lengths are constructible in South Dakota and may slightly cost more than double-tee bridges.

1.5.2 Recommendation 2: Glulam Timber Girder Bridges

The guidelines as detailed in Section A.2 of Appendix A should be adopted for the construction of "glulam timber girder bridges". A span length of 30 ft to 70 ft is recommended for this bridge type.

Glulam timber girder bridges generally consist of glulam girders, glulam deck panels, and diaphragms. The test results of a full-scale 50-ft long glulam girder bridge showed that this bridge type is a viable alternative to double-tee girder bridges. Glulam timber bridges with the recommended span lengths can be fabricated in South Dakota and will be more cost-effective than double-tee bridges.

1.5.3 Recommendation 3: Glulam Timber Slab Bridges

The guidelines as detailed in Section A.3 of Appendix A should be adopted for the construction of "glulam timber slab bridges". A span length of 30 ft or less is recommended for this bridge type.

Glulam timber slab bridges generally consist of glulam deck panels and glulam stiffeners. The test results of a full-scale 16.5-ft long glulam slab bridge showed that this bridge type is a viable alternative to double-tee girder bridges. Currently, glulam slab bridges with a span length of 20 ft

can be fabricated in South Dakota and will be more cost-effective than double-tee or glulam timber bridges.

2 PROBLEM DESCRIPTION

Numerous bridges in the South Dakota local highway system are in need of replacement. South Dakota has 5,870 bridges, of which 1,208 are structurally deficient and 237 are functionally obsolete according to the Federal Highway Administration (FHWA, 2012). This equates to 24.6 percent of bridges in South Dakota being structurally deficient or functionally obsolete. There are more than 700 bridges in South Dakota with precast double-tee girder systems. This type of bridge is very common since it is economical and quick to construct. Bridges are designed for a service life of 75 years, but many double-tee bridges have not met that expectation because of deterioration or the need for replacement after about half the expected service live.

The main problem associated with the currently used precast double-tee bridge in South Dakota (Figure 2.1) is that it is prone to cracking along the longitudinal joints. The cause is an inadequate longitudinal joint detail that uses discrete welded plates to transfer shear forces through the joint. These cracks provide a pathway for water and deicing agents to seep through the joint, spall the concrete, and reach the girder top prestressing steel tendons. Deterioration is initiated when the joint cracks, followed by corrosion of steel plates and girder top reinforcement.

There is only one double-tee girder supplier in South Dakota. Alternative durable precast bridge systems are needed to provide more design options to local governments. Different alternatives will also give local governments more flexibility to select the best system by comparing the performance, availability, durability, and cost of different options. This study investigated the feasibility and structural performance of three alternative prefabricated bridge systems that can be deployed in South Dakota: fully precast superstructure consisting of inverted tee girders and full-depth deck panels, glulam girder, and glulam slab bridges.

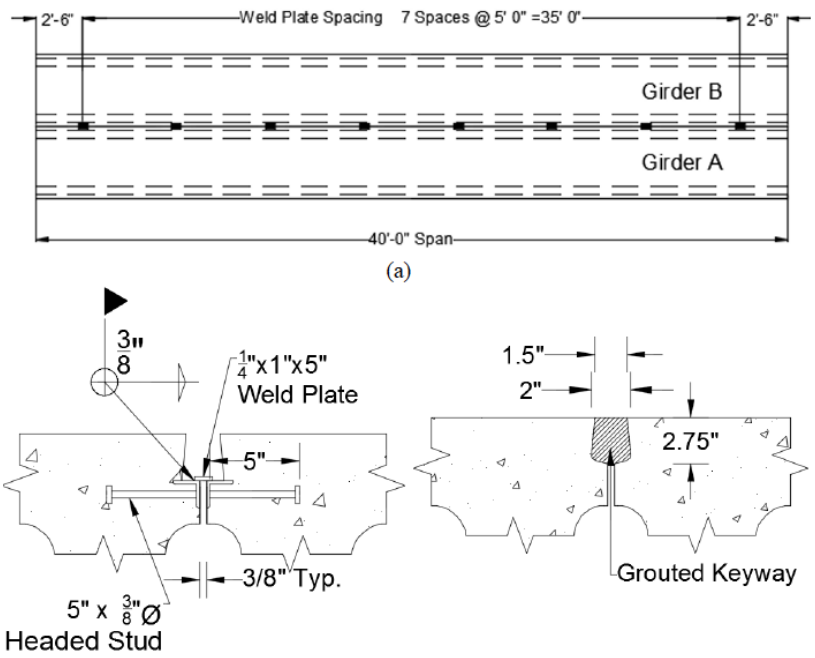

Figure 2.1: Current Double-Tee Bridge Longitudinal Joint Detailing
(after Konrad, 2014)

3 RESEARCH OBJECTIVES

Following are the main research objectives.

3.1 Identify Alternatives to Double-Tee Bridges

Determine bridge system alternatives to the double-tee precast girder system meeting HL93 load requirements and 75-year design life for single span bridges of less than 70 feet.

An extensive review of the literature and practice at the state and national levels was performed, and local precast companies were consulted to find feasible alternatives to the double-tee bridges. Based on the typical properties of local bridges, a few criteria were selected to narrow down the literature review to alternatives that (1) are suitable for single-span bridges with a length of 70 ft or less, (2) can withstand the AASHTO HL93 load, (3) are designed for a service life of at least 75 years, and (4) incorporate accelerated bridge construction (ABC) techniques. Nine bridge systems were identified, and a summary of findings was submitted for discussion with the project technical panel. The panel selected two bridge systems for further investigation: (1) a fully precast bridge model, and (2) two types of glulam timber bridges.

3.2 Experimental Programs

Perform ultimate and fatigue load testing on alternative bridge system(s).

Three full-scale prefabricated bridge specimens were tested at the Lohr Structures Laboratory at South Dakota State University (SDSU): (1) a fully precast bridge consisting of two precast inverted tee girders supporting five precast full-depth deck panels, (2) a glulam timber girder bridge consisting of three glulam girders and 13 glulam deck panels connected using epoxy, and (3) a glulam timber slab bridge consisting of two glulam deck panels placed in the longitudinal direction of the bridge connected together incorporating three glulam stiffeners. Each specimen represented approximately one lane of a typical bridge. The main objective for the laboratory tests was to evaluate the structural performance of the proposed systems under fatigue and ultimate loading.

3.3 Evaluation of Different Bridge Alternatives

Compare cost, construction process, and performance of alternative bridge system(s) to the revised double-tee girder system from SD2013-01.

The constructability, structural performance, and costs of the three alternative bridge systems were compared to those of the modified and original double-tee bridges. Comparisons were made with the results obtained from project SD2013-01. Detailed design and construction guidelines were proposed to facilitate the adoption of the new bridges.

This is a black, white and red line graph that plots Actuator Load, P (kips) from 0 to 300 vs. Strain -500 to 200. It shows results for 5 different strain gauges and 2 embedded gauges. It includes a small digram showing where the strain gauges were tested on the span.

4 TASK DESCRIPTIONS

The research presented in this report includes 12 tasks. The following is a description of activities performed in each task.

4.1 Meet with Technical Panel

Task 1: Meet with the technical panel to review the project scope and work plan.

A kickoff meeting with the technical panel was held on June 16, 2015. A presentation on the project scope and work plan, along with a preliminary literature review, was presented by the research team. A copy of the presentation slides was uploaded to the SDDOT FTP research site.

4.2 Perform Literature Review

Task 2: Perform a literature review of bridge system alternatives to the double-tee girder system that are low cost, single span less than 70 feet, applicable for use on local roads with service life of at least 75 years.

A comprehensive literature review on the design and performance of simply supported bridge systems with a span length of 70 ft or less was conducted. The search included a variety of material types used for the construction of such bridge systems Nine bridge systems were identified as potential candidates for implementation in South Dakota: (1) full-depth deck panels supported by precast girders, (2) voided slab bridges, (3) ultra-high performance concrete (UHPC) waffle deck panels, (4) carbon fiber composite cable-prestressed decked tee beams, (5) bridge decks reinforced with aramid fiber reinforced polymer, (6) stress-laminated timber bridge decks, (7) glulam timber bridges, (8) advanced composite materials bridges, and (9) recycled plastic bridges. A summary of the findings is presented in Chapter 5 of this report and in-depth review of these bridge systems is presented in Mingo (2016) and Carnahan (2017).

4.3 Send Technical Memorandum Summarizing Literature Review Results

Task 3: Provide the technical panel with a technical memorandum explaining the results of the literature review from task 2.

The results from Task 2 were compiled in a technical memorandum, which was submitted to the technical panel on March 15, 2016 for review. The memorandum covered the different short single-span bridge systems identified in Task 2 along with the advantages and limitations of each system. A copy of the memorandum was uploaded to the SDDOT FTP research site.

4.4 Meet with Technical Panel to Discuss Literature Review

Task 4: Meet with the technical panel to discuss results of the literature review and technical memorandum. Based on discussion, technical panel will decide which option(s), if any, will require structural testing.

A meeting with the technical panel was held on October 8, 2015 to discuss the literature review. Based on the discussion during the meeting on constructability, suitability, performance, and costs, the technical panel approved the testing of two bridge systems: full-depth deck panels supported by precast girders and glulam timber bridges. There are generally two types of glulam timber bridges: girder bridges consisting of longitudinal glulam stems supporting glulam deck panels, and slab bridges consisting of deck panels and stiffeners. Both timber bridge types were selected by the panel for further investigation. A copy of the presentation slides was uploaded to the SDDOT FTP research site.

4.5 Prepare Testing Plan

Task 5: If directed by the technical panel, prepare a technical memorandum describing a complete instrumentation, construction, and testing plan for technical panel review.

Comprehensive test plans based on initial feedback from the technical panel were developed for the three selected bridge systems (fully precast, glulam girder, and glulam slab bridges). The research team met with the technical panel on June 14, 2016 and December 6, 2016 to discuss the detailing of the three bridge test specimens, plans to manufacture the specimens and transport them to SDSU, types of testing (strength and fatigue), test setup, instrumentation plan, cost estimate, and tentative test schedule. The technical panel approved the plan in these meetings to proceed. Copies of the presentation slides were uploaded to the SDDOT FTP research site.

4.6 Construct and Instrument Test Specimens

Task 6: Upon approval of the plan by the technical panel, proceed with instrumentation and construction of test girders. Notify the technical panel of construction schedule to give the option to be present at time of construction.

The test girders and deck panels for the precast full-depth deck panel system were fabricated at the Gage Brothers facility in Sioux Falls, SD in June 2016. The precast bridge components were assembled in the Lohr Structures Laboratory at SDSU in July 2016.

The glulam girder bridge was fabricated and assembled at the Gruen-Wald facility in Tea, SD in October 2016. The glulam slab bridge deck panels and stiffeners were fabricated by the same manufacturer in December 2016 and were shipped to SDSU on December 16, 2016 for assembly.

Instrumentation and construction of the test girders are discussed in Chapter 6 of this report.

4.7 Perform Fatigue and Ultimate Tests

Task 7: Perform and provide the technical panel the opportunity to observe ultimate and fatigue loading of selected structure type.

The fatigue load testing of the full-depth deck panel system started on August 15, 2016 and concluded on August 23, 2016. The joint load testing started on August 26, 2014 and concluded on August 27, 2016. The ultimate test was performed on September 6, 2016.

The fatigue testing of the glulam girder bridge started on October 27, 2016 and ended on November 5, 2016. The ultimate test was carried out on November 8, 2016.

The fatigue testing of the glulam slab bridge started on December 18, 2016 and concluded on December 23, 2016. The ultimate test was performed on January 6, 2017.

The technical panel was notified ahead of time of the testing schedule. Detailed information on the experimental work is presented in Chapter 6 of this report.

4.8 Compare Test Results of the Alternatives with Double-Tee Bridges

Task 8: Compare results of testing with the results from the SD2013-01 project to understand the construction and load capacity differences between bridge systems.

The experimental results from the three test specimens were analyzed and compared with the double-tee bridge system in terms of the constructability, testing, and costs. Included were force-displacement relationship, stiffness degradation under AASHTO fatigue loading, observed damage, maximum principal stresses, strain profiles, and joint rotations and slippage. Detailed information on the experimental results is presented in Chapter 7 of this report.

4.9 Develop Recommendations

Task 9: Develop a recommendation to the SDDOT based on cost and performance of the alternative bridge system compared to the revised double tee section from SD2013-01.

Based on the research work done in this study, the research team developed recommendations for the three bridge systems that were tested. Recommendations are presented in Chapter 8 of this report.

4.10 Meet with Technical Panel to Review Results and Recommendations

Task 10: Meet with technical panel to review and accept results of investigation and proposed recommendations.

The research team met with the technical panel on May 24, 2017 and presented a summary of the results, rationale, and design and construction guidelines. The benefit of adopting the alternative systems over the traditional double-tee bridges was discussed in the meeting. Copies of the presentation slides were uploaded to the SDDOT FTP research site.

4.11 Prepare Final Report

Task 11: Prepare a final report and executive summary of the research methodology, findings, conclusions, and recommendations.

This report is a comprehensive final report prepared by the research team according to SDDOT guidelines. The report documents all aspects of the project and recommendations on implementation of the alternative systems.

Two additional documents were attached to this report in case in-depth discussion of some subject matter is needed.

4.12 Make Executive Presentation

Task 12: Make an executive presentation to the SDDOT Research Review Board at the conclusion of the project.

A final presentation was given to the SDDOT Research Review Board on August 30, 2017.

5 LITERATURE REVIEW

A comprehensive review of literature and practice was performed. Nine bridge systems were identified as potential candidates for implementation in South Dakota: (1) full-depth deck panels supported by precast girders, (2) voided slab bridges, (3) ultra-high performance concrete (UHPC) waffle deck panels, (4) carbon fiber composite cable-prestressed decked tee beams, (5) bridge decks reinforced with aramid fiber reinforced polymer, (6) stress-laminated timber bridge decks, (7) glulam timber bridges, (8) advanced composite materials bridges, and (9) recycled plastic bridges. From among those nine choices of bridge systems a full-depth precast panel on precast girders and two glulam designs were selected by the technical panel for testing. This chapter presents the findings of the literature review on the selected bridges systems. Information regarding the other bridge systems can be found in Attachments A and B.

5.1 Full-Depth Deck Panels Supported on Prefabricated Girders

The main components of a full-depth deck panel (FDDP) system are typically: precast full-depth concrete deck slabs, prestressed concrete or steel girders, transverse joints, longitudinal joints, shear pockets, and horizontal shear reinforcement. The findings of the literature review on these components are briefly discussed.

5.1.1 Transverse Joints

Different detailing has been developed for transverse joints of FDDP systems. The detailing usually incorporates longitudinal post-tensioning to aid in moment and shear transfer and to prohibit reflective cracking. However, post-tensioning was not preferred in this study, since many local counties may not have the technology and skilled labor to use post-tensioning.

It is also common to splice the longitudinal steel reinforcement of precast deck panels to avoid post-tensioning. Badie and Tadros (2008) reported that some highway agencies (e.g. the Alaska DOT and the New Hampshire DOT) did not use any reinforcement crossing the transverse joint (Figure 5.1). The Alaska DOT has not reported any significant joint cracking or leakage on simply supported bridges on low-volume traffic roads when there was no reinforcement in the transverse joints (Badie and Tadros, 2008).

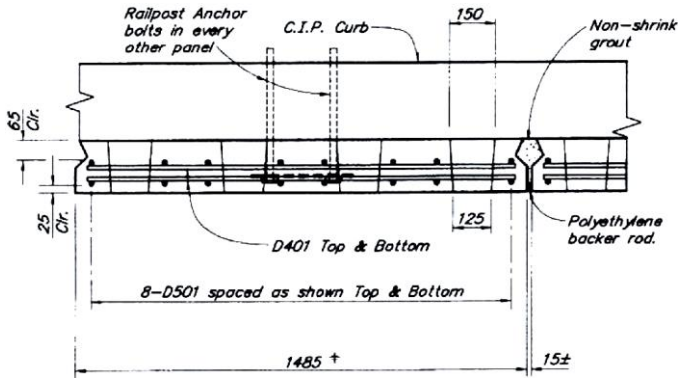

Figure 5.1: Transverse Joint Detailing for Precast Deck Panel Bridges in Alaska

(after Badie and Tadros, 2008)

5.1.1.1 Shear Key Types

Various shear key details exist for FDDP systems (Figure 5.2). Shear keys transfer both shear forces and bending moments. The shear force transfer is achieved through a combination of bearing against the concrete-grout surfaces and the bond between the concrete-grout surfaces.

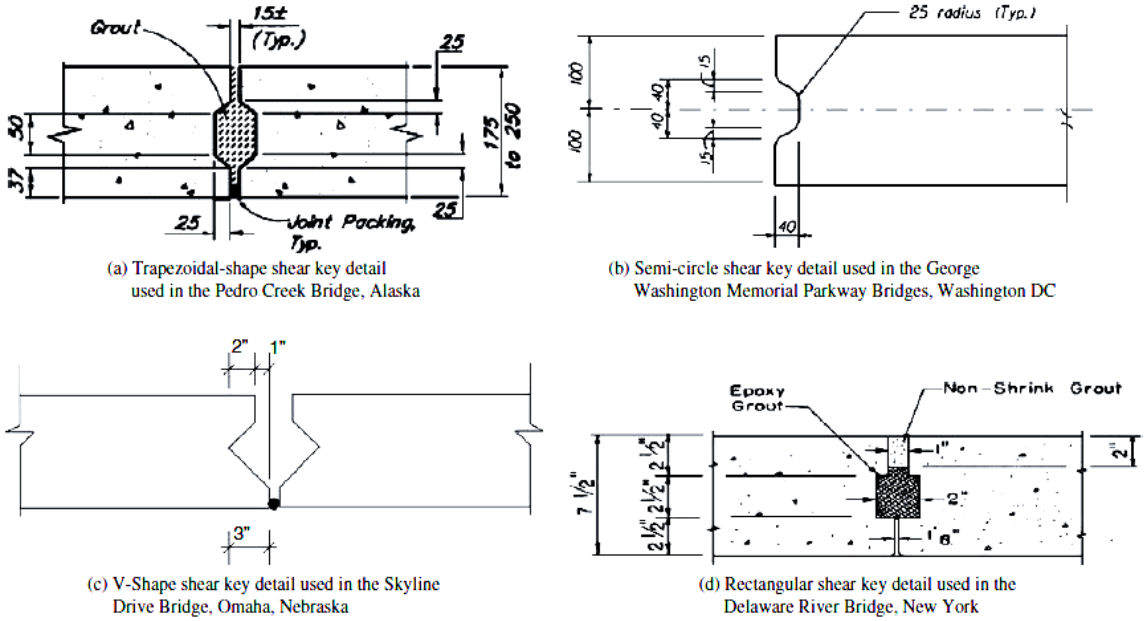

(a) Trapezoidal-shape shear key detail used in the Pedro Creek Bridge, Alaska

(b) Semi-circle shear key detail used in the George Washington Memorial Parkway Bridges, Washington DC

(c) V-Shape shear key detail used in the Skyline Drive Bridge, Omaha, Nebraska

(d) Rectangular shear key detail used in the Delaware River Bridge, New York

Figure 5.2: Grouted Groove-to-Groove Shear Key Details for Transverse Joints

(after Badie and Tadros, 2008)

Two methods have been used to contain the grout poured into the shear keyways: inserting a polyethylene backer rod towards the bottom of the keyway and using wood formwork placed from under the panel. Badie and Tadros (2008) recommended roughening the surface of the shear key for deck systems that do not include post-tensioning.

5.1.1.2 Block-out with Tied-in Lap Splice and Spiral Confinement

For block-out with tied-in lap splice and spiral confinement configurations, the transverse joint detail consists of a series of block-outs along the joint (Figure 5.3). Bridge deck longitudinal reinforcement extends from panels into the block-outs and a steel bar is tied to the deck longitudinal reinforcement. Steel spirals are used to confine the concrete, shorten the lap splice length by 40% to 50%, and simplify the construction, since deck steel does not extend into the transverse joint (Badie and Tadros, 2008).

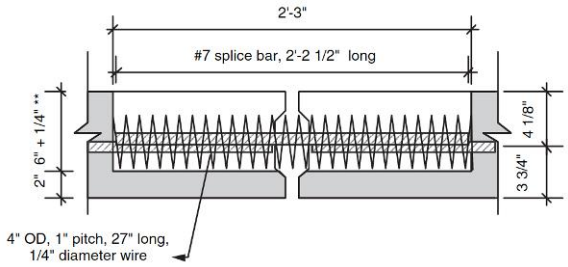

(a) Detailing of Block-out with Tied-in Lap Splice and Spiral Confinement (after Badie and Tadros, 2008)

(b) Photogram of Block-out with Tied-in Lap Splice and Spiral Confinement (after Badie et al., 1998)

Figure 5.3: Spiral Confinement Detailing for Transverse Joints

5.1.1.3 Hollow Structural Steel Confinement

Badie and Tadros (2008) developed two new FDDP transverse joints with external confinement (Figure 5.4and Figure 5.5) in which hollow structural steel (HSS) tubes are embedded in the FDDP decks adjacent to the transverse joint. Figure 5.4 shows one of the joint detailing. Deck steel bars are extended out the transverse joint on one side of the slab and are inserted into the HSS tube in the adjacent slab during construction.

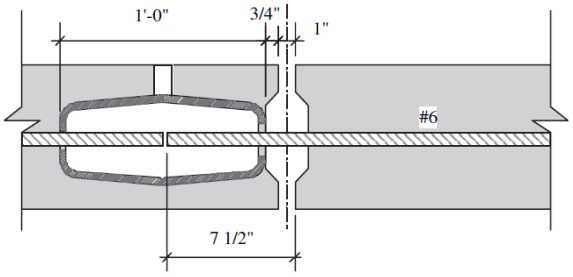

(a) HSS Tube Confinement Detail

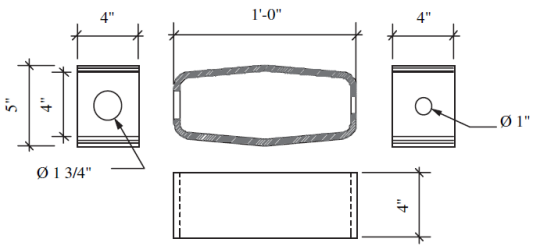

(b) Galvanized Bulged HSS 4x12x3/8 in.

Figure 5.4: HSS Tube Confinement Details for Transverse Joint
(after Badie and Tadros, 2008)

Figure 5.5 shows another joint detailing where HSS tubes are embedded in both adjacent panel transverse joints. Deck steel bars are extended into the HSS tubes. The main difference with respect to the first detailing is that the top portion of the HSS tube is open to allow placement of deck steel bars in the HSS tubes. It should be noted that these types of joints have a tight construction tolerance.

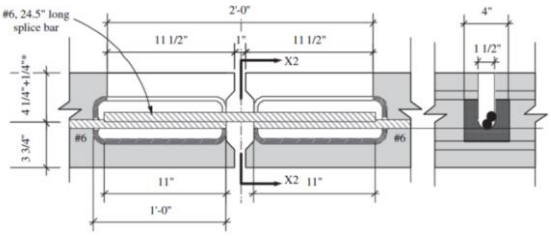

(a) HSS Tube Confinement Detail

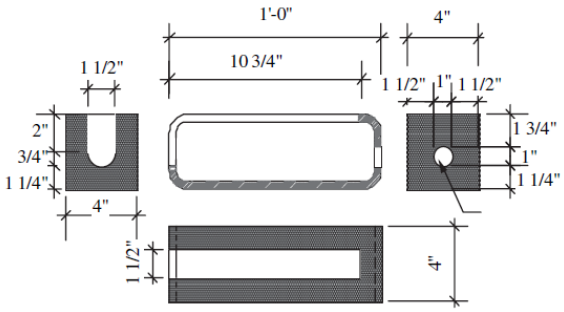

(b) Galvanized Bulged HSS 4x12x3/8 in.

Figure 5.5: Adjacent HSS Tube Confinement Details for Transverse Joints
(after Badie and Tadros, 2008)

5.1.1.4 UHPC for Transverse Joints

Graybeal (2010) tested various transverse joint details incorporating Ultra-High Performance Concrete (UHPC) as joint filler. One detail consisted of non-contact headed mild-steel reinforcement extending from the bridge deck into the joints. Figure 5.6 shows the layout and rebar plan of the connection. Two No. 5 bars were placed along the length of the connection between the heads. Another connection consisted of epoxy-coated No. 4 hairpin bars extending from the deck into the joint (Figure 5.7). Two No. 5 bars were placed inside the hairpins along the length of the joint. The third detail consisted of straight lapped No. 5 mild-steel reinforcement extending from the deck into the joint (Figure 5.8). Two No. 5 bars were placed along the length of the connection between the top and bottom layer of joint reinforcement.

No cracking between the UHPC and the precast panels was observed during cyclic loading. Furthermore, no rebar de-bonding occurred in the joints of the test specimens. Cracks propagated perpendicular to the transverse joints when subjected to ultimate loading. The joint details tested by Graybeal (2010) are expected to perform sufficiently in the field.

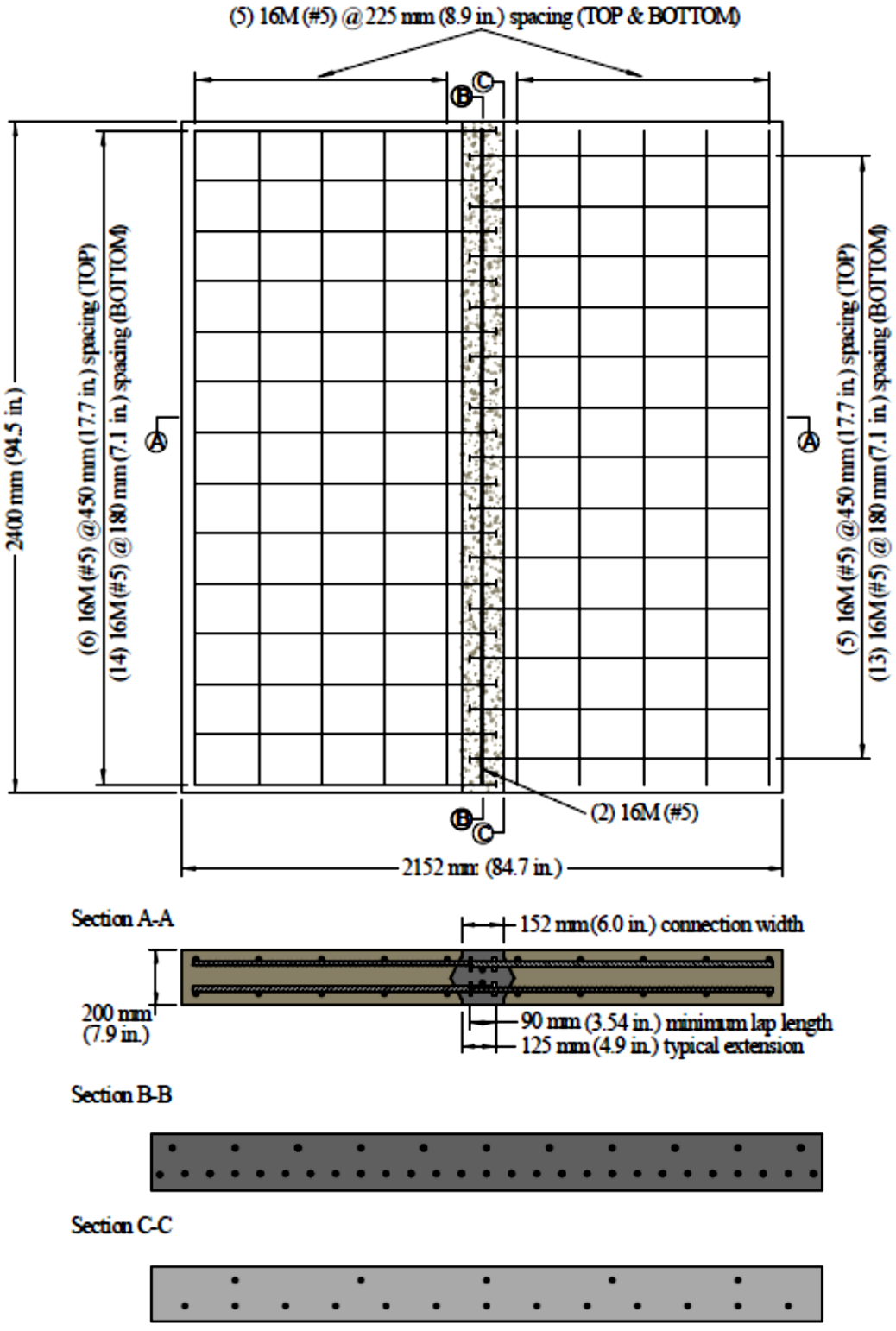

Figure 5.6: UHPC and Headed Steel Bars for Transverse Joints
(after Graybeal, 2010)

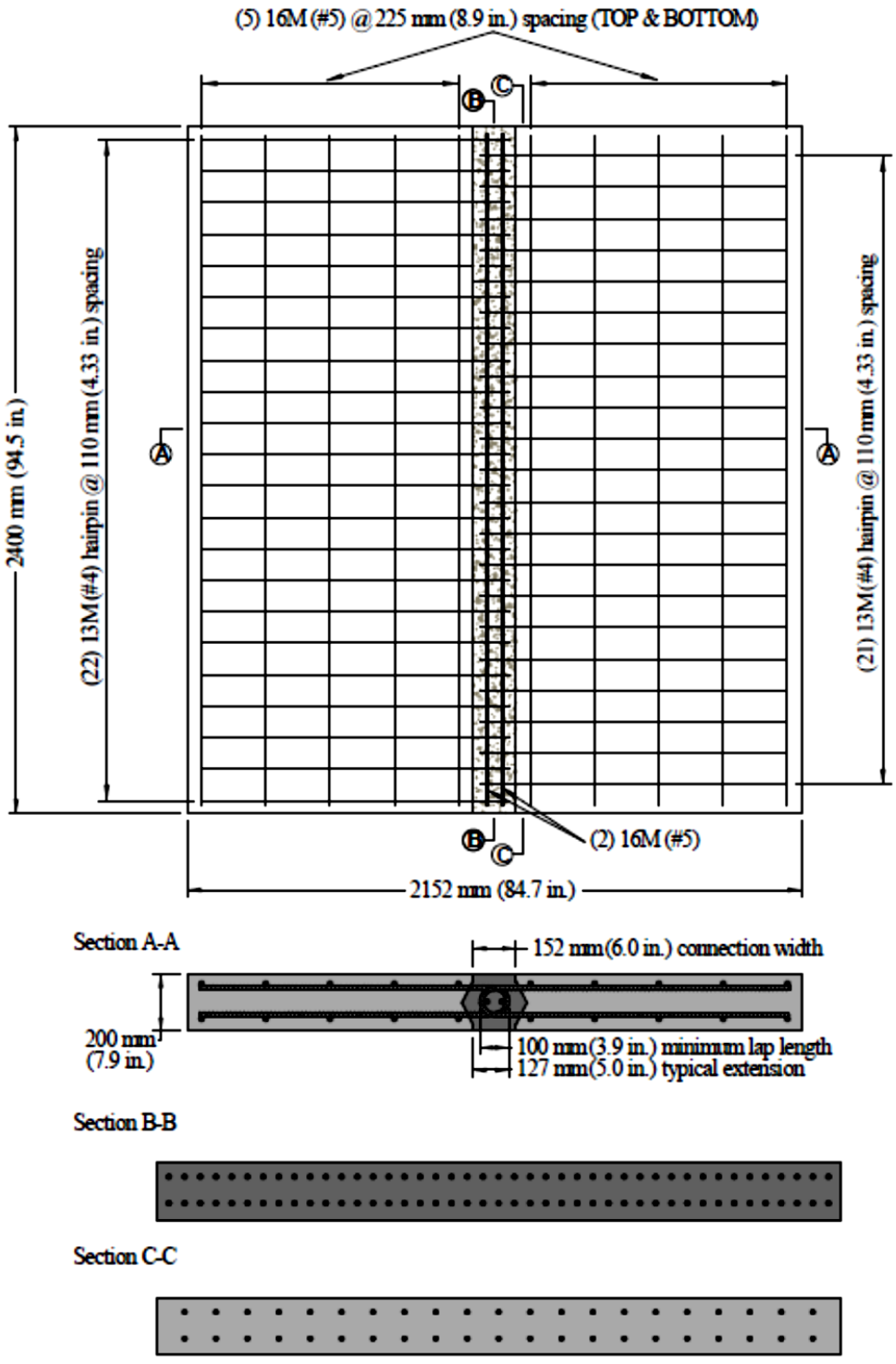

Figure 5.7: UHPC and Hairpin Steel Bars for Transverse Joints
(after Graybeal, 2010)

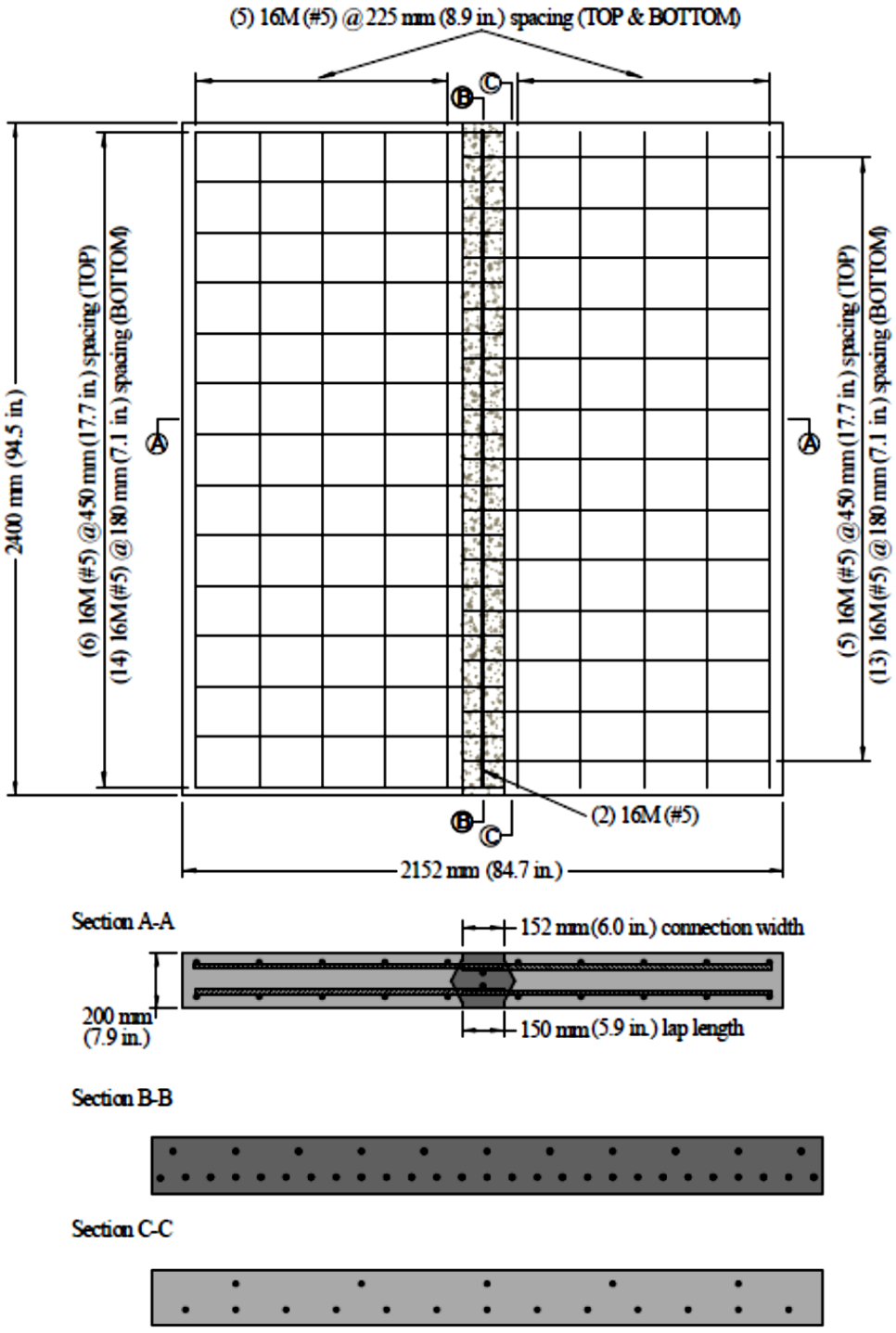

Figure 5.8: UHPC and Straight Lapped Steel Bars for Transverse Joints
(after Graybeal, 2010)

5.1.2 Longitudinal Joint

For FDDP systems, a longitudinal joint is usually used at the centerline of the bridge in the direction of traffic to allow the bridge to be crowned for water drainage. Typically, U-shape steel bars are extended

from two adjacent panels to splice the panels and to provide reinforcement continuity to resist bending moments and shear forces. Longitudinal steel bars are installed along the length of the bridge inside the U-shape bars to increase the bond strength. The Bill Emerson Bridge in Missouri is an example of such longitudinal joint detail (Figure 5.9).

(a) Photograph of Longitudinal Joint

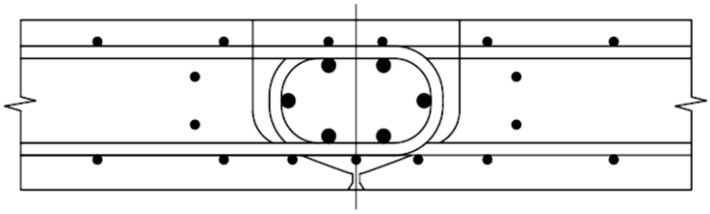

(b) Detailing of Longitudinal Join

Figure 5.9: Longitudinal Joint Detail of Bill Emerson Memorial Bridge, Missouri DOT
(after Badie and Tadros, 2008)

Aaleti and Sritharan (2014) developed a UHPC waffle deck panel system with a longitudinal joint consisting of 1-in. diameter straight dowel bars extending from the deck into the joint and bars running along the length of the joint to aid in development of the dowel bars. Figure 5.10 shows the longitudinal joint detailing for the UHPC waffle deck panel system.

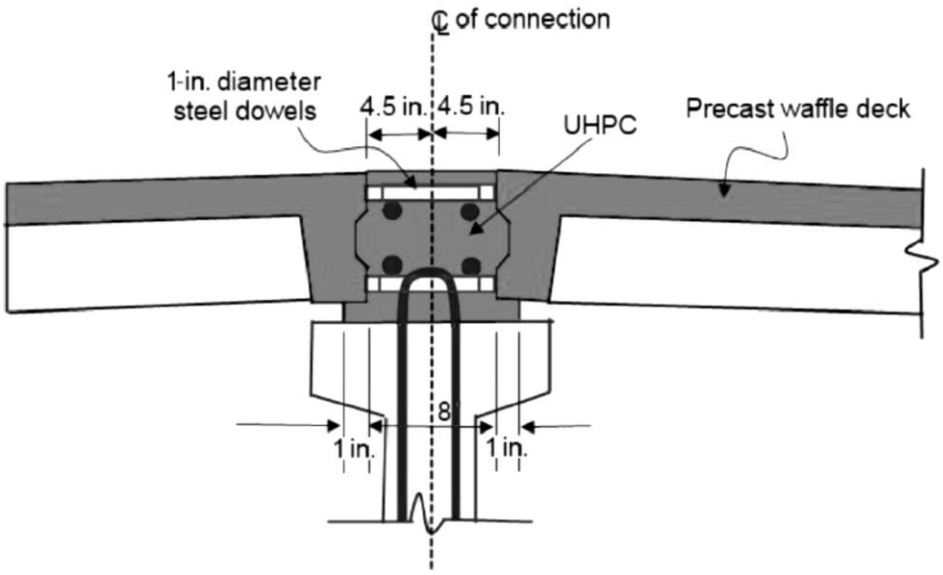

Figure 5.10: Longitudinal Joint Detailing for UHPC Waffle Deck Panel System
(after Aaleti and Sritharan, 2014)

5.1.3 Shear Pockets

The shear pockets connect the concrete panels to the girder to create composite action. Scholz (2007) performed a study on shear pocket connections funded by the Virginia DOT. Eight grout types were

investigated to determine the best grout. This study also investigated the bond between the girder-grout and grout-deck interfaces. Flow and workability, horizontal shear strength with two planes of shear, various shear pocket reinforcement types, grout compressive and tensile strength, shrinkage, and bond strength between the grout-to-concrete interface were measured. Both grout and extended grout with pea gravel were used. Inverted U-shape stirrups and headed shear studs were tested through push-off tests.

Two grouts were found to be suitable for use in an FDDP system based on this research: Five Star® Highway Patch and Set® 45 Hot Weather. Two types of shear reinforcement between the precast concrete I-beams and bridge deck panels were tested, and they provided adequate shear resistance. These included two No. 4 or No. 5 bars extending from the I-beam into the shear pocket and headed shear studs, which were welded to steel plates embedded in the I-beams.

Badie et al. (2006) developed two types of shear pockets that can be used in FDDP systems: partial-depth and full-depth shear pockets (Figure 5.11 and Figure 5.12, respectively). The partial-depth shear pocket was recommended when no overlay is used to protect the deck from water leakage at the grout and surrounding concrete interface.

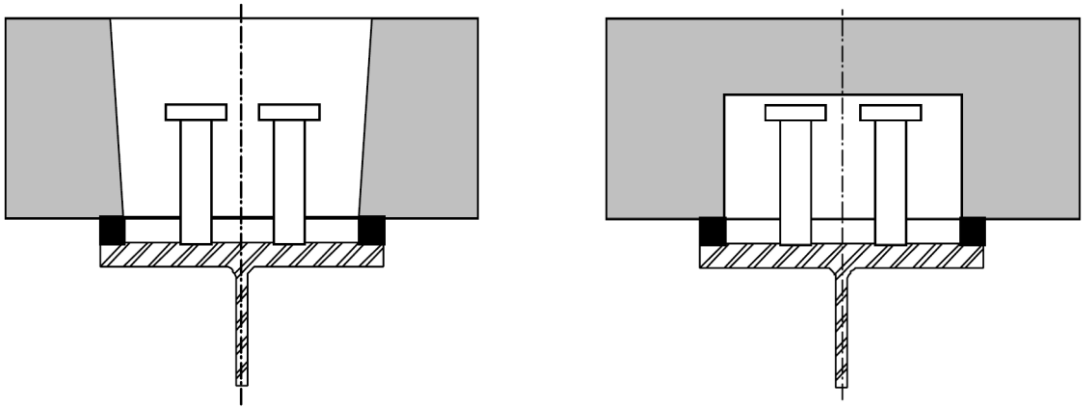

(a) Full-depth Shear Pocket (b) Partial-depth Shear Pocket

Figure 5.11: Shear Pocket Details
(after Badie et al., 2006)

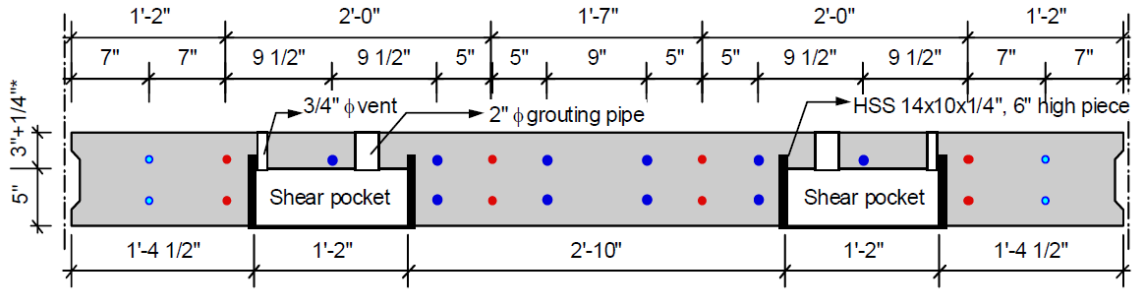

Figure 5.12: FDDP System with Partial-Depth Shear Pockets
(after Badie et al., 2006)

5.1.4 Horizontal Shear Reinforcement

Two types of reinforcement detailing were used in the past to transfer horizontal shear forces between the girder and the deck: inverted U-shape bars and headed shear studs (Figure 5.13 - Figure 5.15). The U-shape bars placed transversely minimize the length of shear pockets, and the U-shape bars placed longitudinally can be used in girders with small web widths. The headed shear stud detail (Figure 5.15) proposed by Badie and Tadros (2008) requires welding of shear studs to a steel plate and embedding the plate in the top flange of the prestressed concrete girder.

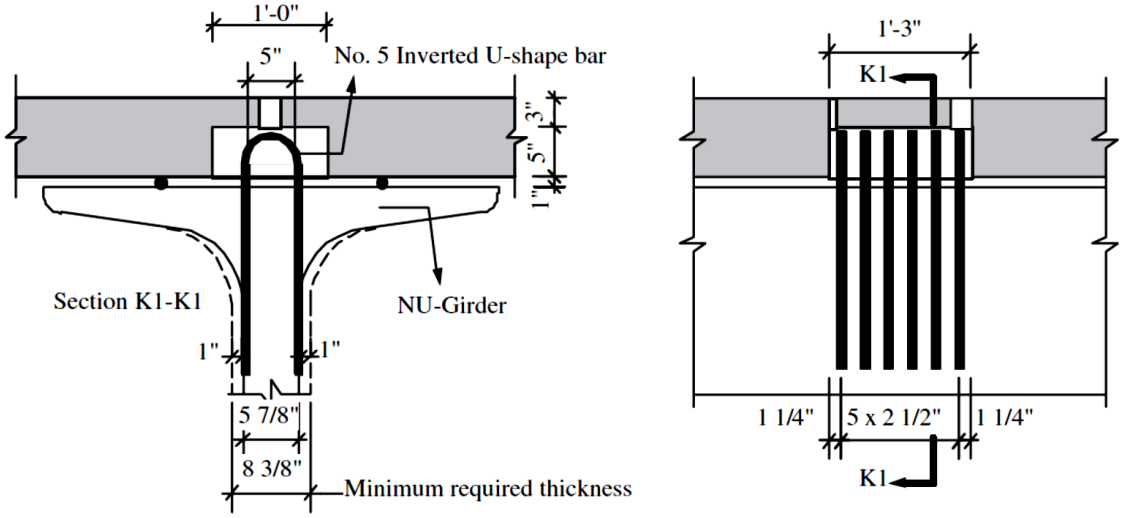

Figure 5.13: Inverted U-Shape Horizontal Shear Reinforcement Placed Transversely
(after Badie and Tadros, 2008)

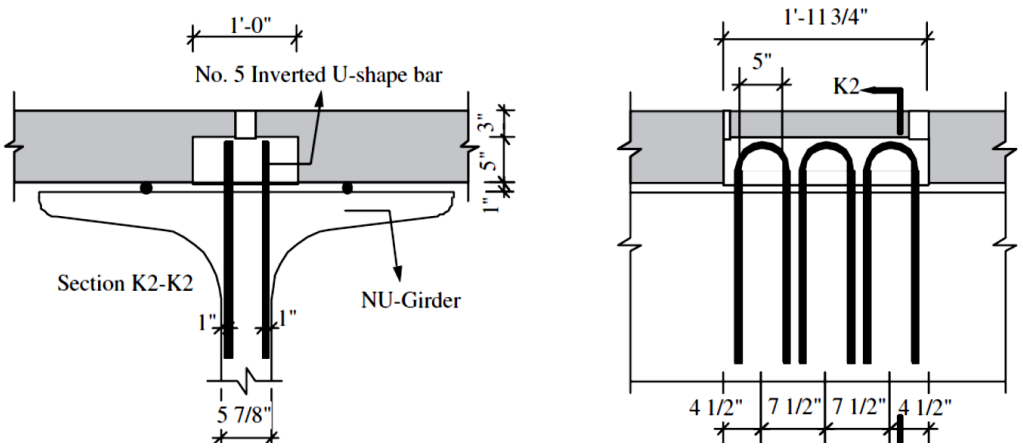

Figure 5.14: Inverted U-Shape Horizontal Shear Reinforcement Placed Longitudinally
(after Badie and Tadros, 2008)

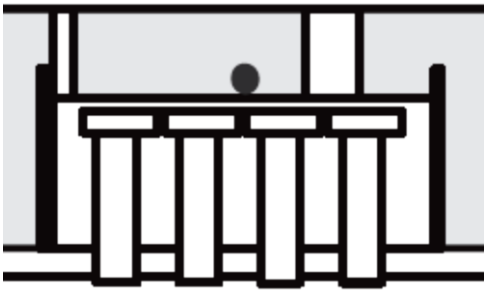

Figure 5.15: Headed Stud Horizontal Shear Reinforcement
(after Badie and Tadros, 2008)

5.2 Glulam Timber Bridges

This section includes a summary of findings in the literature review on the feasibility, performance, and past application of two different glulam timber bridge systems.

5.2.1 Overview of Glulam Timber Bridges

Glulam timber bridges (Figure 5.16) are constructed of glulam members manufactured from lumber laminations that are bonded together on their wide faces with waterproof structural adhesives. According to Ritter (1990), glulam is the most common material used for the fabrication of timber bridges because glulam members can be manufactured to any size and shape. In general, the span length of glulam bridges ranges from 20 to 80 ft, but construction of longer bridges with span lengths of 140 ft or longer is possible (Ritter, 1990). Important design and construction considerations such as design method, wearing surfaces, railing systems, and abutments are discussed in the following sections.

Figure 5.16: Glulam Timber Bridge in Buchanan County, Iowa

Wood is a renewable material that is readily available in South Dakota. Ritter (1990) states that glulam timber bridges are very economical, light-weight, easy to fabricate, and environmentally friendly. Construction of glulam timber bridges is relatively simple and usually can be done without highly skilled labor. Since they can be fabricated off-site and installed in place in a short period of time, glulam bridges are suitable for accelerated bridge construction (ABC) and can be installed in most weather conditions.

Glulam timber bridges are not very common; therefore, data on the long-term performance of such bridges is scarce. Timber bridges will deteriorate rapidly if exposed to moisture for a long duration; therefore, frequent inspection and retreating are needed. It is also highly recommended that timber bridges be inspected every two years and any wood that is exposed be retreated every six years (Ritter, 1990). Early detection of moisture is critical in extending the life of timber bridges (Ritter 1990).

5.2.2 Types of Glulam Timber Bridges

Two main types of glulam timber bridges have been used in the field: longitudinal glulam deck bridges (Figure 5.17a), and transverse glulam deck bridges (Figure 5.17b). The former type consists of glulam deck panels, typically 4 ft wide, spanning in the longitudinal direction of the bridge. These panels are held together by transverse stiffeners, which cannot be spaced more than 8 ft apart. The longitudinal glulam deck bridges can only span up to 38 ft (Wacker and Smith, 2001). The latter type of glulam bridge consists of transverse glulam deck panels supported by stringers placed in the longitudinal direction of the bridge. The deck panels are typically 4 ft wide and the stringers are typically spaced at 4-ft intervals. These bridges typically span up to 80 ft.

(a) Longitudinal Glulam Deck (Slab Bridge)

(b) Transverse Glulam Deck (Girder Bridge)

Figure 5.17: Glulam Timber Bridge Types

5.2.3 Timber Bridge Structural Components

The material and various structural components of a glulam timber bridge include girders, deck panels, connections, and stiffeners discussed here.

5.2.3.1 Glulam Materials

Timber is a nonhomogeneous and brittle material as evidenced by bending and axial compressive behavior (Figure 5.18). The strength of glulam timber is evaluated (rated) either mechanically or visually. Design values for typical glulam timber are specified in Chapter 8 of AASHTO LRFD Bridge Design Specifications (AASHTO, 2013). Other glulam materials and species are allowed by the code, however. These design values are then adjusted by correction factors as specified by AASHTO, accounting for several parameters affecting the behavior of wood such as wet service conditions, temperature, member size, member volume, and load duration.

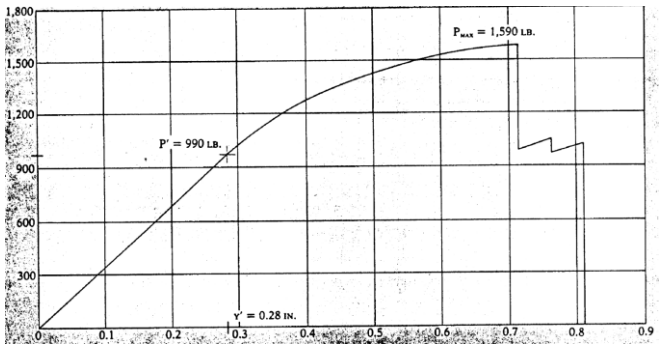

Vertical Axis = Load (lb)

Horizontal Axis = Displacement (in.)

(a) Force-Displacement Relationship under Bending

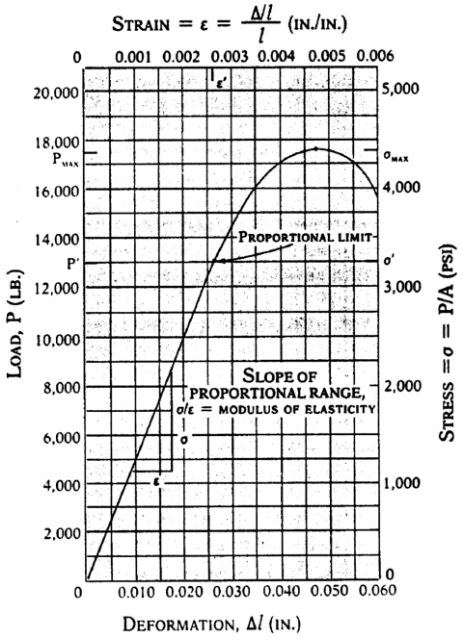

(b) Axial Compressive Behavior

Figure 5.18: Force-Displacement Relationship for Wood
(after Hoadley, 1980)

5.2.3.2 Girders (Stringers)

The size of glulam girders varies based on the bridge span length, the girder spacing, lamination species, and design loads. The nominal width of a glulam girder is typically ranges from 8 to 12 in. The nominal depth of a glulam girder can vary from 12 to 60 in. The lamination species is selected based on the availability of the material and the cost. Southern Pine is the most commonly used species for wood bridge girders in South Dakota.

5.2.3.3 Deck Panels

The deck panels for the girder bridges are typically 4 ft wide. A weaker species of wood, rather than Southern Pine, may be used in the panels due to low stress demands. The panels should have a minimum nominal depth of 6 in. to meet AASHTO (2013) LRFD standards. The deck panels for the slab bridges are typically 4 ft wide. The strong, inexpensive, and easily available wood material is normally used due to high stress demands on the slab. The nominal depth of a deck panel varies from 6 to 16 in. Nominal depths greater than 12 in. are not common.

5.2.3.4 Stiffeners

For glulam slab bridges, stiffeners are required to unify the deformation of the individual panels and to make the panels act as one system. One stiffener must be placed at the mid-span of the bridge, and the additional stiffeners should be placed no more than 8 ft apart on the remainder of the span length according to AASHTO LRFD (2013). AASHTO (2013) in Section 9.9.4.3.1 also requires that the rigidity, defined as the product of the modulus of elasticity and the moment of inertia (*EI*), of a stiffener beam shall not be less than 80,000 kip-in^2. Any size and material can be used as long as it satisfies the rigidity standard.

5.2.3.5 Diaphragms

AASHTO LRFD (2013) currently specifies that either solid diaphragms (Figure 5.19a) or steel cross braces (Figure 5.19b) be installed on the timber bridges to improve the stability of the bridge. The feasibility and performance of glulam cross braces was investigated in this study (Figure 5.20).

(a) Solid Glulam Diaphragm (after Hosteng, 2013)

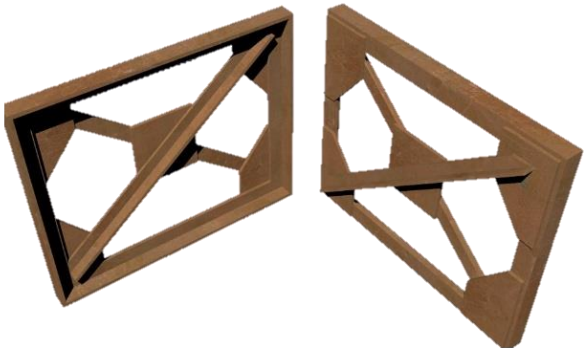

(b) Steel Cross Braces (etraxx.com)

Figure 5.19: Diaphragm Types for Girder Timber Bridges

Figure 5.20: Glulam Cross Braces for Girder Timber Bridges

5.2.3.6 Deck to Stringer Connections

Currently two methods are primarily used to connect deck panels to stringers. One method is to install lag bolts from the top of the deck through the entire panel into the top of the beam (Figure 5.21). One of the disadvantages of using lag bolts is their large size, requiring field boring for installation. Since it is impractical to drill lag bolt holes before the pressure treatment of the lumber, the bridge is more susceptible to decay due to water penetration. Furthermore, it is not possible to retighten these bolts if they loosen since the wearing surface will cover them.

Figure 5.21: Lag Bolt Deck-to-Stringer Connection for Timber Bridges
(after Hosteng, 2013)

Another connection detailing is with deck brackets (Figure 5.22). Aluminum brackets usually have small teeth that bite into a routed slot that is cut into the girder. The top portion of the bracket is then bolted to the deck. The deck bracket connection offers a tight connection that can be retightened if needed. Deck bracket connections also do not affect the deck preservative treatment since lag bolts can be placed from the bottom of the deck. Disadvantages of this type of connection are that a large number of brackets is required and the slots require removal of a large volume of the wood to accommodate the size of the bolt head. Furthermore, many holes are drilled into the deck if bolts are installed from the top of the bridge.

Figure 5.22 : Aluminum Clip Deck-to-Stringer Connection for Timber Bridges
(after Hosteng, 2013)

The third deck-to-stringer connection that has been incorporated in the Cedar Rock Bridge in Buchanan County, Iowa (Figure 5.16), is with epoxy (Figure 5.23). Epoxy provides a strong bond between the deck and the stringer. This connection reduces the areas where water can seep into the deck, since only small structural screws are needed to hold the deck panels to the stringers as the epoxy cures. The performance of this type of deck-to-stringer connection was investigated in this study.

Figure 5.23: Epoxy Deck-to-Stringer Connection

5.2.4 Long Term Performance of Glulam Timber Bridges

Ritter (1990) states that while timber has been used as a bridge material for hundreds of years, the application of treated timber was very rare until the early 1900s. Numerous untreated timber bridges

performed well in the past, but untreated timber bridge numbers have declined in the modern era due to the reduction in naturally weather resistant North American wood species formerly used in bridge construction. It is no longer feasible or economical to cover bridges for protection against moisture if the wood is untreated.

Brashaw et al. (2013) investigated the long-term performance of many different types of bridges, including five glulam timber bridges. The study included the National Bridge Inventory (NBI) ratings for those five bridges in Faribault County, Minnesota (Table 5.1).

Table 5.1: Glulam Timber Girder Bridges in Minnesota (Brashaw et al., 2013)

Bridge ID	Year Built	Span (ft)	Average Daily Traffic	Width (ft)	Wearing Surface	NBI Condition Rating - Deck	NBI Condition Rating-Superstructure
22508	1968	33.5	95	33.3	Bituminous	7	7
22514	1968	40	35	26	Gravel	6	7
22518	1969	38.5	70	33.1	Gravel	7	7
22519	1969	33.5	539	32	Bituminous	6	7
9967	1951	36.2	175	27.4	Bituminous	7	6

Figure 5.24 through Figure 5.28 show these five bridge conditions in 2016. It can be concluded that glulam timber bridges can last more than 60 years if they are properly maintained.

Figure 5.24: Glulam Timber Bridge No. 22508 in Faribault County, Minnesota

Figure 5.25: Glulam Timber Bridge No. 22514 in Faribault County, Minnesota

Figure 5.26: Glulam Timber Bridge No. 22518 in Faribault County, Minnesota

Figure 5.27: Glulam Timber Bridge No. 22519 in Faribault County, Minnesota

Figure 5.28: Glulam Timber Bridge No. 9967 in Faribault County, Minnesota

5.2.5 Wearing Surface for Timber Bridges

According to Ritter (1990), a wearing surface is the top layer placed on the bridge deck to form the road surface. The main purpose of a wearing surface is to improve safety, provide a smoother surface, improve skid resistance, and protect the deck. Typically, a wearing surface for a timber bridge can consist of (1) an asphalt overlay, (2) an asphalt chip seal, (3) sacrificial lumber covering the whole deck, (4) cover steel plates, (5) cover lumber planks, and (6) aggregate overlay. In the case that no wearing

surface is used, routine inspections must be performed to ensure that the deck remains properly sealed to maintain the acceptable condition.

Asphalt is the most commonly used wearing surface since it provides a smooth and skid-resistant surface. Asphalt provides a tight waterproof layer that protects the timber deck from abrasion. The only negative aspect of using asphalt is that reflective cracks can form allowing water to seep into the wood, decreasing the service life of the bridge. Geotextile fabrics are highly recommended to help prevent reflective cracking and to improve the bond between the glulam deck and the asphalt wearing surface. To prevent any moisture from reaching the deck, the asphalt needs to be maintained. The asphalt approaches must be paved a minimum of 75 ft beyond the ends of the bridge to prevent the formation of potholes at the ends of the bridge. Examples of the asphalt wearing surface on timber bridge decks are shown in Figure 5.24, Figure 5.27, and Figure 5.28 where the surfaces performed reasonably well with minor cracks and potholes.

Another commonly used wearing surface is asphalt chip seal (Ritter, 1990). An asphalt chip seal is formed by placing a layer of aggregate onto liquid asphalt. Like the asphalt wearing surface, chip seal is smooth and skid-resistant. The main advantage of asphalt chip seal compared to regular asphalt is that the chip seal is thinner and more flexible with less reflective cracks. Two 3/4-in thick layers of chip seal are recommended to seal the deck. Geotextile fabric is also recommended for an asphalt chip seal wearing surface.

The use of an aggregate wearing surface is not common. Two examples are given in Figure 5.25 and Figure 5.26. Both bridges with the aggregate wearing surface were in reasonable condition in 2016. They might need some grading soon to remove the ruts from daily traffic.

The remaining wearing surface types were not recommended by Ritter (1990) since they can trap water. These types of wearing surfaces are typically used on very low volume of traffic roads when no other options are feasible.

A new wearing surface was recently used on the Cedar Rock Bridge in Buchanan County, Iowa (Figure 5.29). The bridge deck was flooded with epoxy to fill all the gaps in the wood. Then very small rocks were imbedded into the epoxy to improve traction. The epoxy is typically applied in three layers of 3/8-in thickness each. The life of the epoxy depends on its exposure. This wearing surface was applied in 2015, too recent for full performance evaluation.

Figure 5.29: Epoxy with Embedded Grit Wearing Surface for Glulam Timber Bridge in Buchanan County, Iowa

5.2.6 Preservative Treatment of Wood

All wood used in the construction of glulam bridges must be treated with preservatives as required by AASHTO (2013) LRFD specifications (Section 8.4.3). Water repellents are used to slow the absorption of water and to keep the moisture content low, which helps prevent decay and slows the weathering process. Wood preservatives are used to prevent biological deterioration. These preservatives are applied to the wood by vacuum-pressure treatment (FHWA, 2012a).

Fire retardant treatments are generally not recommended by AASHTO (2013), since the large size of the timber components used in bridge construction have inherent fire resistance characteristics. A fire retardant must not be applied unless it is compatible with the preservative treatment used in the wood. The strength and stiffness of fire treated wood should be reduced as recommended by the product manufacturer (AASHTO, 2013, Article 8.4.3.4).

5.2.7 Maintenance and Inspection Required for Glulam Timber Bridges

Since dry wood lasts longer than wood that has been exposed to moisture, it is necessary to perform routine maintenance on glulam timber bridges to keep the wearing surface and other exposed areas in good condition. It is also highly recommended that timber bridges be inspected every two years and any wood that is exposed be retreated every six years (Ritter, 1990). Retreatment can be done by applying the preservative with a brush.

According to Ritter (1990), several methods can be used for timber bridge inspection. Visual inspection is the most convenient method. An inspector looks over the bridge for signs of deterioration, decay, mold, fungi, insect activity, or any other abnormal changes in the wood. Probing is another inspection method usually performed as part of the visual inspection. A moderately pointed tool is used to probe for any soft spots in the wood. The third and most common inspection method for wood is to use

sounding in which the bridge inspector strikes the wood with a mallet or another object. The inspector can determine if there is decay by listening to the sound feedback. If decay is suspected, the inspector then must drill or core the area for further inspection. If decay is found, a plan of action must be made to fix the distressed region.

Preventative maintenance is crucial for long-term serviceability of timber bridges. For example, resealing the exposed wood can prevent decay and deterioration by keeping out moisture. Remedial maintenance should be performed when decay is present. However, remedial maintenance is only applicable where the distress is not severe enough to affect the overall performance of the bridge. In this case, a small section of a timber bridge can be replaced. Major maintenance is usually performed when deterioration results in strength degradation. In that case, a few members of the bridge have to be replaced to increase the bridge's load-carrying capacity. When the deterioration is severe, the bridge has to be replaced.

5.2.8 Railing Systems

A bridge railing system must be positioned to safely contain an impacting vehicle without allowing it to pass over, under, or through the rail elements. A proper railing system must be free of features that may catch on the vehicle or cause it to overturn or decelerate too rapidly. Any crash-tested railing configuration or any railing designed according to Section 13.7 of AASHTO LRFD (2013) can be used for timber bridges. The connecting components should be designed adequately. The rail material can be timber, metal, or concrete. One example of a timber railing is shown in Figure 5.30.

Figure 5.30: Railing on a Glulam Bridge
(after laminatedconcepts.com)

5.2.9 Timber Bridge Abutments

Many studies note that existing abutment detailing can be used for glulam timber bridges (Ritter (1990). Timber bridge abutments are typically constructed using either timber or concrete (Figure 5.31). The connections should be designed to resist appropriate design loads.

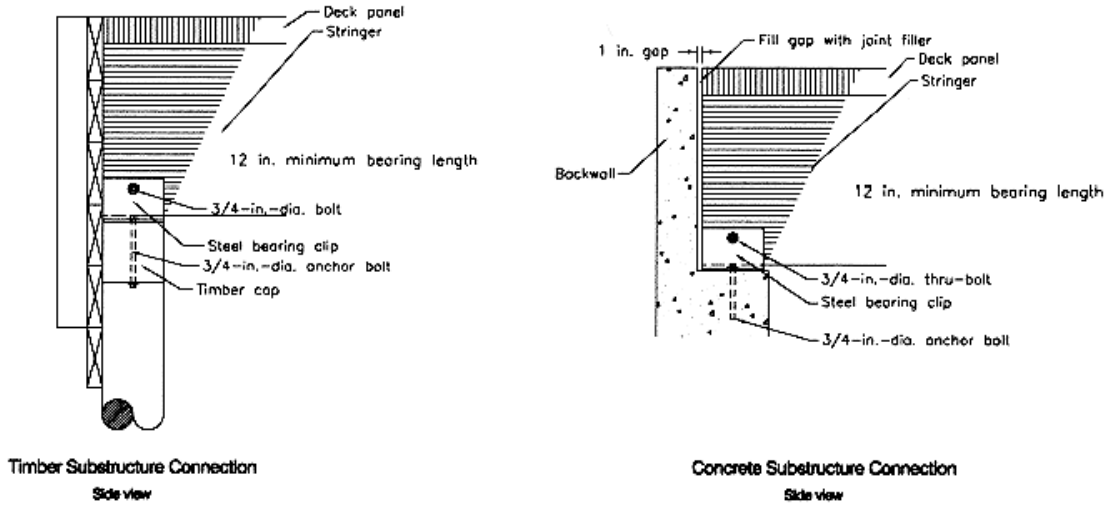

Figure 5.31: Glulam Timber Bridge Abutment Connections
(after Wacker and Smith, 2001)

5.2.10 Timber Bridge Fabrication

One of the advantages of glulam timber bridges is that they can be completely prefabricated offsite and then shipped to the project site for installation (Figure 5.32). This feature is in-line with Accelerated Bridge Construction (ABC), which has been recently emphasized in the United State. For wide timber bridges, the bridge can be prefabricated in segments of one or two lanes to be shipped and assembled onsite.

Figure 5.32: Erie Canal Bridge Being Placed in Port Byron, NY in 2014
(after laminatedconcepts.com)

For onsite construction of glulam girder timber bridges, assembly is typically started by placing the center girder, followed by the placing of the other girders, working outwards. Subsequently, the deck

panels are placed; then curbs and railings are installed. Once the bridge superstructure is completed, the substructure back-walls can be placed and the approach can be backfilled. The last step is the wearing surface application. The entire construction process for a bridge 60 ft long can be completed in 60 hours or less (Ritter, 1990). The construction time for prefabricated timber bridges is expected to be significantly less than that for timber bridges built onsite.

6 EXPERIMENTAL FINDINGS

Full-scale experiments were conducted in this study to evaluate the structural performance of the selected bridge systems: (1) precast full-depth deck panel supported on inverted precast prestressed tee girders bridge, (2) glulam timber girder bridge, and (3) glulam timber slab bridge. This chapter covers design, fabrication, test setup, instrumentation, test procedures, and test results for the three test specimens.

6.1 Precast Full-Depth Deck Panel Bridge Specimen

The structural performance of a full-scale bridge specimen incorporating precast full-depth deck panels supported on inverted tee girders was experimentally evaluated under fatigue and ultimate loading. A summary of the experimental program and findings are presented. An in-depth discussion can be found in Attachment A.

6.1.1 Precast Bridge Test Specimen

6.1.1.1 Design of Precast Bridge Test Specimen

A full-scale 50-ft long by 34.5-ft wide prototype bridge was selected for experimental studies. The bridge was designed for HL-93 loading according to AASHTO (2013), which includes both the design truck or tandem load and the design lane load. Because of test setup limitations, only a 10-ft width of the prototype bridge could be tested in the Lohr Structures Laboratory at South Dakota State University (SDSU). Therefore, two interior girders of the prototype bridge were selected for further investigation. The full-scale bridge test specimen consisted of five precast full-depth deck panels with a 9.5-ft total width (in the bridge transverse direction) and a 10-ft length (in the bridge longitudinal direction) and two prestressed precast inverted tee girders 50 ft long spaced 4.67 ft on center.

The main objective of the laboratory tests was to assess the bridge system performance under fatigue and strength loading. A summary of the design and detailing of the girders and the panels are presented.

6.1.1.1.1 Inverted Tee Girders

PS Beam (Ericksson Technologies, 2011) software was used to design the prestressed inverted tee girders according to AASHTO (2013). A total of 20 Grade 270 low relaxation prestressing strands with a diameter of 0.6 in. were used in the inverted tee girders to meet the design requirements (Figure 6.1). Two of the strands were harped to avoid concrete cracking at the girder ends. The girders were transversely reinforced with ASTM A615 Grade 60 No. 4 bars at a spacing varying from 6 to 18 in.

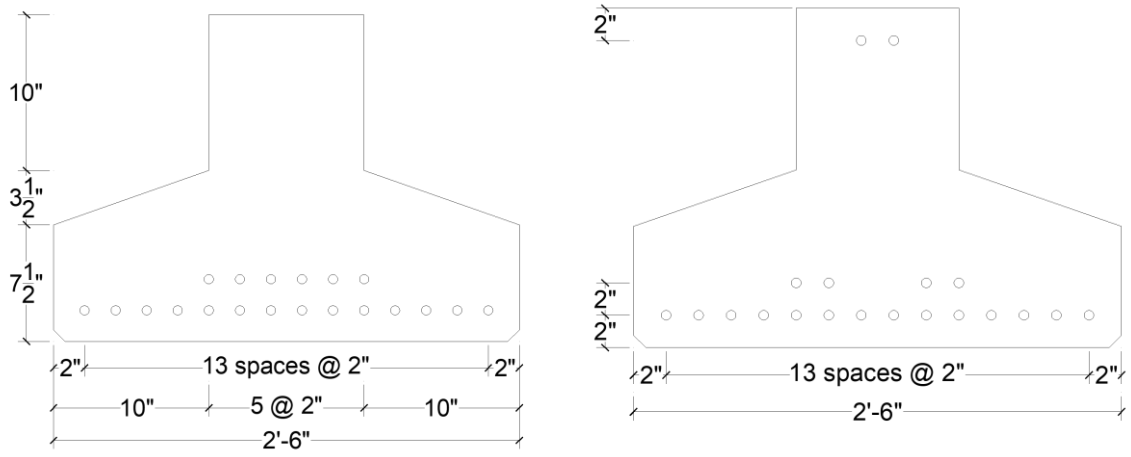

(a) Mid-span Section (b) Girder End Section

Figure 6.1: Inverted Tee Girder Cross Section with Two Harped Strands

6.1.1.1.2 Full-Depth Deck Panels for Precast Bridge

The full-depth deck panel top and bottom reinforcement in the transverse direction of the bridge was designed using table A4-1 in AASHTO (2013), which provides maximum live load moments per unit width for both positive and negative transverse deck moments. The tabulated values are based on the equivalent strip method. The deck longitudinal reinforcement was designed to accommodate creep and shrinkage requirements and to allow splicing of reinforcement at transverse joints to provide adequate shear and moment transfer between the transverse joints. The deck longitudinal steel was placed in one layer 4.25 in. below the deck surface to allow for splicing of the steel at the transverse joints.

6.1.1.1.3 Shear Pockets for Precast Bridge

The precast girders and panels were connected using shear studs extending from the girder web into the panel shear pockets to make the deck-girder system composite. The deck system was composite since horizontal shear stresses were transferred through the bond in the haunch region as well as the shear studs when the grout was cured.

Two types of shear pockets were incorporated in the test bridge: (1) full-depth pocket in which the full-depth of the deck was open (Figure 6.2), and (2) hidden pocket in which the large portion of the pocket was covered with 3 in. of concrete (Figure 6.3). Grout can be poured from the top of the pockets into the full-depth pocket or through pipes in the hidden pocket. Figure 6.4 shows the location of the two pocket types in the bridge test model.

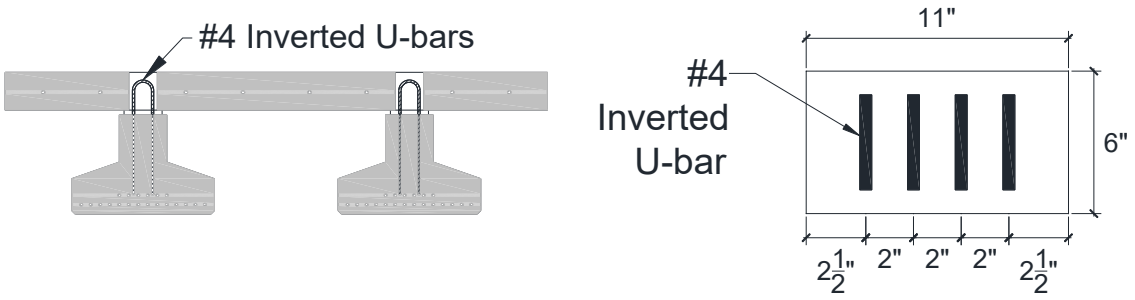

(a) Test Girder Cross Section

(b) Full-depth Pocket Plan View

Figure 6.2: No. 4 Inverted U-Shape Bars in Full-Depth Shear Pockets

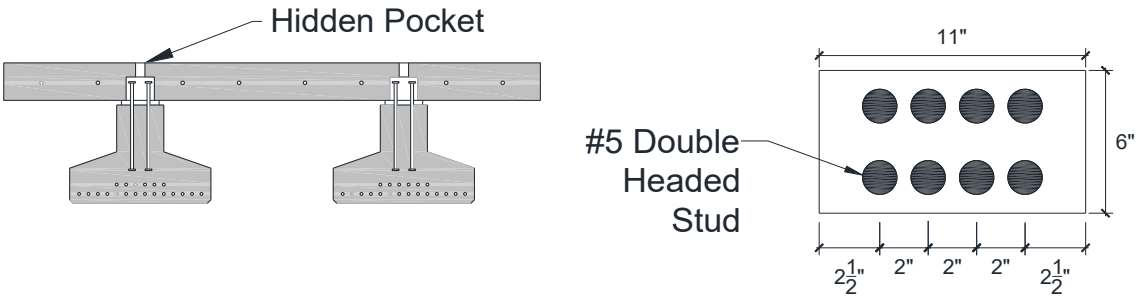

(b) Hidden Pocket Plan View

(a) Test Girder Cross Section

Figure 6.3: No. 5 Double Headed Studs in Hidden Shear Pockets

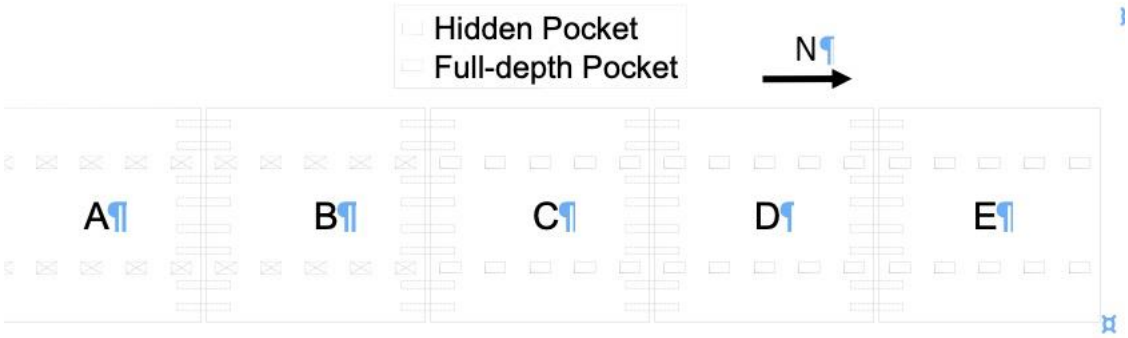

Figure 6.4: Test Bridge Shear Pocket Locations

6.1.1.1.4 Horizontal Shear Studs for Precast Bridge

Two types of horizontal shear studs were incorporated in this study: (1) inverted U-shape bars in the full-depth pockets (Figure 6.2), and (2) double headed studs in the hidden pockets (Figure 6.3). ASTM A615 Grade 60 No. 4 bars were used to form the inverted U-shape studs. Each full-depth pocket

contained eight legs of No. 4 inverted U-shape bars and was spaced 2 ft on center. The double headed studs were made of ASTM A615 Grade 60 No. 5 bars. Eight double headed studs were used in the hidden pockets, and the pockets were spaced 2 ft on center. Horizontal shear studs were designed based on AASHTO (2013) standards.

6.1.1.1.5 Transverse Joint for Precast Bridge

The Full-Depth Deck Panel (FDDP) transverse joints consisted of (1) groove-to-groove grouted shear keys (Figure 6.5) in the transverse direction of the bridge and (2) dowel bars in the bridge longitudinal direction to be embedded in hollow structural steel (HSS) members (Figure 6.6). The gap between the two adjacent precast deck slabs in the bridge longitudinal direction is usually 1 in. to 1.5 in. for a typical FDDP transverse joint. However, a transverse joint 2.75 in. wide was used to allow a transverse steel bar to be placed in the joint to meet maximum rebar spacing requirements of 18 in. and to allow 1 in. of clear cover from the face of the joint. Two No. 5 bars were placed beneath HSS sections to meet creep and shrinkage requirements (Figure 6.6c).

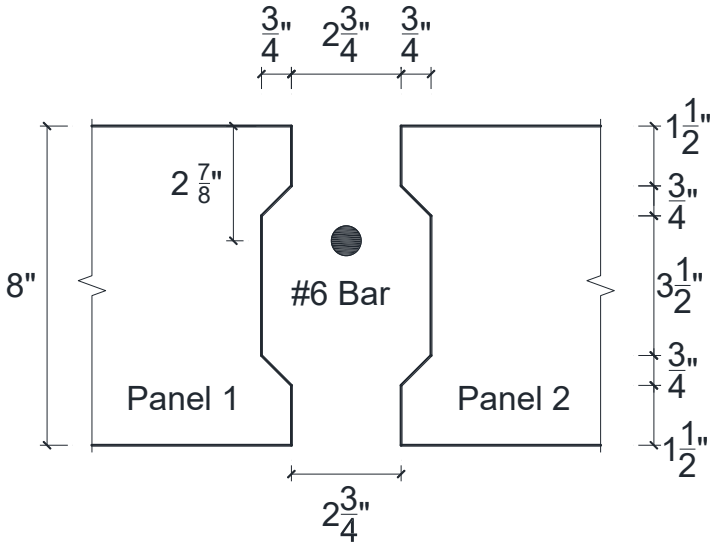

Figure 6.5: Groove-to-groove Transverse Deck-to-Deck Joint Detailing

The deck longitudinal reinforcing bars were spliced using 25.75-in long No. 6 ASTM A615 Grade 60 dowels, which were inserted into HSS from the top of the deck after the panels were placed. ASTM A500 Grade B steel was used to form HSS. The HSS increased the confinement resulting in a shorter lap-splice for dowels.

Two types of failure were assumed for the proposed transverse joint: bearing and vertical shear. Modified shear friction theory was used to check the strength of the transverse joints with the longitudinal dowels (Badie and Tadros, 2008).

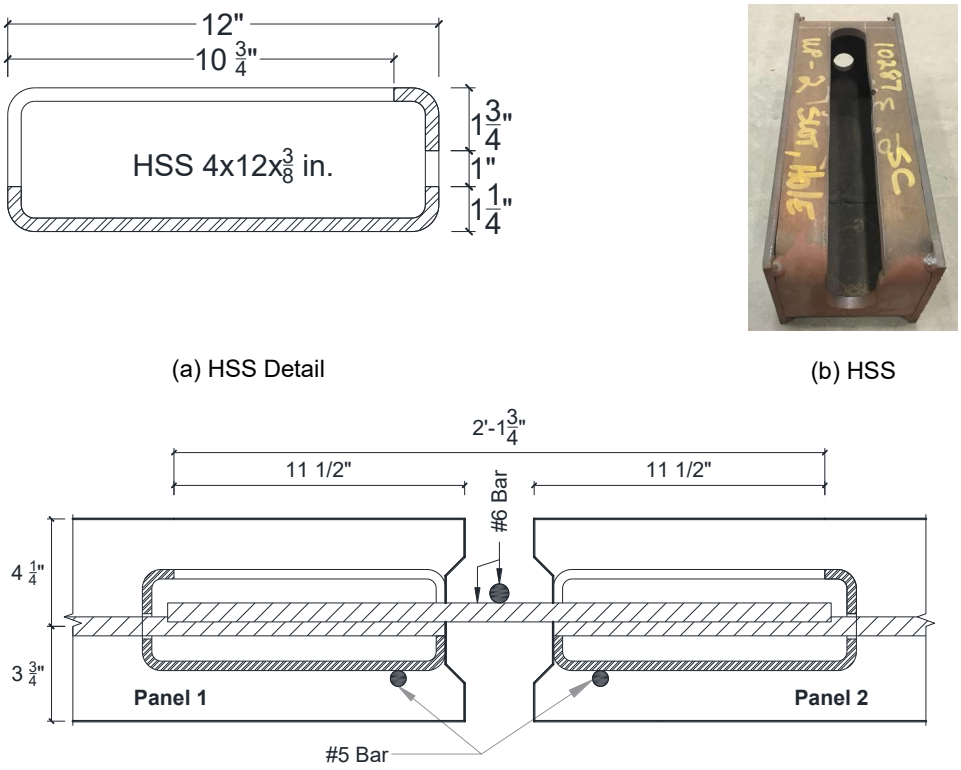

(a) HSS Detail

(b) HSS

(c) Transverse Joint Reinforcement

Figure 6.6: Transverse Joint Reinforcement for Full-Depth Precast Panels

6.1.1.2 Fabrication and Assembly of Precast Bridge Test Specimen

The girders and panels for the test bridge specimen were fabricated at Gage Brothers Concrete Products in Sioux Falls, SD. This section includes the fabrication of bridge members and construction stages for the bridge test specimen.

6.1.1.2.1 Inverted Tee Girders

The inverted tee girders were prepared and cast on a single bed (Figure 6.7). Low relaxation Grade 270 prestressing strands were initially tensioned to 10,000 lbs to eliminate slack and to straighten tendons for instrumentation. Then, the girder shear reinforcement and shear studs were installed. Strain gauge data from strands were obtained before tensioning. Finally, each strand was tensioned to 44,000 lbs, equivalent to 75% of the ultimate stress. Strain gauge readings were also taken during jacking.

The girders were cast in two consecutive days. The one-day concrete compressive strengths of the first and the second girders were 6,820 and 6,190 psi, respectively. Since the specified concrete strength at the time of tendon release was 6,000 psi, the strands were concurrently cut one-day after casting. Strains were also measured during the tendon release.

(a) Placement of Bars and Prestressing Strands

(b) Formwork Removal

Figure 6.7: Fabrication of Inverted Tee Girders

The test girders were shipped to the Lohr Structures Laboratory at SDSU after releasing the tendons. The girders were unloaded using a 15-ton overhead crane and placed on concrete reaction blocks (Figure 6.8).

(a) Girder Unloading

(b) Girder Placement on Abutments

Figure 6.8: Unloading and Positioning of Test Girders

6.1.1.2.2 Full-Depth Deck Panels

Five precast panels were fabricated in an indoor construction site

(

(a) Panel Formwork

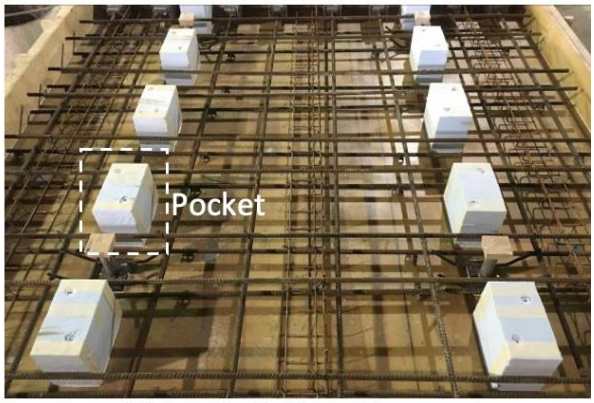

(b) Full-Depth Pocket Formwork

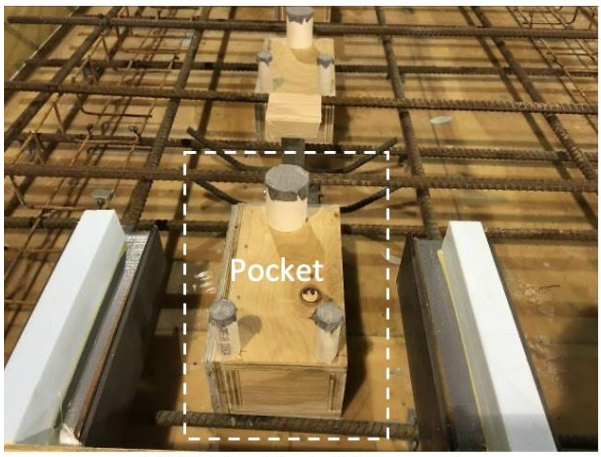

(c) Hidden Pocket Formwork

(d) Leveling Bolt

Figure 6.9). Three interior panels were 9.5 ft wide in the transverse direction of the bridge and 9.77 ft long in the longitudinal direction. Two exterior panels had the same width, but were 9.89 ft long.

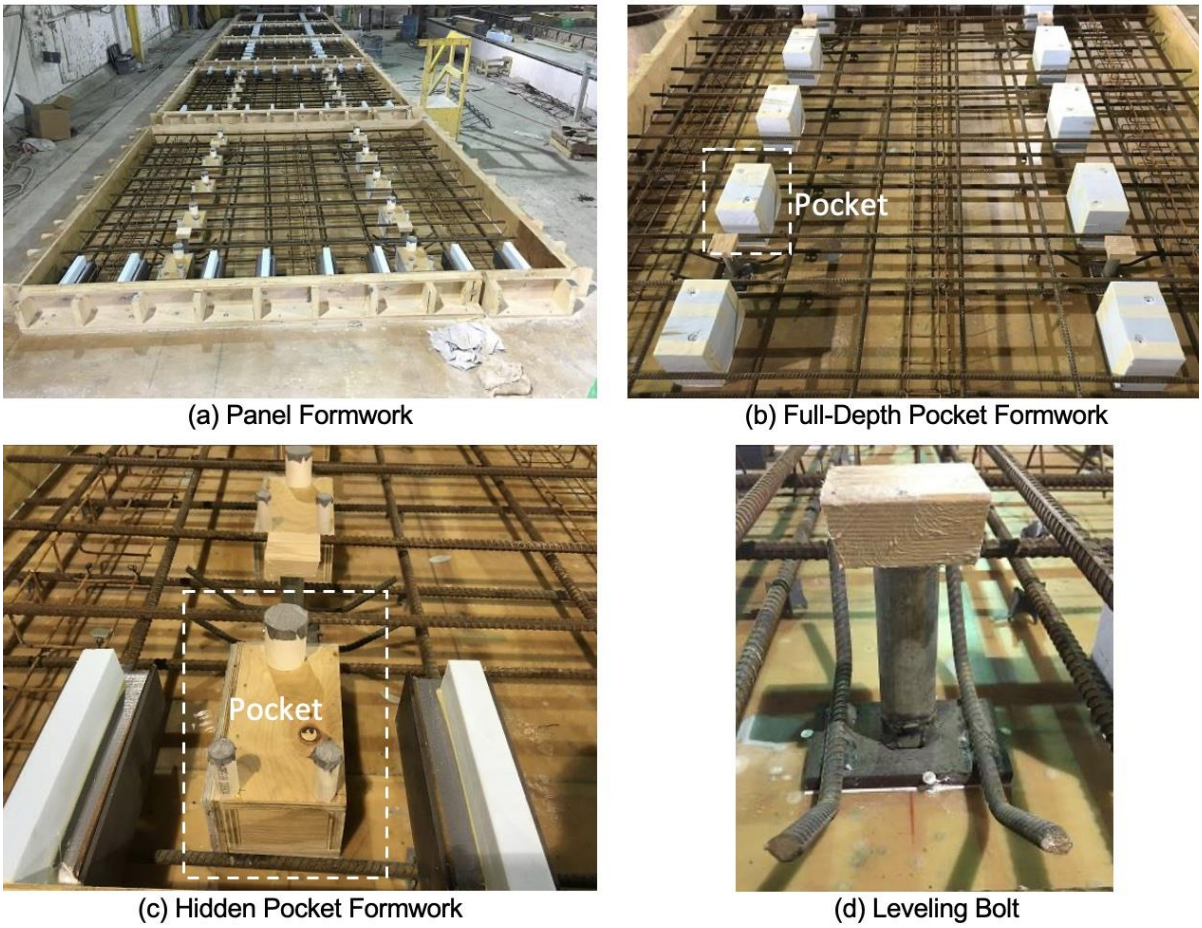

(a) Panel Formwork (b) Full-Depth Pocket Formwork

(c) Hidden Pocket Formwork (d) Leveling Bolt

Figure 6.9: Fabrication of Full-depth Deck Panels

Each of the five panels contained 10 pockets. Three panels (C, D, and E in Figure 6.4) had full-depth pockets (Figure 6.2) while the remaining two panels (A and B) had hidden pockets (Figure 6.3). The full-depth pocket forms were constructed using cut-out hardboard insulation in stacked layers

(

(a) Panel Formwork

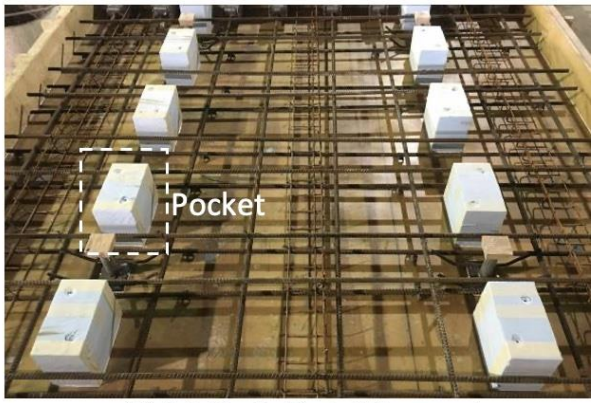

(b) Full-Depth Pocket Formwork

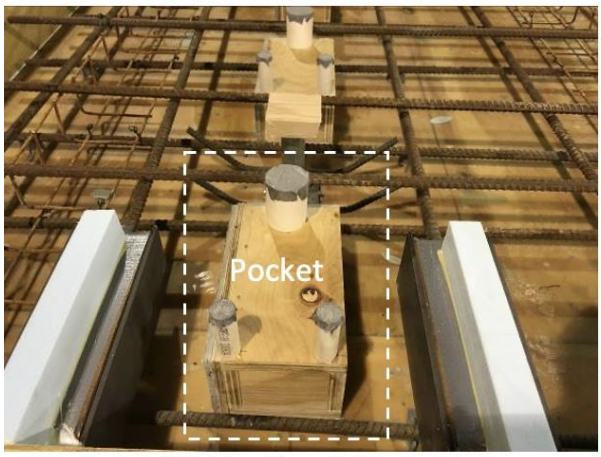

(c) Hidden Pocket Formwork

(d) Leveling Bolt

Figure 6.9b). The hidden pocket forms were constructed using plywood for the pockets (

(a) Panel Formwork

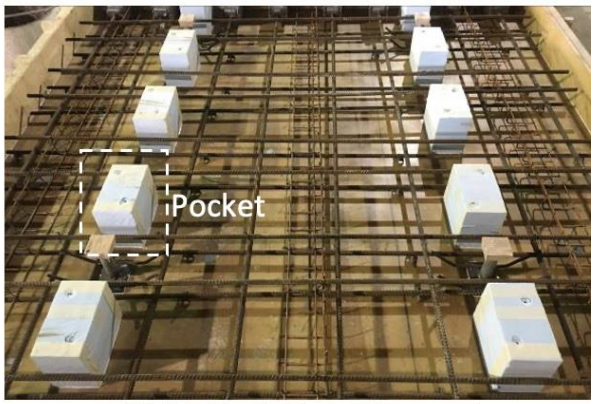

(b) Full-Depth Pocket Formwork

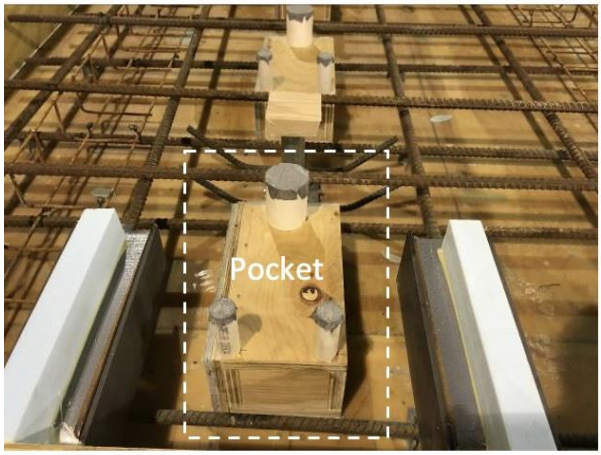

(c) Hidden Pocket Formwork

(d) Leveling Bolt

Figure 6.9c). The PVC pipes were installed to form the grouting vents. Four leveling bolts were placed in each panel

(

(a) Panel Formwork

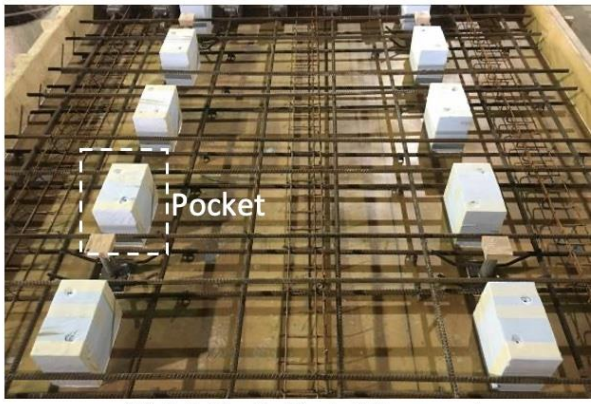

(b) Full-Depth Pocket Formwork

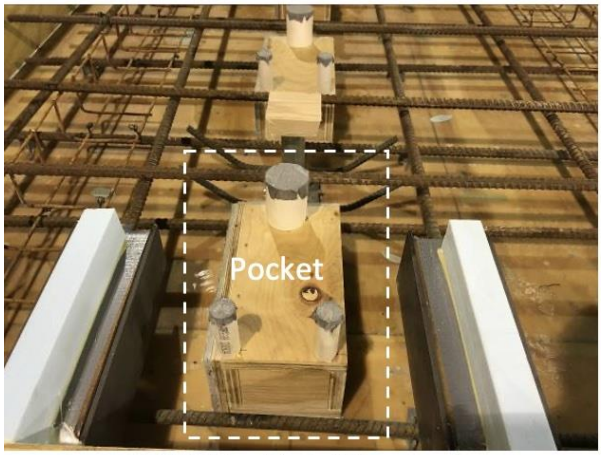

(c) Hidden Pocket Formwork

(d) Leveling Bolt

Figure 6.9d). Leveling bolt forms consisted of a nut tack-welded to a vertical steel pipe, and a 2 in. by 4-in. lumber piece to form a blockout at the top of the steel pipe.

The full-depth deck panels were shipped to the Lohr Structures Laboratory and unloaded using a 15-ton overhead crane. The pockets, joints, and embedded hollow structural steel members were cleaned to avoid any bonding issues. Petroleum jelly was applied to the leveling bolt shaft at the bottom end to allow bolt removal after pouring the grout in the haunch. Next, the panels were placed (Figure 6.10) starting from one end of the bridge specimen (the south end) toward the other end (the north end). Then, the leveling bolts were adjusted with a wrench to level the deck panels. The target grouted haunch depth was 1 in. at the mid-span, which was achieved using the leveling bolts.

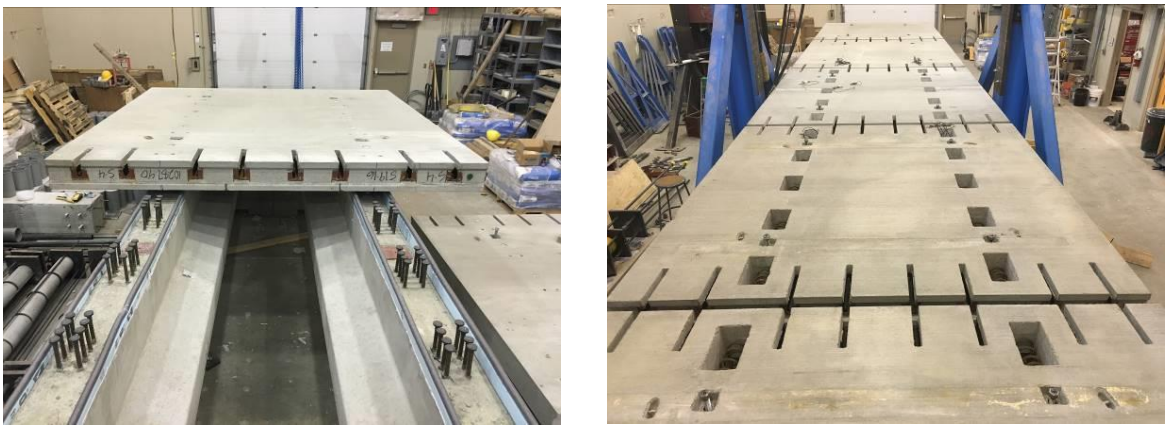

Figure 6.10: Installation for Full-depth Deck Panels on Precast Girders

Plywood was attached at the bottom of the transverse joints using tie wires (Figure 6.11) tied to the transverse joint reinforcement. The plywood and tie wires were installed from the top of the bridge. Silicone was applied around the concrete-plywood edges from the top of the bridge to create water-tight joints. A No. 6 bar was placed and centered on the spliced bars of each transverse joint.

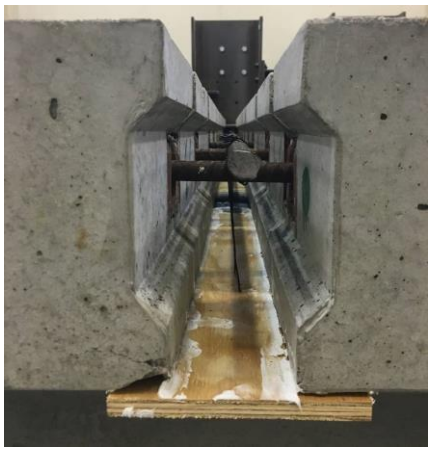

Figure 6.11: Transverse Joint Formwork

Figure 6.12 Grout Haunch Region Formwork

The grouted haunch dam was formed using ¾-in. plywood and 2 in. by 4-in. nominal dimension lumber (Figure 6.12), which was used as a strut to hold the plywood in place. For the exterior of the girders, longitudinal lumber was clamped to the deck and used as a reaction block for the transverse struts.

Two types of filler materials were incorporated into the grouted haunch, shear pockets, and transverse joints: conventional non-shrink grout and latex modified concrete (LMC). As was discussed before, two types of pockets were used in the test specimen: (1) hidden and (2) open (full-depth). Since durability of the open pockets was a concern, LMC was proposed as an alternative filler material for this type of pocket because the durability of LMC is better than conventional grout (Wenzlick, 2006; BASF, 2011; Baer, 2013). Half of the open pockets were filled with LMC and the remaining pockets were cast with conventional grout as shown in Figure 6.13. Figure 6.14shows the grout pour in the hidden and open pockets.

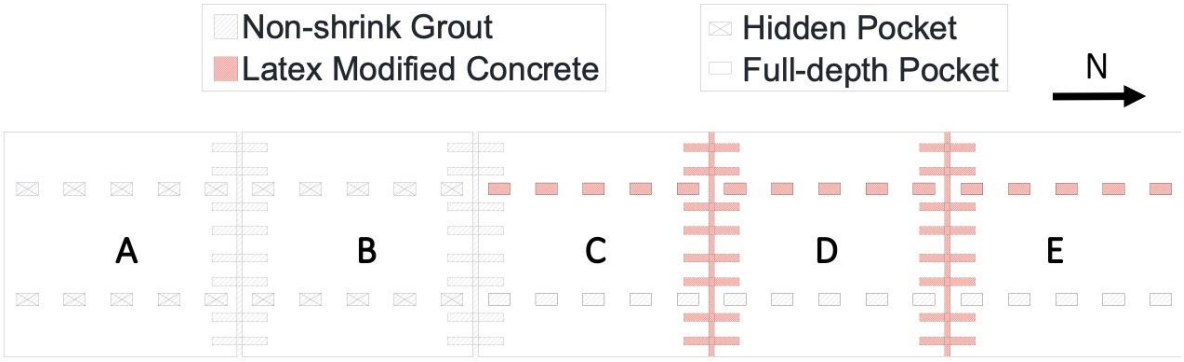

Figure 6.13: Filler Materials and Shear Pocket Locations

(a) Pouring in Hidden Pockets (b) Pouring in Open Pockets

Figure 6.14: Filling Shear Pockets, Haunch Region, and Transverse Joints

6.1.1.3 Precast Bridge Test Setup

The test bridge was placed in a vertical loading frame so that a 146-kip hydraulic actuator was at the centerline of the bridge at the mid-span. The girders were supported on concrete reaction blocks. A 6-in by 6-in elastomeric bearing pad was placed between each girder and the reaction block. The effective span length of the test bridge was 49.13 ft. Water ponds were formed on the top of the pockets and joints to investigate the integrity of the precast joint detailing during fatigue testing.

Fatigue testing was performed in two phases: (1) Phase I, in which the bridge overall performance was investigated, and (2) Phase II, in which the performance of the transverse joint was emphasized. In Phase I, a single point load was applied at the centerline of the bridge at the mid-span using a 146-kip actuator (Figure 6.15a). The load was applied to a 10-in. by 20-in. steel plate to simulate AASHTO (2013) design truck tire bearing area. A 0.5-in. thick layer of plaster was poured beneath the steel plate to ensure a level and uniform bearing surface.

(a) Single Point Load in Phase I (b) Two-Point Loads in Phase II

Figure 6.15: Test Setup for the Precast Bridge Specimen

An 8-ft long W12x93 steel spreader beam was used in Phase II to spread the load directly to the transverse joints and to maximize the shear transfer from panel to panel (Figure 6.15b). Two 10 in. by 20 in. steel plates were positioned at the ends of the spreader beam and were leveled. The center-to-center distance between the two loading plates was 7.5 ft.

After the completion of the fatigue testing, an ultimate test was conducted using a 328-kip actuator. A W12x93 steel beam was used to spread the load over the two girder centerlines at the mid-span to avoid punching shear failure of the deck. Figure 6.16 shows the test setup for the strength test.

Figure 6.16: Ultimate Test Setup for the Precast Bridge Specimen

6.1.1.4 Instrumentation Plan for the Precast Bridge Specimen

The test bridge was heavily instrumented with axial strain gauges, shear strain gauges, linear variable differential transducers (LVDTs), and load cells. The instrumentation plan is briefly discussed.

6.1.1.4.1 Strain Gauges Used in the Precast Bridge

Three types of strain gauges were used on different materials: (1) surface-mounted axial strain gauges were used to measure axial strains in mild and prestressing reinforcement; (2) surface-mounted shear strain gauges were used to capture shear strain data on mild steel bars; and (3) embedded concrete strain gauges were used to measure the concrete strain.

Figure 6.17 shows the bridge strain gauge plan at the mid-span. Five axial strain gauges were mounted to the top surface of the deck longitudinal mild steel bars. Two axial strain gauges were installed on the prestressing tendons at the bottom layer of each girder. One embedded concrete strain gauge per girder was installed slightly above the composite bridge section neutral axis. A total of nine axial strain gauges and two embedded concrete strain gauges were used at the mid-span.

Strain gauges were installed on the studs in four of the shear pockets. Two were hidden pockets with No. 5 double-headed studs and filled with non-shrink grout, and the other two were full-depth pockets with No. 4 inverted U-shape bars (one filled with non-shrink grout and the other with latex modified concrete). Eight studs/legs were extended into each pocket to resist horizontal shear. Two axial strain gauges were mounted to the pocket corner studs in a diagonal pattern and two shear strain gauges were mounted on the opposite two diagonal studs. The combination of one axial and two shear strain gauges enabled the measurement of strains in three different directions. Thus, principal strains and stresses of shear studs could be measured.

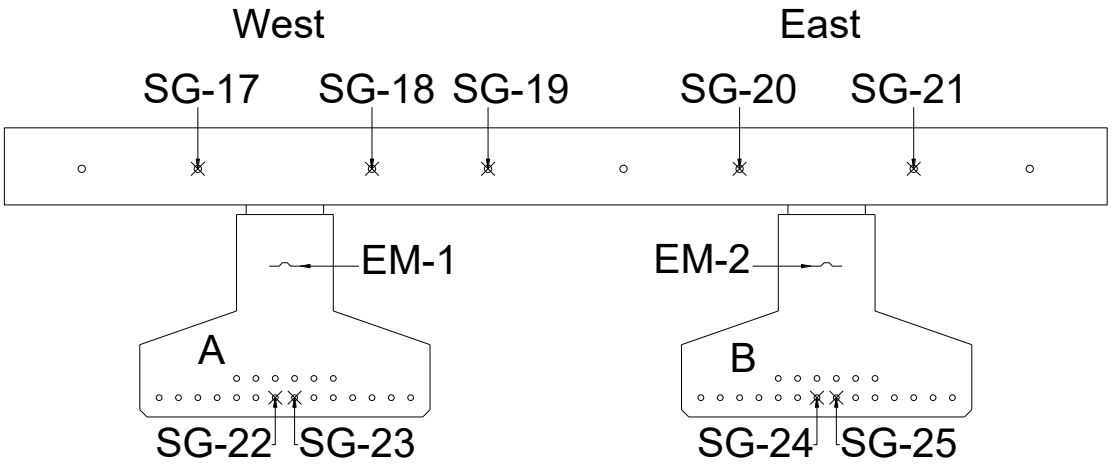

Figure 6.17: Strain Gauge Configuration at Mid-span of the Precast Bridge Specimen

6.1.1.4.2 Linear Variable Differential Transformers Used for the Precast Bridge Specimen

Thirteen linear variable differential transformers (LVDTs) were attached to the test specimen to measure deflections and rotations in various directions (Figure 6.18).

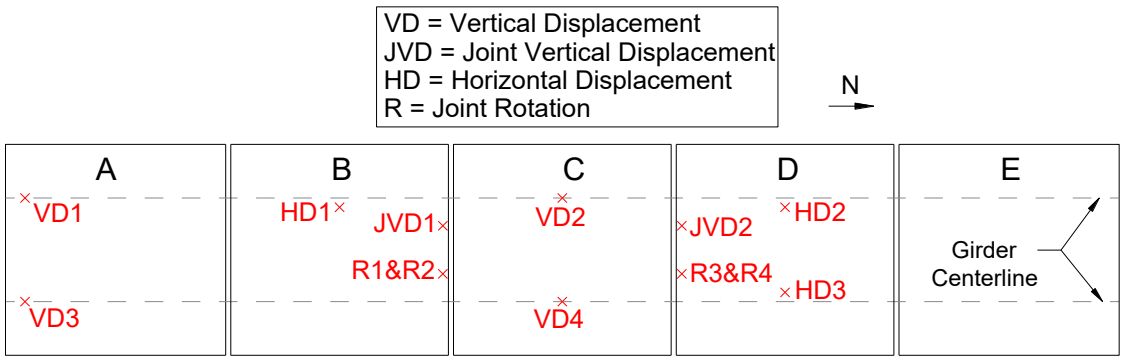

Figure 6.18: LVDT Installation Plan for the Precast Bridge Specimen

Vertical deflections were measured both at the mid-span of the bridge as well as the girder ends using LVDTs. The difference between the girder mid-span and the girder end displacements was reported as actual (net) girder deflections to account for compression of the elastomeric bearing pads.

Deck-to-girder slippage was measured using horizontal LVDTs mounted to the top of the girder. They were mounted at three locations to observe the performance of: (1) full-depth pockets with latex modified concrete and No. 4 inverted U-shape bars, (2) full-depth pockets with non-shrink grout and No. 4 inverted U-shape bars, and (3) hidden pockets with non-shrink grout and No. 5 double headed studs. Each HD LVDT was installed 15 ft away from the mid-span.

Joint rotations were also measured with LVDTs mounted adjacent to the two transverse joints of the middle panel. Each joint had an LVDT mounted horizontally in the longitudinal direction of the bridge on the top and bottom of the deck at the same section. The LVDTs were offset 13 in. from the longitudinal centerline of the bridge to allow ponding of the joint.

The relative vertical deflection across the two transverse joints of the middle panel was measured with a single vertical LVDT mounted adjacent to each joint. Similar to the previous measurement, these LVDTs were offset 13 in. from the longitudinal centerline of the bridge to allow ponding of the joint.

6.1.1.4.3 Load Cells Used in the Precast Bridge Specimen

Four load cells were placed under the south end of the girders to measure support reactions. Two load cells were used per girder, offset 6.25 in. from the girder centerline to enhance overall stability and 6 in. from the girder end to provide sufficient seat length. Steel plates with a dimension of 6 in. by 6 in. by 1 in. were placed at the top and the bottom of the load cells to create a level bearing surface. Elastomeric bearing pads were placed on top of the steel plates to allow the girders to freely rotate.

6.1.1.4.4 Data Acquisition System

A 128-channel data acquisition device was used, which could record between 10 and 2,048 readings per second. Stiffness and ultimate tests were scanned at a rate of 10 readings per second. For the fatigue testing, cyclic data was recorded at a scan rate of 100 points per second for 30 load cycles at the beginning and the end of each fatigue test.

6.1.1.5 Test Procedure for the Precast Bridge Specimen

The full-scale bridge was tested under fatigue, stiffness, and ultimate loading. Fatigue testing was performed by applying cyclic loads either at the mid-span (phase I) or close to the transverse joints (phase II). Stiffness tests, which consisted of applying a monotonic point load or loads, were performed at intervals of 50,000 cycles to determine the effect of fatigue on the bridge performance and to measure the bridge overall stiffness. The ultimate test was carried out by applying point loads to the girders at the mid-span with a monotonic loading protocol.

6.1.1.5.1 Fatigue Testing of the Precast Bridge Specimen

For Phase I, a 27.7-kip point load was applied at the center of the bridge at the mid-span at a loading rate of 1 cycle per second. The actuator was controlled by force to ensure that the cyclic load magnitude remained the same even if the bridge stiffness degraded. The magnitude of the point load was calculated according to AASHTO (2013) Fatigue II limit state load combination.

Since the proposed bridge will be used on local roads in South Dakota, the average daily traffic (ADT) was assumed to be 100 vehicles per day with a 15% truck density (ADTT=15). Therefore, 410,625 trucks would cross the bridge over a 75-year design life. The test bridge was subjected to 500,000 load cycles to account for the possibility of increased truck traffic.

After the completion of the Phase I loading, fatigue testing was continued with two point loads adjacent to the transverse joints. The distance between the two point loads was 7.5 ft. on center. The same load magnitude as that of Phase I was applied to the beam resulting in a 13.9-kip load at each end of the spreader beam. The load magnitude was determined by matching the girder shear demand in the test girder from the Phase I loading. The test was terminated at 150,000 cycles since no stiffness degradation was observed.

6.1.1.5.2 Stiffness Testing of the Precast Bridge Specimen

Stiffness tests were performed at the beginning of the testing and then at every 50,000 load cycle increment thereafter. The stiffness load magnitude was 55.4 kips, which was applied monotonically using a displacement-control loading protocol. The load was calculated according to the AASHTO (2013) Fatigue I limit state. Displacements were applied with an interval of 0.01 in. with a speed of 0.007 in/sec.

6.1.1.5.3 Strength Testing of Precast Bridge

A point load at the mid-span of the bridge was monotonically applied to a beam placed in the transverse direction of the bridge to spread the load to the two girders. The girders were loaded under a displacement-control loading protocol, in which displacements were applied with an increment of 0.02 in. and a rate of 0.007 in/sec.

6.1.2 Material Properties of the Precast Bridge Specimen

Different materials were incorporated in different bridge components. In this section the following mix design and mechanical properties are presented: (1) concrete used in the deck, (2) concrete used in the girders, (3) conventional non-shrink grout used in the joints, (4) latex modified concrete used in

the joints, (5) deck mild steel, (6) inverted U-shape shear studs, (7) double headed shear studs, and (8) prestressing strands used in the girders are presented in this section.

6.1.2.1 Properties of Concrete Used in the Precast Bridge Specimen

The design concrete compressive strength at 28 days was 6,000 psi and 8,000 psi for the full-depth deck panels and the prestressed inverted tee girders, respectively. The properties of the fresh concrete used in the full-depth deck panels and inverted tee girders were measured in accordance with ASTM C143 and C231 standards (2010).

Standard 6-in. by 12-in. cylinders were used for concrete sampling. The cylinders were first placed next to the deck panels and girders for 24 hours. Molded girder samples were stored in the Lohr Structures Laboratory while deck concrete samples were unmolded and placed in a moist cure room. Note that both methods are acceptable by the ASTM standard. Compressive strength tests were performed in accordance with ASTM C39 standard (2010).

6.1.2.2 Properties of Grout Used in the Precast Bridge Specimen

Fifteen standard 2-in.by 2-in. cube samples were collected for each mix of conventional non-shrink grout and LMC, which were used as filler materials in different precast joints. The non-shrink grout had a 28-day strength of approximately 9 ksi and the latex modified concrete had a 28-day strength of approximately 7.5 ksi. Detailed measured material properties can be found in Mingo (2016).

6.1.2.3 Properties of Prestressing Strands Used in the Precast Bridge Specimen

Low-relaxation Grade 270 prestressing strands with a diameter of 0.6 in. were used in this project. The mechanical properties of the strands are summarized in Table 6.1.

Table 6.1: Mechanical Properties of Prestressing Strands Used in the Precast Bridge Specimen

Cross-Sectional Area ($in.^2$)	Modulus of Elasticity (ksi)	Yield Stress (ksi)	Ultimate Stress (ksi)
0.22	29,000	254.4 at 1% extension	287.8 at 7.4% extension

6.1.2.4 Properties of Horizontal Shear Studs Used in Precast Bridge

Dog-bone samples were prepared for the tensile testing of reinforcement used as horizontal shear studs in accordance with ASTM 370. This section includes a summary of the measured data.

6.1.2.4.1 Inverted U-Shape Bars Used in Precast Bridge

No. 4 inverted U-shape bars that extended from the girder top into the full-depth shear pockets were made of ASTM A615 Grade 60 reinforcing steel bars. Table 6.2 presents the measured mechanical properties for the inverted U-shape bars.

Table 6.2: Mechanical Properties of Inverted U-Shape Bar Used in Precast Bridge

Bar Size	ASTM Type	Yield Strength, f_y (ksi)	Ultimate Strength, f_u (ksi)	Strain at Peak Stress (%)	Strain at Fracture (%)
No. 4	A615 Grade 60	74.9	113.6	7.0	13.4

Note: Measured data were based on the average of two tensile tests.

6.1.2.4.2 Double Headed Studs Used in Precast Bridge

No. 5 ASTM A706 Grade 60 double headed reinforcing steel bars were used in the hidden shear pockets as shear studs. Table 6.3 presents the mechanical properties of the double headed stud according to the mill certificate provided by the manufacturer.

Table 6.3: Mechanical Properties of Double Headed Stud Used in Precast Bridge

Cross-Sectional Area (in.^{2})	Yield Stress (ksi)	Ultimate Stress (ksi)	Strain at Fracture (%)
0.31	69.9	90.7	17

6.1.2.5 Properties of Reinforcement in Panels and Joints Used in Precast Bridge

Tensile tests were performed on dog-bone samples of steel bars used in the test bridge transverse joints and deck panels. A summary of the test data is presented in Table 6.4 and Table 6.5.

Table 6.4: Mechanical Properties of Transverse Joint Reinforcement Used in Precast Bridge

Bar Size	ASTM Type	Yield Strength, f_y (ksi)	Ultimate Strength, f_u (ksi)	Strain at Peak Stress (%)	Strain at Fracture (%)
No. 6	A615 Grade 60	71.5	112.5	7.4	14.8

Note: Measured data were based on the average of two tensile tests.

Table 6.5: Mechanical Properties of Deck Reinforcement Used in Precast Bridge

Bar Size	ASTM Type	Yield Strength, f_y (ksi)	Ultimate Strength, f_u (ksi)	Strain at Peak Stress (%)	Strain at Fracture (%)
No. 6	A615 Grade 60	63.4	107.3	7.2	14.9

Note: Measured data were based on the average of two tensile tests.

6.1.2.6 Properties of Elastomeric Neoprene Bearing Pads Used in Precast Bridge

A 6-in. by 6-in. by ⅜-in. elastomeric neoprene pad was tested in a compression machine to determine the force-deformation relationship of the bearing pads used at the supports. The stiffness of the linear portion of the force-displacement relationship was 1,128 kip/in.

6.1.3 Test Results for Precast Bridge

As mentioned, the precast bridge specimen was first tested under 500,000 cycles of the Fatigue II loading using a point load applied at the mid-span. Then, it was subjected to 150,000 cycles using two point loads applied adjacent to the middle panel (Panel C) transverse joints. Finally, it was loaded monotonically to failure.

6.1.3.1 Phase I – Fatigue II Loading of Precast Bridge

A summary of the Phase I testing results for the precast prestressed bridge including observed damage, stiffness degradation, and joint rotation and slippage is presented in this section.

6.1.3.1.1 Observed Damage

At 25,000 load cycles, which corresponds to 4.6 years of service, a vertical hairline crack was observed on the grouted haunch of Girder A located approximate 4.2 ft south of the mid-span in one of the LMC

joints. One of the water ponds was on the top of this joint. Since (1) the crack width did not change over the entire fatigue test (Figure 6.19), (2) the pond did not lose water from this leak, and (3) this joint was the last joint filled with LMC (LMC sets in approximately 30 min.), it was concluded that the leak was because of construction issues but not structural degradation due to fatigue. Furthermore, there was no change in bridge overall stiffness due to this crack.

(a) Observed Crack at 25,000-Load Cycle

(b) Close Up of Crack

(c) Pocket and Water Pond from Bridge Top

(d) Crack Condition after 650,000 Load Cycle

Figure 6.19: Observed Damage in LMC Full-Depth Pocket of Girder A

At 125,000 load cycles, which corresponds to 22.8 years of service, vertical hairline cracks were observed along the length of the grouted haunch of both girders approximately evenly spaced between 2 in. to 4 in. (Figure 6.20). Both the conventional non-shrink grout and the latex modified concrete exhibited vertical hairline cracking in the haunch area. Since the haunch region was in compression, it was concluded that these cracks were mainly shrinkage not flexural. Most likely, the fatigue loads made these shrinkage cracks wider and visible at this load cycle.

(a) Shrinkage Cracks in Haunch Region of Girder A Filled with Latex Modified Concrete

(b) Close Up of Girder A Haunch Region Filled with Latex Modified Concrete

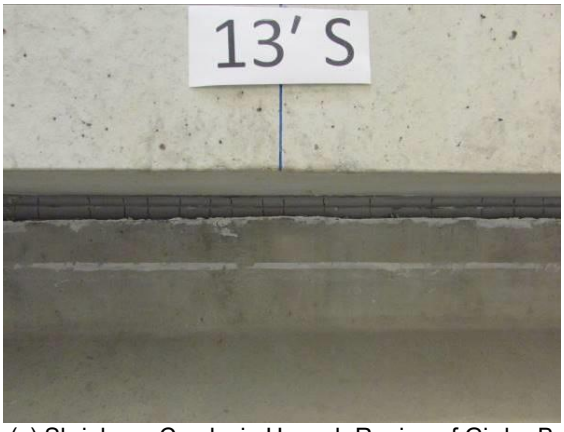

(c) Shrinkage Cracks in Haunch Region of Girder B Filled with Non-Shrink Grout

(d) Close Up of Girder B Haunch Region Filled with Non-Shrink Grout

Figure 6.20: Haunch Region Shrinkage Cracks at 125,000 Load Cycle

Also, hairline shallow cracks were observed in all transverse joints (Figure 6.21) and most shear pockets (Figure 6.22). Since (1) water did not leak through these cracks, (2) the crack width did not increase over time, and (3) there was no change in the bridge overall stiffness, it was concluded that these hairline cracks were caused by shrinkage, not fatigue loading.

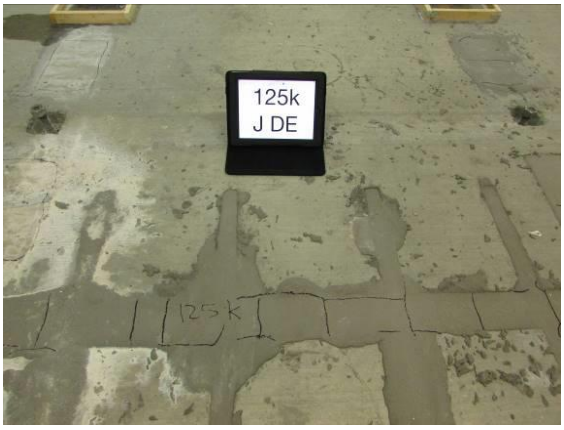

(a) Latex Modified Concrete at 125,000 Cycle

(b) Latex Modified Concrete at 650,000 Cycle

Figure 6.21: Transverse Joint Cracks in the Precast Bridge Specimen

(a) Non-Shrink Grout at 125,000 Cycle

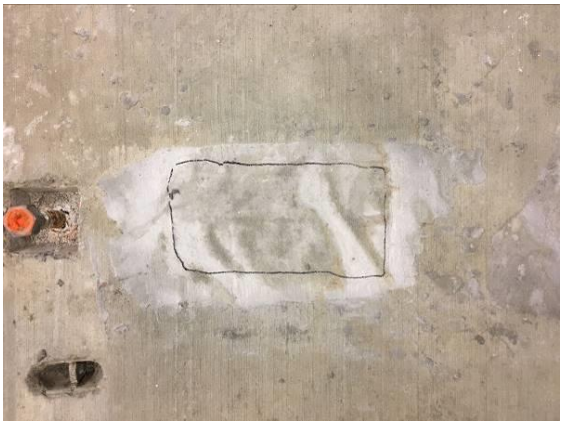

(b) Non-Shrink Grout at 650,000 Cycle

(c) Latex Modified Concrete at 125,000 Cycle

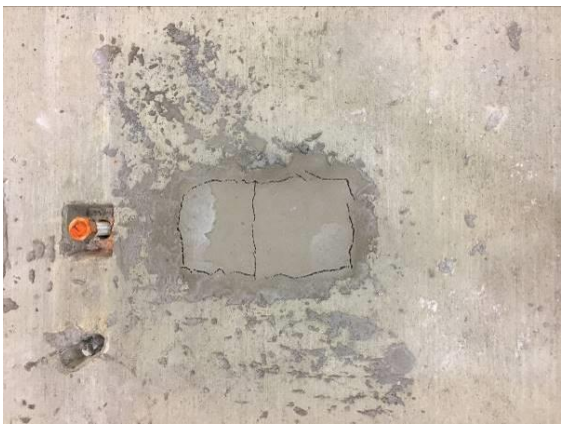

(d) Latex Modified Concrete at 650,000 Cycle

Figure 6.22: Full-Depth Shear Pocket Cracks in the Precast Bridge Specimen

6.1.3.1.2 Stiffness Degradation and Joint Integrity

The measured force-displacement relationship for each stiffness, which was test performed after every 50,000 load cycles, is shown in Figure 6.23. The measured effective stiffness (*EI*) of the bridge versus the number of load cycles is shown in Figure 6.24. The stiffness was measured based on the applied loads and the average girder net mid-span deflections. The bridge overall stiffness remained essentially the same throughout the fatigue testing, indicating sufficient detailing for the proposed bridge system.

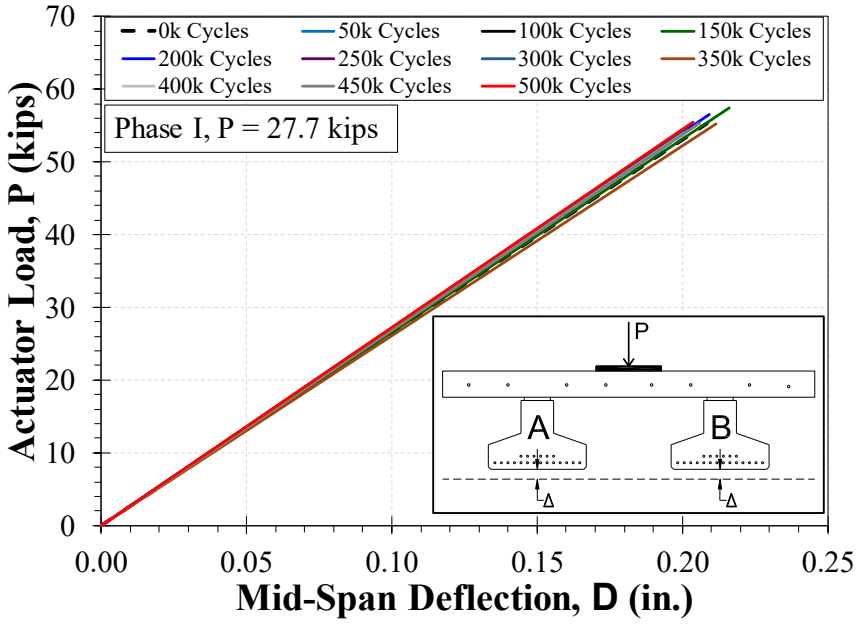

Figure 6.23: Measured Stiffness During Phase I Fatigue Loading – Precast Bridge Specimen

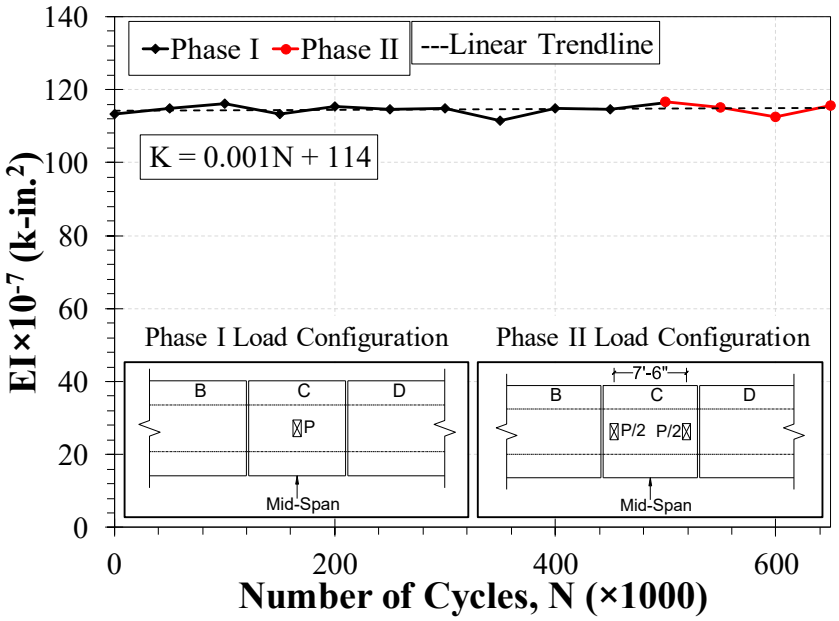

Figure 6.24: Stiffness Degradation During Fatigue Testing – Precast Bridge Specimen

Figure 6.25 shows the measured joint relative deflections versus the number of load cycles for the two joints of Panel C. The joint's relative deflections were negligible and remained essentially constant through all 500,000 load cycles of the Phase I fatigue testing. Figure 6.26 shows the measured joint rotations versus number of load cycles for the two joints of Panel C. The joint rotations were negligible and remained essentially constant through all 500,000 load cycles of the Phase I fatigue testing.

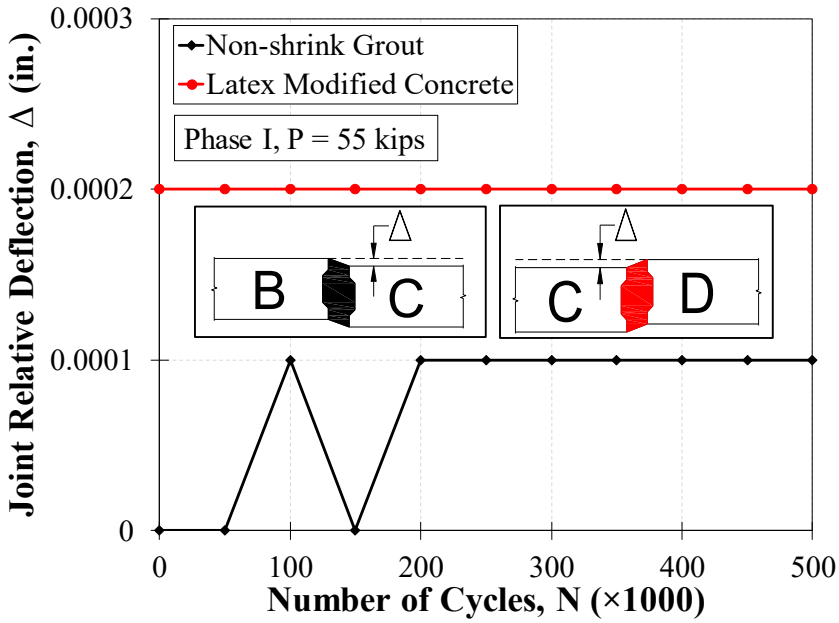

Figure 6.25: Transverse Joint Relative Deflection During Phase I Fatigue Testing – Precast Bridge Specimen

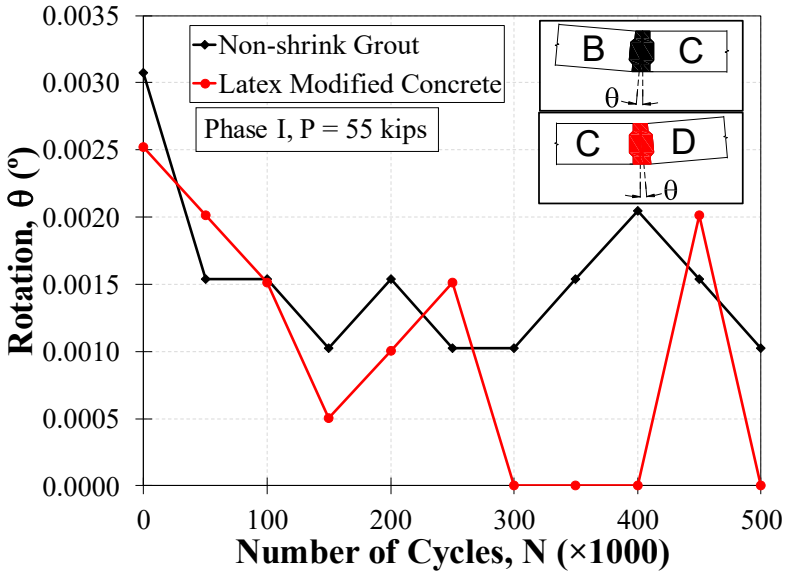

Figure 6.26: Transverse Joint Rotation During Phase I Fatigue Testing – Precast Bridge Specimen

The relative displacement between the girder top flange and the deck bottom (deck-to-girder slippage) was measured during each stiffness test (Figure 6.27). The slippage was negligible and remained essentially constant through all 500,000 load cycles of the Phase I fatigue testing.

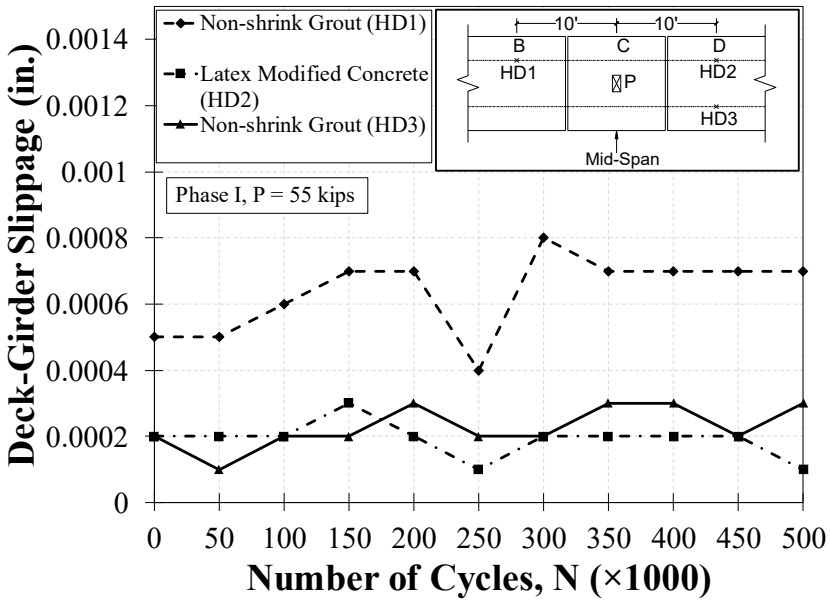

Figure 6.27: Deck-to-Girder Slippage During Phase I Fatigue Testing – Precast Bridge Specimen

6.1.3.2 Phase II – Joint Loading of Precast Bridge

A summary of the Phase II testing results for the precast prestressed bridge including observed damage, stiffness degradation, and joint rotation and slippage is presented in this section.

6.1.3.2.1 Observed Damage

Figure 6.28 shows the middle panel transverse joints with either non-shrink grout or latex modified concrete after applying 150,000 cycles of joint loading. All joints remained water tight through the fatigue loading. No significant damage of the bridge components, in addition to what was reported in Phase I testing, was observed.

(a) Joint with Non-Shrink Grout – Deck Underneath (b) Joint Latex Modified Concrete – Deck Underneath

Figure 6.28: Transverse Joint Damage During Phase II Fatigue Testing – Precast Bridge Specimen

6.1.3.2.2 Stiffness Degradation and Joint Integrity

Figure 6.29 shows the measured force-displacement relationship for each stiffness test performed at every 50,000 load cycles during the Phase II fatigue testing. The stiffness was measured based on the applied loads and the girder net mid-span deflections. The bridge overall stiffness essentially remained the same throughout the transverse joint fatigue testing indicating sufficient transverse joint detailing for the proposed bridge system.

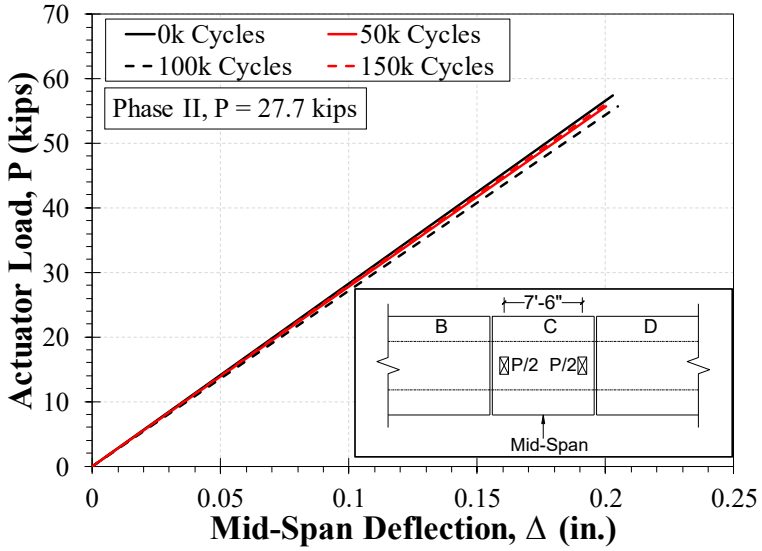

Figure 6.29: Measured Stiffness During Phase II Fatigue Loading – Precast Bridge Specimen

Figure 6.30 shows the measured joint relative deflections versus number of load cycles for both joints of Panel C during the Phase II testing. The joint relative deflections were negligible and remained essentially constant through all 150,000 load cycles. Figure 6.31 shows the measured joint rotations versus number of load cycles for both joints of Panel C under the Phase II loading. The joint rotations were negligible.

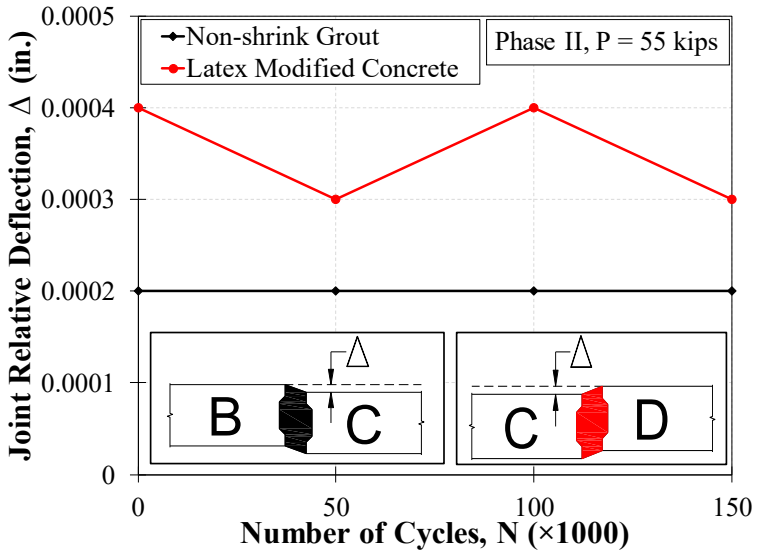

Figure 6.30: Joint Relative Deflection During Phase II Testing – Precast Bridge Specimen

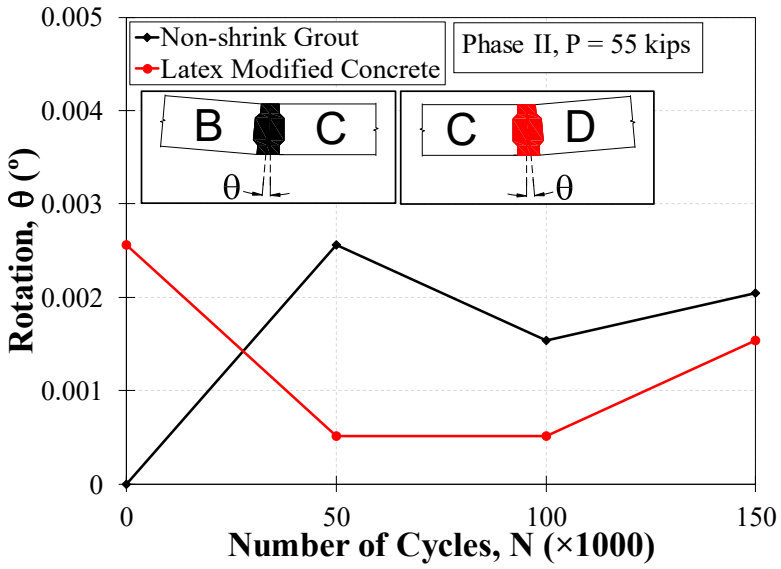

Figure 6.31: Joint Rotation During Phase II Testing – Precast Bridge Specimen

Figure 6.32 shows the deck-to-girder slippage versus number of load cycles. The slippage was negligible through all 150,000 load cycles of the Phase II testing.

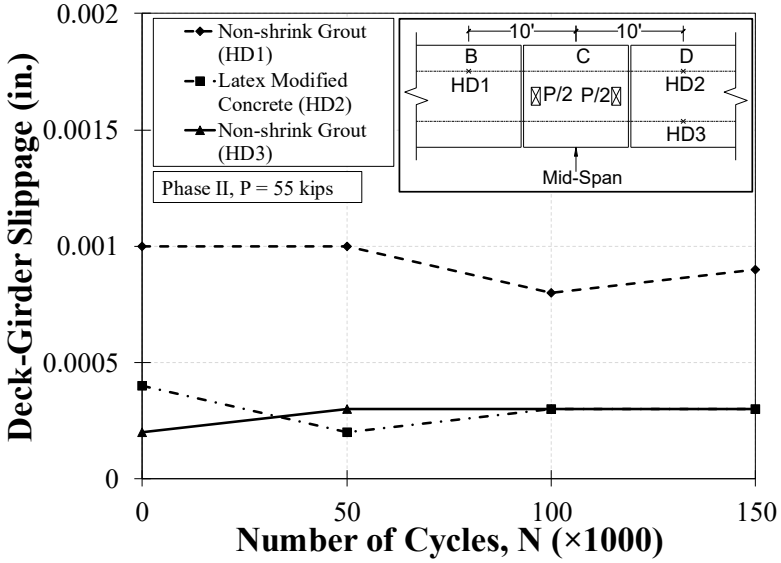

Figure 6.32: Deck-to-Girder Slippage During Phase II Testing – Precast Bridge Specimen

6.1.3.3 Strength Testing Used in the Precast Bridge Specimen

A summary of strength test results for the precast prestressed bridge including observed damage, force-displacement relationship, strain profiles, and joint performance is presented in this section.

6.1.3.3.1 Observed Damage

The first crack in the girder was observed at the mid-span at an actuator load of 149 kips (Figure 6.33a). Subsequently, more cracks were developed on both girders close to the mid-span at higher loads as shown in Figure 6.33b to Figure 6.33d.

(a) First Crack, Mid-span of Girder A at P = 251 kips

(b) First Crack, Mid-span of Girder B at P = 251 kips

(c) Crack Pattern for Girder A at P = 263 kips

(d) Crack Pattern for Girder B at P = 263 kips

Figure 6.33: Girder Cracks During Strength Testing of the Precast Bridge Specimen

The first horizontal shear crack in the grouted haunch region of the precast bridge (Figure 6.34) was observed at an actuator load of 200 kips, which corresponds to a girder load of approximately 100 kips. However, horizontal shear stud strain gauge data suggests that cracking occurred at lower loads. Additional shear cracks appeared at an actuator load of 226 kips (Figure 6.35). Note that shear cracks did not form under an equivalent Strength I Limit State load for this bridge, which was 131.4 kips, indicating that the shear reinforcement detailing was sufficient.

(a) 14-ft Noth of Mid-span (Girder A) (b) 14-ft South of Mid-span (Girder A)

Figure 6.34: Haunch Region Horizontal Shear Cracks at an Actuator Load of 200 kips During Strength Testing of the Precast Bridge Specimen

(a) 16-ft North of Mid-span (Girder B) (b) 14-ft South of Mid-span (Girder B)

Figure 6.35: Haunch Region Horizontal Shear Cracks at an Actuator Load of 226 kips During Strength Testing of the Precast Bridge Specimen

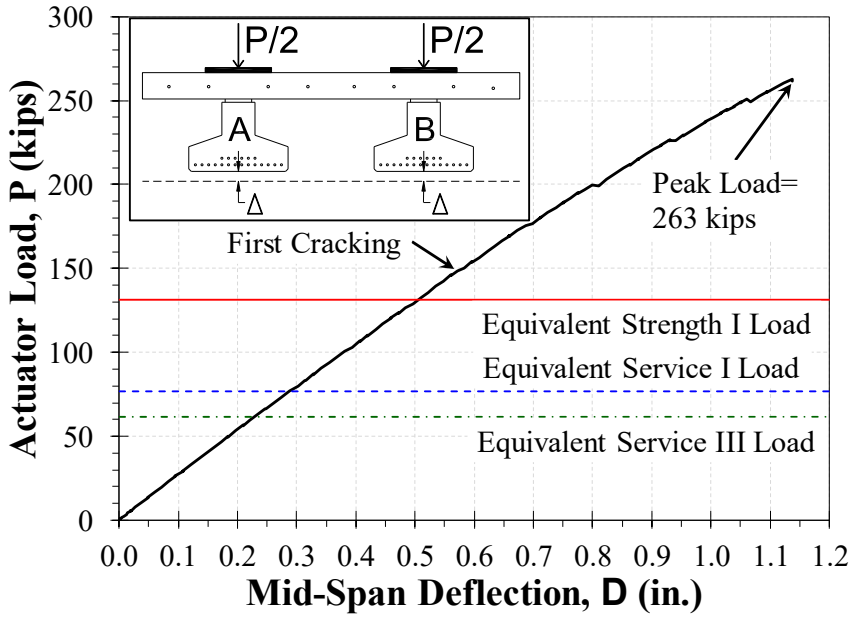

Figure 6.36: Measured Mid-Span Force-Deformation Relationship Under Strength Testing of the Precast Bridge Specimen

6.1.3.3.2 Force-Displacement Relationship

Figure 6.36 shows the force-displacement relationship for the bridge at the mid-span during the strength testing. The figure also shows the equivalent loads for different limit states. The mid-span net girder deflection at the Service I limit state load of 76.7 kips was 0.29 in., which was only 39% of the AASHTO allowable deflection at this limit state (0.74 in.) for this bridge. The girder deflection at the peak applied load of 263 kips was 1.14 in. The test was stopped at 263 kips because of the setup limitation. Furthermore, Figure 6.36 shows that the first girder cracking occurred at a higher load than that of the Strength I limit state indicating that the bridge design was sufficient (since the superstructure should remain capacity-protected). No yielding of the prestressing tendons was observed during the ultimate test. The calculated tendon yield force based on a moment-curvature analysis was 362 kips. Overall, the bridge showed satisfactory performance in terms of displacement and force capacities.

Four load cells were installed under the south end girders to measure the girder reactions continuously. Reactions at applied loads corresponding to the Service I limit state, the Strength I limit state, first cracking, and the ultimate load are shown in Figure 6.37. Approximately 49% of the applied load was resisted by Girder A and the remaining load was resisted by Girder B. The total south end reaction was 24.9 kips under the equivalent Service I limit state load, 58.8 kips under the equivalent Strength I limit state load, 67.0 kips under the first cracking load, and 119.1 kips under the peak load. The south end measured reactions were always 10% lower than the calculated reactions from statics. The cause was probably a slight offset in the actual location of the applied load or a minor gradient in the bridge deck.

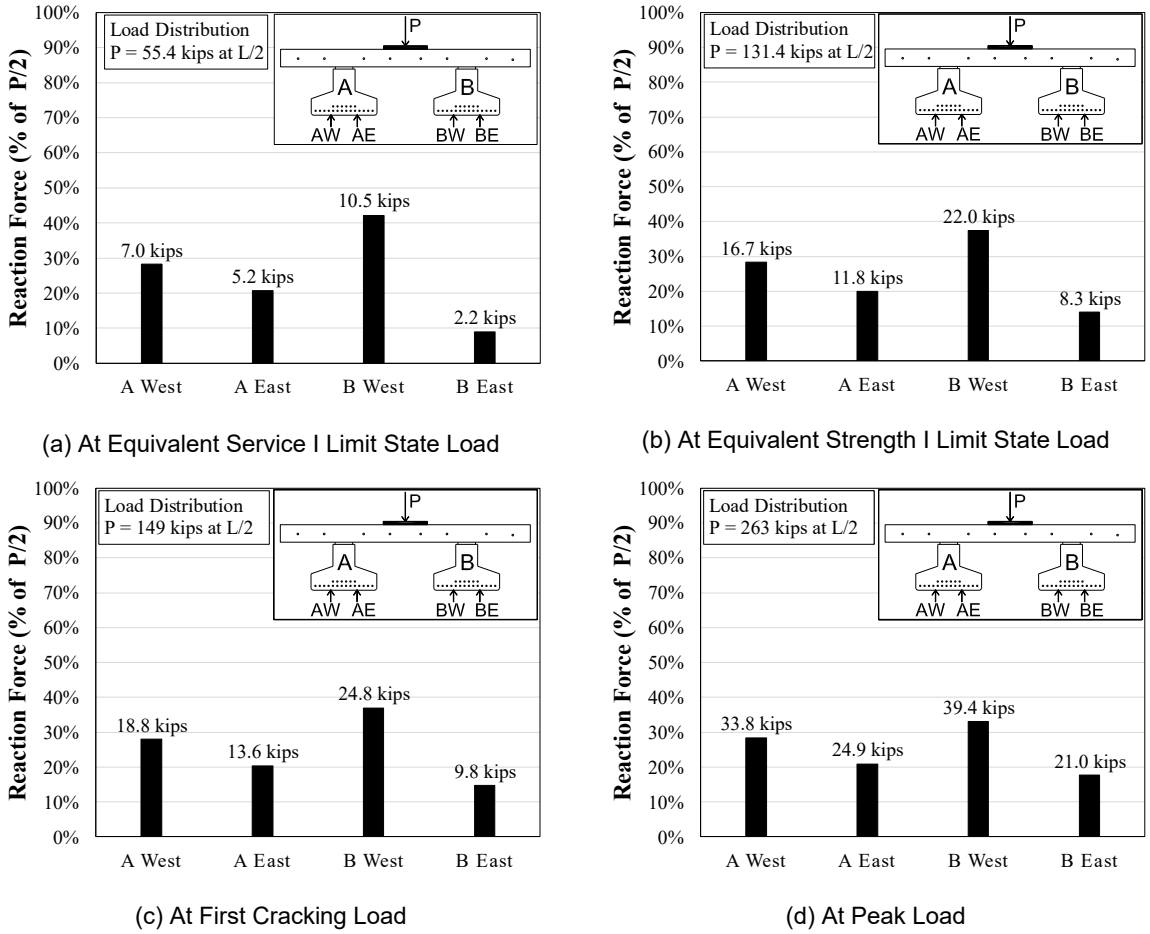

Figure 6.37: Measured Girder End Reactions Under Strength Testing of the Precast Bridge Specimen

6.1.3.3.3 Measured Strains

Strain gauges were installed on prestressing strands and reinforcing steel bars. The measured strain data during the strength test is discussed.

6.1.3.3.3.1 Tendon and Reinforcement Strains

Figure 6.38 shows the measured strain of prestressing strands during the strength testing. The initial strains of the strands were determined using strain gauge data collected during stressing. Note that the strands' initial strains account for the short-term losses such as elastic shortening but not long-term losses such as relaxation, creep, and shrinkage. The tendons did not yield up to 263 kips where the test was stopped. The yield strain of the tendons was 8,772 microstrain. Figure 6.39 shows the measured strains for the longitudinal deck mild steel and the embedded concrete strain gauges during ultimate loading. The measured data for the embedded concrete strain gauges also include the initial strains recorded during cutting of the prestressing strands. The longitudinal deck mild steel did not yield up to 263 kips. The embedded concrete strain gauges were located 1.6 in. below the theoretical composite girder section neutral axis. The measured concrete strains agree with calculated strains from statics.

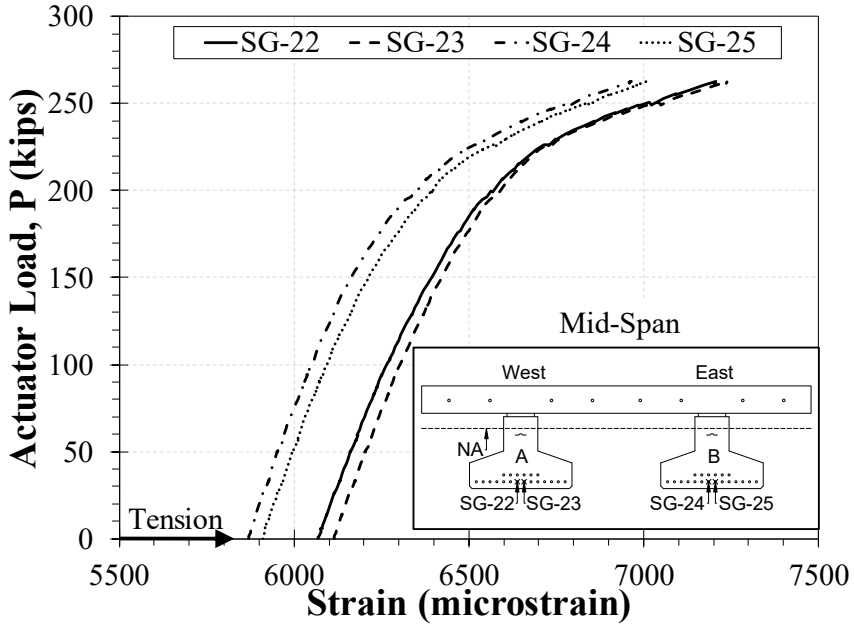

Figure 6.38: Measured Prestressing Strand Strains During Strength Testing of the Precast Bridge Specimen

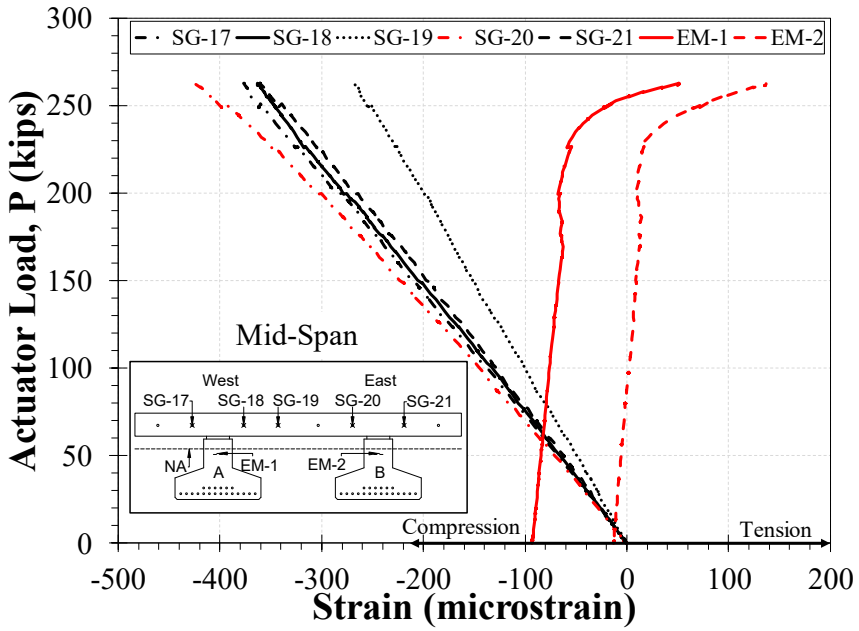

Figure 6.39: Measured Longitudinal Deck Steel Strain and Girder Concrete Strain During Strength Testing of the Precast Bridge Specimen

6.1.3.3.3.2 Shear Stud Strains and Stresses

The actuator load versus measured strain for the double-headed shear studs is shown in Figure 6.40. The double-headed studs did not yield in any direction. Since the strain gauges were installed in a rosette layout in each pocket (one in the axial direction of the stud, and two at ±45 degrees with

respect to the stud's longitudinal axis), the maximum principal stresses (Figure 6.41) could be estimated for the studs in each pocket. The maximum principal stress of the double-headed studs was 19.4 ksi, well below the yield stress (69.9 ksi), indicating sufficient design.

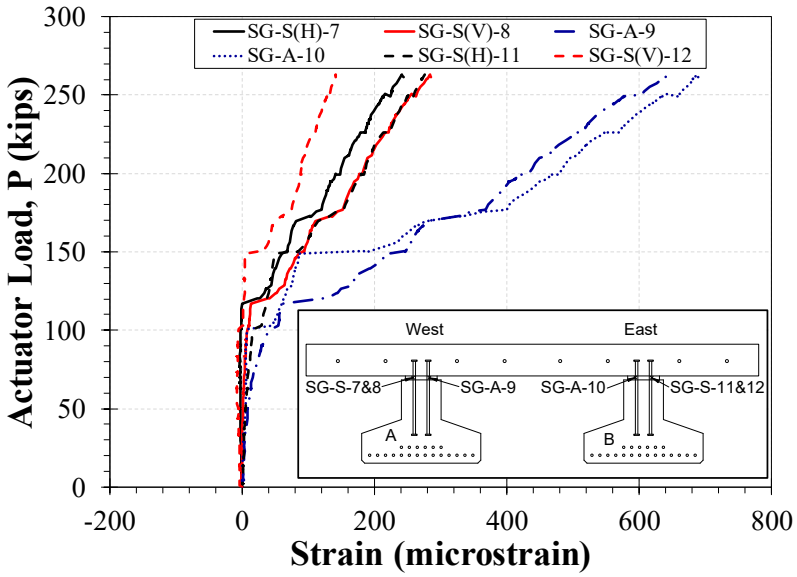

Figure 6.40: Measured Strain for No. 5 Double Headed Studs During Strength Testing of the Precast Bridge Specimen

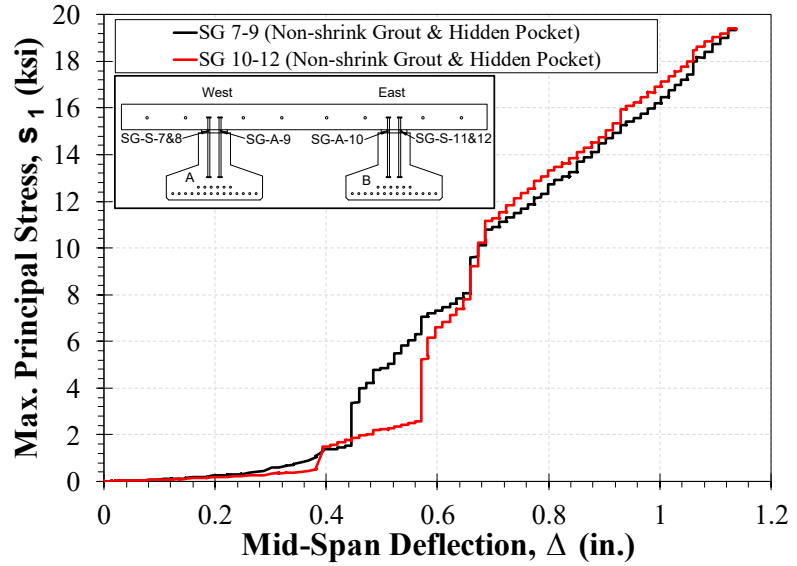

Figure 6.41: Maximum Principal Stresses for No. 5 Double Headed Studs vs. Mid-Span Deflection During Strength Testing of the Precast Bridge Specimen

The load required to cause horizontal shear cracks in the girder haunch can be determined using the stud strain or stress data where strains or stresses suddenly change (Figure 6.41). The deflection associated with the sudden change of strains in studs was identified then converted to the actuator

load using the force-displacement relationship. The first haunch cracks, based on the measured data (Figure 6.41) of the headed studs in the hidden pockets filled with non-shrink grout, occurred at an actuator load of 100.6 kips, which is larger than the Service I limit state load of 76.7 kips.

The actuator load versus measured strain for the inverted U-shape shear studs is shown in Figure 6.42. These studs did not yield in any direction. The maximum principal stresses (Figure 6.43) were estimated in each pocket similar to what was done for the double-headed studs. The maximum principal stress for the inverted U-shape shear studs was 23.9 ksi for the pocket filled LMC and 27.6 ksi for the pocket filled with non-shrink grout. Therefore, the principal stresses were well below the stud yield stress, indicating sufficient design.

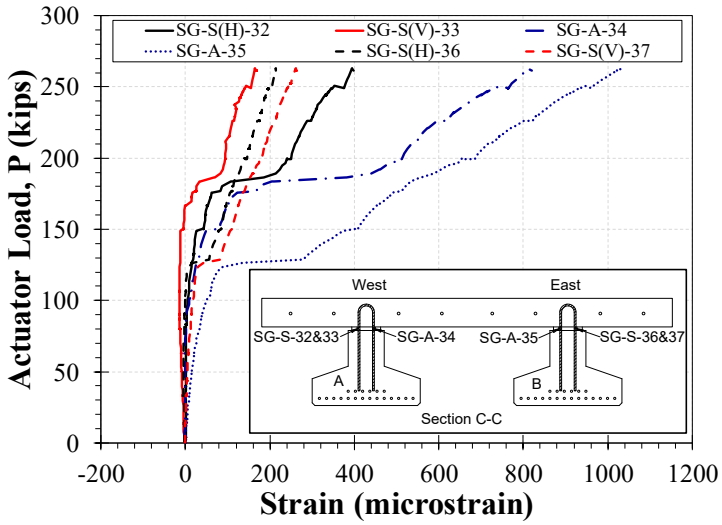

Figure 6.42: Measured Strain for No. 4 Inverted U-Shape Studs During Strength Testing of the Precast Bridge Specimen

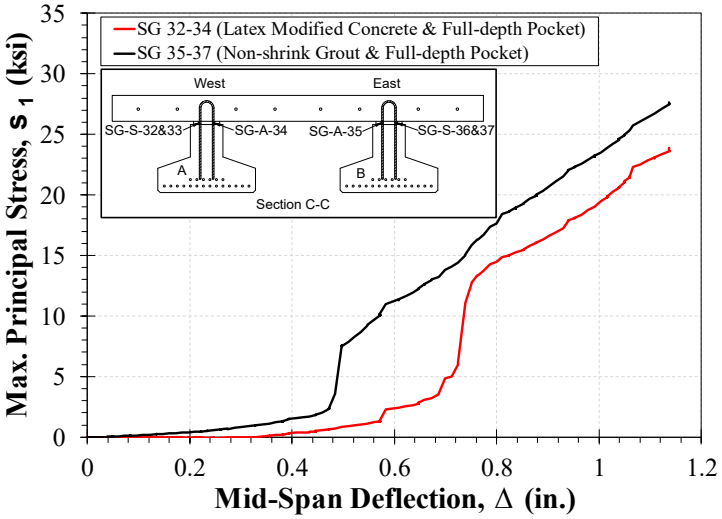

Figure 6.43: Maximum Principal Stresses for No. 4 Inverted U-Shape Studs vs. Mid-Span Deflection During Strength Testing of the Precast Bridge Specimen

The load required to cause horizontal shear cracks in the girder haunch was also determined. The first haunch cracks based on the measured strain data (Figure 6.43) for the inverted U-shape shear studs in the full-depth pockets filled with non-shrink grout occurred at an actuator load of 124 kips, and at a load of 149 kips for the full-depth pockets filled with LMC. Both loads are larger than the Service I limit state load of 76.7 kips, confirming that the shear pocket detailing was sufficient.

6.1.3.3.3.3 Transverse Joint Reinforcement Strains

Figure 6.44 shows the measured strains of the transverse bars in the transverse joints during the strength testing. Strain gauge SG-A-15 failed at 170 kips (marked with * in the figure). The strains were negligible. None exceeded 50 microstrain.

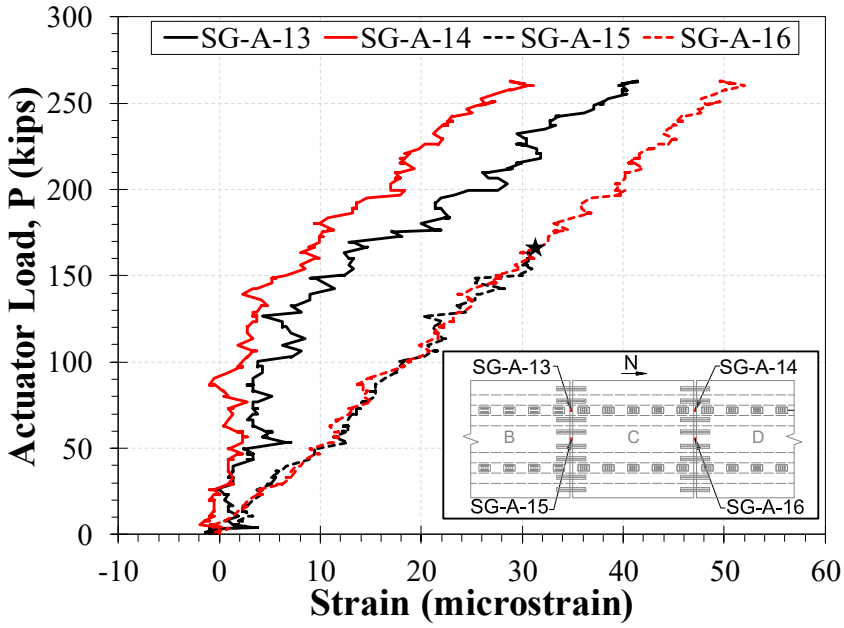

Figure 6.44: Measured Strains of No. 6 Transverse Bars in Transverse Joints During Strength Testing of the Precast Bridge Specimen

Two No. 6 dowel bars installed in the transverse joints had strain gauges in a rosette layout to estimate the maximum principal stresses (Figure 6.45) transferred between the two adjacent decks. The maximum principal stress for the reinforcement in the joints filled with either non-shrink grout or LMC was well below the yield strength, indicating sufficient design.

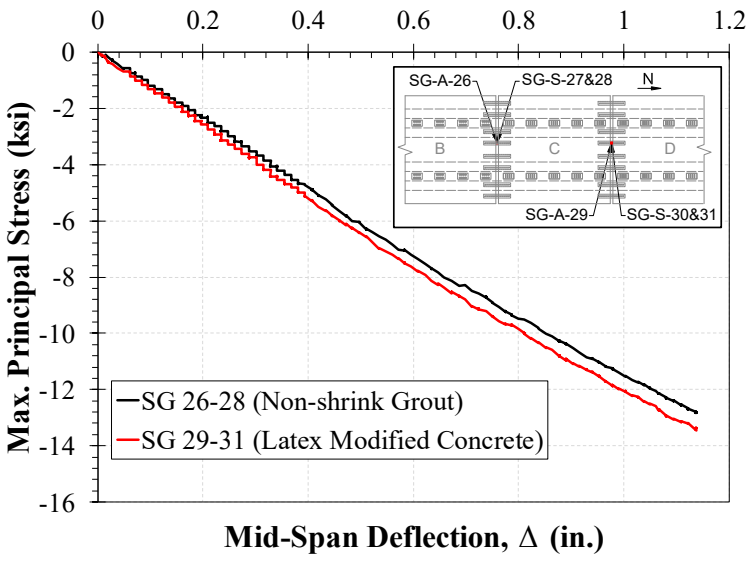

Figure 6.45: Maximum Principal Stresses for No. 6 Lap-Spliced Bars vs. Mid-Span Deflection During Strength Testing of the Precast Bridge Specimen

6.1.3.3.4 Performance of Joints

The mid-panel joints' relative deflections and rotations during strength testing are shown in Figure 6.46. The joint filled with non-shrink grout had a relative deflection of 0.0014 in. at 263 kips. The joint filled with latex modified concrete had a relative deflection of 0.0015 in. at 263 kips. Both deflections were negligible. Furthermore, the joint filled with non-shrink grout had a rotation of 0.009 degrees at 263 kips. The joint filled with latex modified concrete had a rotation of 0.01 degrees at 263 kips. Both joint rotations were negligible.

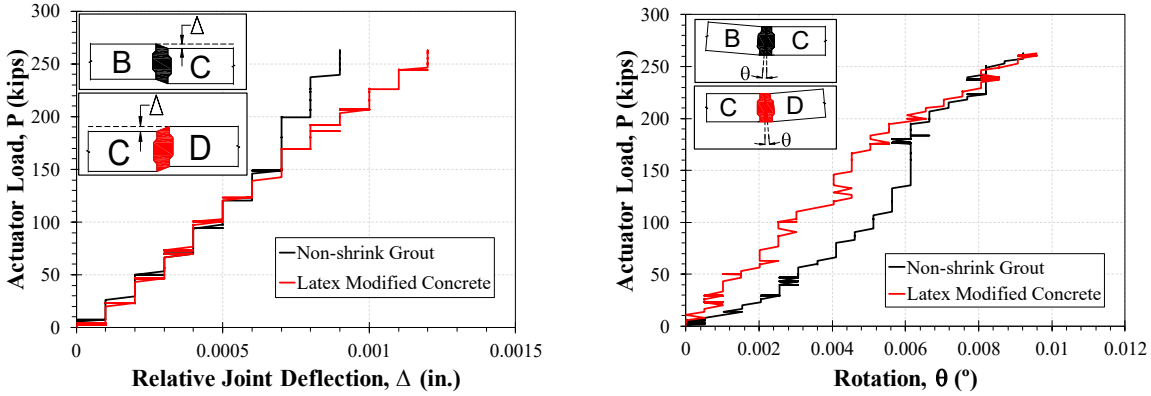

(a) Relative Joint Deflection

(b) Joint Rotation

Figure 6.46: Measured Relative Deflections and Joint Rotations During Strength Testing of the Precast Bridge Specimen

The relative displacement between the bottom of the deck and the top of the girder (deck-to-girder slippage) was measured in three locations. Figure 6.47 shows the deck-to-girder slippage during the strength testing. A plateau can be seen at a girder load of approximately 60 kips, which can be

attributed to the cracking of the haunch region (e.g., Figure 6.34), and the relatively small shear deformations of the haunch region.

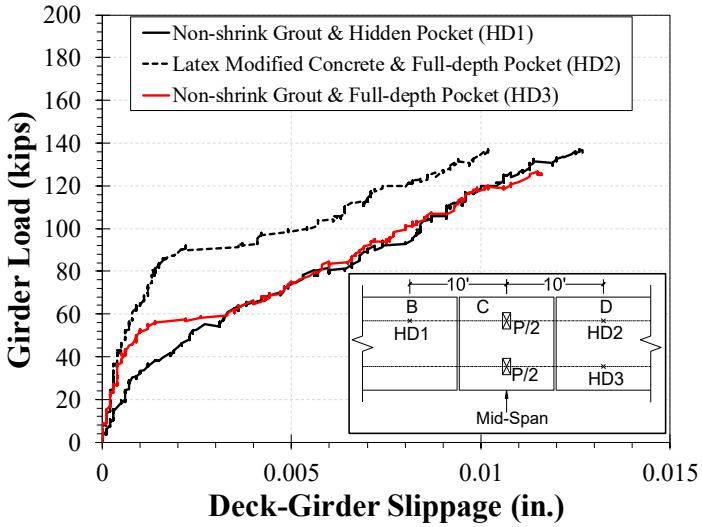

Figure 6.47: Measured Deck-to-Girder Slippage During Strength Testing of the Precast Bridge Specimen

6.2 Glulam Timber Girder Bridge Specimen

Two types of glulam timber bridges (Figure 5.17) were introduced in the previous chapter: (1) bridges built with transverse glulam decks supported on glulam stringers (hereafter referred to as the "girder bridges"), and (2) longitudinal glulam deck bridges (hereafter referred to as "slab bridges"). The structural performance of a glulam girder bridge was evaluated through full-scale experiment. This section includes a summary of the design, construction, instrumentation, test setup, loading protocols, and test results for the full-scale girder bridge test specimen.

6.2.1 Glulam Timber Girder Bridge Test Specimen

6.2.1.1 Design of Test Specimen

The prototype glulam girder bridge was assumed to be 50-ft long and 34.5 ft wide (**Figure 6.48**a). A full-scale bridge model was selected for testing but with a width approximately equal to the width of one lane of traffic. The bridge test specimen (**Figure 6.48**b) consisted of (1) three 50 ft long girders with a depth of 30.25 in. and a width of 8.5 in., (2) thirteen deck panels each 48 in. long (in the longitudinal direction of the bridge), 110.75 in. wide (in the transverse direction of the bridge), and 5.5-in. thick (6 in. nominal thickness), and (3) ten rectangular glulam cross braces each with a dimension of 5 in. by 10 in. to improve the stability of the bridge.

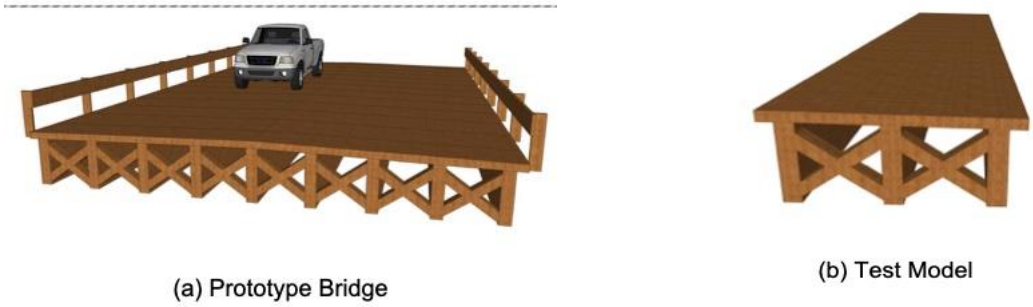

(a) Prototype Bridge

(b) Test Model

Figure 6.48: Glulam Girder Bridge Test Model

AASHTO (2013) was used for the design of the bridge components. This bridge was designed for the HL-93 loading, which consists of a design truck or tandem accompanied by the design lane load.

6.2.1.1.1 Design of Glulam Deck Panels

The deck panels were analyzed and designed according to AASHTO (2013). A structural analysis was performed using the Strength I limit state loads with the assumptions that the deck panels are continuous beams and that the girders are simply supported at the ends. According to the structural analysis, the deck could be less than 6 in. However, the depth of the deck was controlled by the minimum nominal thickness of 6 in. required by AASHTO. The width of the deck panels was determined to be 4 ft for ease of fabrication and installation.

6.2.1.1.2 Design of Glulam Girders (Stingers)

The girders were also designed according to AASHTO (2013). Live load distribution factors were used to calculate the moment demand for an interior girder, since the girders used in the test bridge simulate interior girders of the prototype bridge model.

The girders were assumed to be partially composite with the deck and were designed based on the mechanical properties for 26F-1.9E Southern Yellow Pine. The design girder was 30.25 in. deep and 8.5 in. wide. To provide sufficient bearing area for girders at the ends and to have a 50-ft clear span, the girder length was increased from 50 to 52 ft.

To further aid bridge designers, a spreadsheet was developed for the design of glulam girders, checking the capacity to demand ratio for all design parameters as well as the girder deflection.

(a) Installation of Cross Braces

(b) Placement of Epoxy between Girder and Deck

(c) Drilling GRK Screws

(d) Placing Epoxy in Deck-to-Deck Connection

(e) Placement of Second Panel

(f) Interlocking Deck Panels

Figure 6.49: Assembly of Glulam Timber Girder Bridge Test Specimen

6.2.1.1.3 Design of Cross Braces

The cross braces were designed to resist lateral loads according to AASHTO (2013), Section 8.11. Even though solid diaphragms and steel cross braces are recommended by AASHTO, the use of glulam cross braces was proposed and investigated in this project due to the ease of construction. The final glulam rectangular cross braces were 6.875-in. wide and 8-in. deep.

6.2.1.1.4 Design of Deck-to-Stringer Connection

As discussed in the previous chapter, there are three main types of deck-to-stringer connections: (1) lag bolt connection, (2) aluminum bracket connection, and (3) epoxy connection. The use of epoxy to connect the deck to the stringers was proposed in this study, and the connection performance was evaluated experimentally. This connection type was expected to perform better than the other types due to minimal drilling from the top of the deck. The deck panels were attached to the girders using a layer of epoxy (Figure 6.49b). Note that some screws were used to compress the deck to the girder to activate the epoxy.

6.2.1.2 Fabrication and Assembly of Glulam Timber Girder Bridge Test Specimen

The entire test bridge was fabricated by the manufacturer then shipped as one piece to the Lohr Structures Laboratory. The following sections discuss the fabrication, assembly, and transportation of the test specimen.

6.2.1.2.1 Fabrication of Deck Panels

The glulam deck panels were built from M-29 Southern Yellow Pine. Thirty-five 1.375 in. thick laminations were glued together to form 48-in. deck panels. Each panel was clamped to apply pressure and to activate the epoxy between the laminations. This type of epoxy does not activate until a minimum pressure of 150 psi is applied. The panels were stored in the construction facility with ambient room temperature to allow the epoxy to dry and harden. After epoxy hardening, the panel edges were grooved and routed to form a tongue-and-groove connection.

6.2.1.2.2 Fabrication of Girders

The girders were specified to be built using 26F-1.9E Southern Yellow Pine. However, the ultimate testing showed that a wrong type of wood (24F-2.0E) was used in the fabrication process by mistake. This issue will be discussed later under the testing results. Twenty-two 1.375-in. thick laminations were glued together to form the girders. Each girder was clamped to apply pressure and to activate the glue after placing the epoxy between the laminations. The girders were placed in the construction area with an ambient room temperature to allow the epoxy to dry and harden.

6.2.1.2.3 Fabrication of Cross Braces

The cross braces were specified to be built with 26F-1.9E Southern Yellow Pine. However, they were also built with 24F-2.0E by mistake. The cross braces were cut and prepared with high precision to easily fit between the stringers.

6.2.1.2.4 Assembly of Bridge Test Specimen

The test specimen was completely assembled at the manufacturing site then shipped to the Lohr Structures Laboratory for testing. First the girders were placed beside one another (Figure 6.49a); then the cross braces were installed between them. Epoxy was placed between the cross braces and the girders were installed.

After completion of the diaphragms, the first deck panel was placed at the south end of the specimen. The panel was held upright by a fork lift while the epoxy was placed on the top of the girders (Figure 6.49b). Long screws were then installed to hold the panel in place and allow the epoxy to cure (Figure 6.49c). The next panel was installed with the same method but placed with care to ensure that the panel-to-panel connection was adequate. A bead of epoxy was placed along the tongue connection before the second panel was in place (Figure 6.49d to Figure 6.49f). This process continued until the deck system was completed.

6.2.1.2.5 Transportation of Test Specimen

The test specimen was transported from the manufacture site in Tea, SD, to the Lohr Structures Laboratory in one piece. The bridge was loaded on a truck using two fork lifts. Upon arrival at the lab, the truck backed as far into the lab as possible. Two straps were placed approximately 20 ft apart. Wooden blocks were installed at these points to keep the straps in place and to avoid stressing the deck during lifting. The straps were hooked to a chain, which was connected to a 15-ton crane. The test specimen was then lifted, and the truck drove away. Finally, the abutments (reaction blocks) were placed and the test specimen was slowly dropped in place.

6.2.1.3 Test Setup for Glulam Timber Girder Bridge

The girder bridge specimen was tested under two different loading scenarios: (1) fatigue loading and (2) ultimate (strength) loading. The test setups for the two test procedures were slightly different and are discussed.

6.2.1.3.1 Fatigue Test Setup

The bridge was supported on three reaction blocks at each end (Figure 6.50). The reaction blocks at the north end were 28.5 in. tall while the reaction blocks at the south end were 4.5 in. shorter (24 in. tall) to allow for placement of load cells. Rectangular neoprene bearing pads each with a dimension of 6 in. by 12 in. were placed under each girder. The length of the pad was based on the AASHTO requirements. Two 22-kip actuators were used to apply the load at the mid-span at 6.6 in. from the inside edge of the exterior girders. The location of the point loads was selected to produce equal reactions in the three girders. The load frame used to support the actuators had a height of 20 ft and a clear spacing of 10 ft between the columns.

Figure 6.50: Fatigue Test Setup for Timber Girder Bridge

6.2.1.3.2 Ultimate (Strength) Test Setup

For the ultimate test, a 328-kip actuator was used to monotonically apply the load at the mid-span of the bridge. The load was distributed directly to the three girders using a spreader beam (Figure 6.51).

Figure 6.51: Ultimate Test Setup

6.2.1.4 Instrumentation Plan for Glulam Timber Girder Bridge

The bridge test specimen was instrumented with strain gauges, Linear Variable Differential Transformers (LVDTs), load cells, and string potentiometers (string pots) to measure the response of the bridge at different load levels. Note that actuators also provide load and displacement data at the location of the applied load. This section presents the bridge instrumentation detailing.

6.2.1.4.1 Strain Gauges

Figure 6.52 shows the strain gauge plan for the test bridge. Strain gauges were installed only at the mid-span where the bending moment was maximum. Three strain gauges were installed on the interior girder, and two gauges were placed on the exterior girders. Sixteen strain gauges were installed on the top of the deck to investigate the effective width of the deck for composite action. Wood strain gauges (PFL-30-11-5L) each with a length of 30 mm (1.18-in) were used in this project.

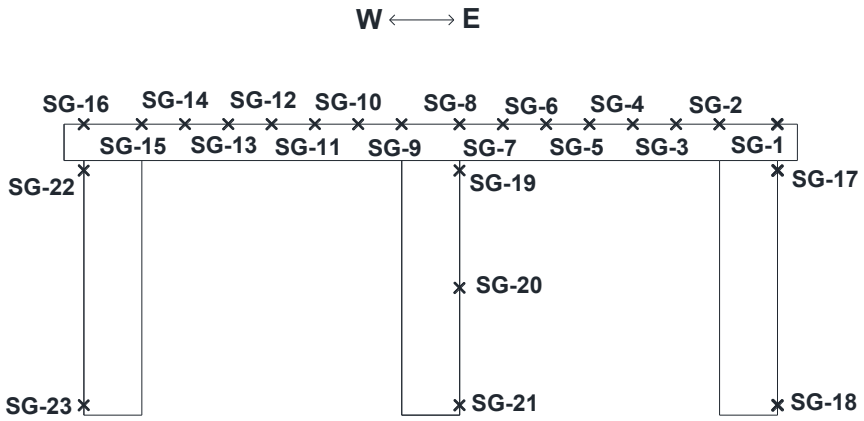

Figure 6.52: Strain Gauge Plan for Timber Girder Bridge

6.2.1.4.2 Linear Variable Differential Transformers (LVDTs)

Fourteen LVDTs were used to record displacements and rotations at various locations on the bridge (Figure 6.53). Since the girders were placed on bearing pads, which compress under applied load, vertical LVDTs were installed at the end of each girder to measure the deformation of the pads and to calculate the net mid-span deflection. Three additional vertical LVDTs were installed at the mid-span to measure the girder deflections. Six horizontal LVDTs were used to measure either the relative displacements of the joints or the rotations.

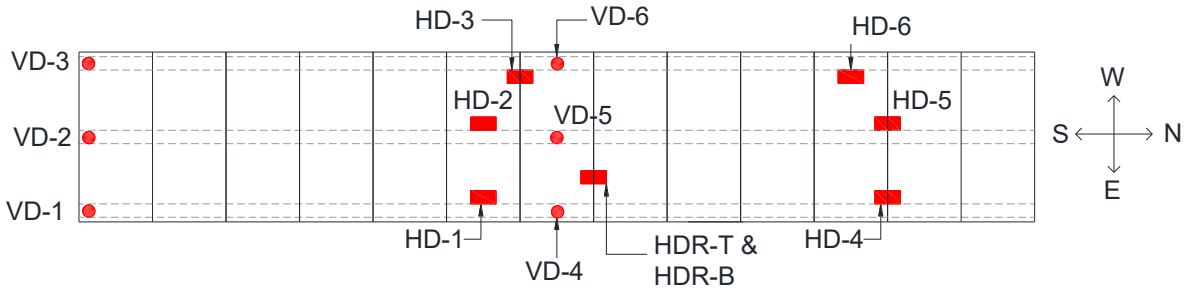

Figure 6.53: LVDT Installation Plan for Fatigue Testing of Glulam Timber Girder Bridge

For the ultimate testing, the LVDT installation plan was slightly modified. Since large displacements were expected under the ultimate load, the LVDTs at the mid-span of the bridge were removed (due to a small measuring range) and placed in other locations. VD-4 was removed and placed as HD-7 to measure the opening of the joint at the bottom of the bridge (2 joints south of HD-6). Note that VD-5 and VD-6 were removed at 1.25 in. displacement to avoid damage of the device.

6.2.1.4.3 String Potentiometers (String POTs)

Since string pots have a larger measuring range than LVDTs, they were used at the mid-span of the bridge during the ultimate test to measure deflections. The string pots were installed at the centerline of the girders at their bottom face.

6.2.1.4.4 Load Cells

Load cells, which have been calibrated regularly, were placed under each of the three girders at the south end to measure the support reactions. It was assumed that the reactions at both ends of the girders were equal because the load was applied at the mid-span.

6.2.1.4.5 Data Acquisition System

All of the instrumentation was connected to a 128-channel data acquisition system by Vishay. A scan rate of 10 readings per second was used for the monotonic loading and a scan rate of 100 readings per second was used for the cyclic loading.

6.2.1.5 Test Procedure for Glulam Timber Girder Bridge

The bridge specimen was tested under two loading scenarios: fatigue and ultimate. Fatigue testing was performed to investigate the performance of the bridge under 75 years of service life, and the ultimate testing was carried out to determine the capacities of the bridge. The test procedures are described in detail herein.

6.2.1.5.1 Fatigue Testing

Phase I of the bridge testing consisted of fatigue testing. Two 16-kip point loads were cyclically applied at the mid-span of the bridge (Figure 6.50). The fatigue loading protocol was determined using AASHTO (2013) Fatigue II Limit State specifications. The number of the fatigue loading cycles was determined to be 410,625 cycles based on an Average Daily Truck Traffic (ADTT) of 15 for the 75 years of the design life. The total load cycle was increased to 500,000 to account for unexpected higher traffic. Force-based controlled cyclic loads were applied at a frequency of 0.7 Hz. The lower bound of the applied load during the fatigue testing was 300 lbs to prevent the actuator from uplifting. Stiffness tests were performed at an interval of 50,000-load cycles including an initial stiffness test. The stiffness load amplitude was 30 kips. The load was applied under a displacement-based control condition at a displacement rate of 0.007 in/sec.

6.2.1.5.2 Ultimate Testing

After completion of the fatigue testing, an ultimate test was carried out to determine the capacity of the timber girder bridge and to investigate the failure mode. A point load was applied at the mid-span

of the bridge. The specimen was loaded under a monotonic displacement-controlled protocol to failure with a displacement rate of 0.007 in/sec. The data was recorded after completion of each displacement step. The displacement step was 0.05 in. up to a displacement of 1.30 in. then the displacement step was increased to 0.1 in. to the end of the testing.

6.2.2 Material Properties for Timber Girder Bridge

Table 6.6 presents mechanical properties of the timber that was used in the as-built test specimen (24F-2.0E), the timber that was specified to be used in the bridge (26F-1.9E), and M-29 glulam, which was used to construct the deck panels.

Table 6.6: Mechanical Properties of Glulam Timber Used in Girder Bridge

Properties	Notation	Unit	26F-1.9E	24F-2.0E	M-29
Tension Zone Stressed in Tension	F_{bxo}^{+}	ksi	2.6	2.4	1.55
Compression Zone Stressed in Tension	F_{bxo}^{-}	ksi	1.95	1.45	1.55
Shear Parallel to Grain	F_{vxo}	ksi	0.265	0.265	0.175
Modulus of Elasticity	E_{xo}	ksi	1900	2000	1700

The girders were specified to be built using 26F-1.9E Southern Yellow Pine. However, the ultimate testing showed that the wrong type of wood (24F-2.0E) was used in the fabrication process by mistake.

6.2.3 Test Results for Timber Girder Bridge

The girder bridge specimen was first tested under 500,000 cycles of the AASHTO (2013) Fatigue II loading using two 22-kip actuators at the mid-span. Then, it was loaded monotonically to failure using a 328-kip actuator applying point loads at the mid-span. Results of both tests are presented.

6.2.3.1 Fatigue Testing of Glulam Timber Girder Bridge

6.2.3.1.1 Observed Damage

No damage to any components of the bridge was observed up to 250,000 load cycles, which was approximately equivalent to 46 years of service. However, deck-to-deck connections cracked at the 250,000 load cycle, and then the crack extended and widened at higher load

cycles.

(b) Panel I-to-J Connection (East Side) at 0 Cycles

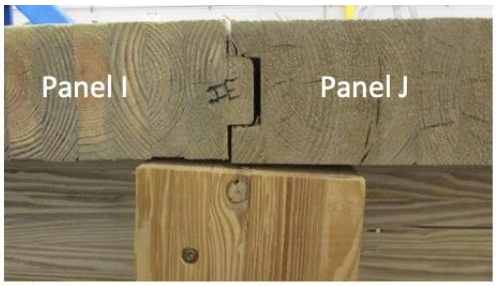

(c) Panel I-to-J Connection at 250,000 Cycles

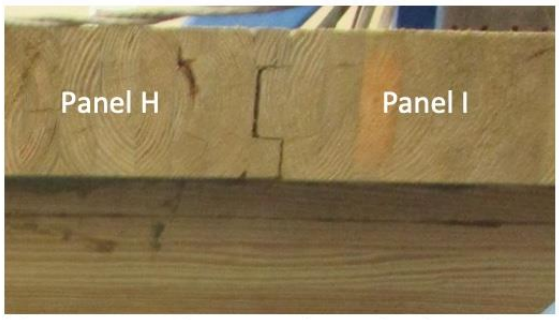

(d) Panel H-to-I Connection (West Side) at 0 Cycles

(e) Panel H-to-I Connection after 250,000 Cycles

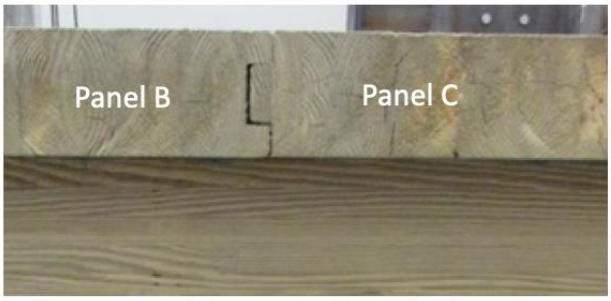

(f) Panel B-to-C Connection (West Side) at 0 Cycles

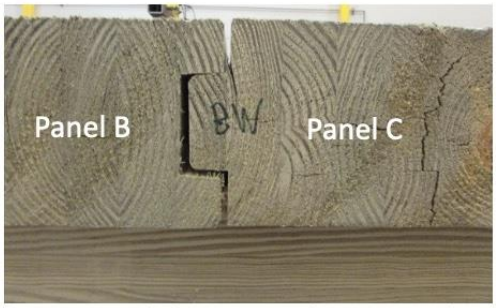

(g) Panel B-to-C Connection after 250,000 Cycles

Figure 6.54 shows the damage to some of the joints before and after loading.

No damage to any other components was apparent during the fatigue testing.

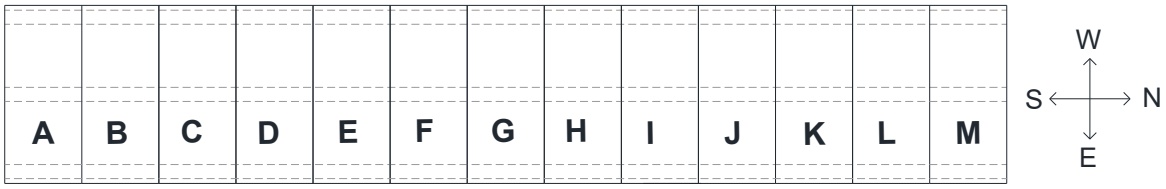

(a) Plan View of Bridge Deck

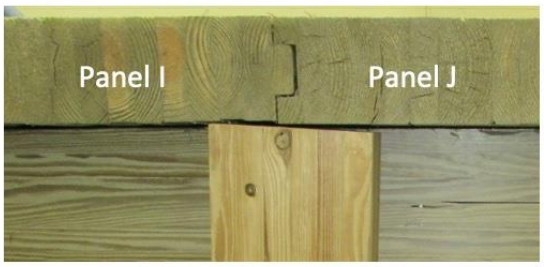

(b) Panel I-to-J Connection (East Side) at 0 Cycles

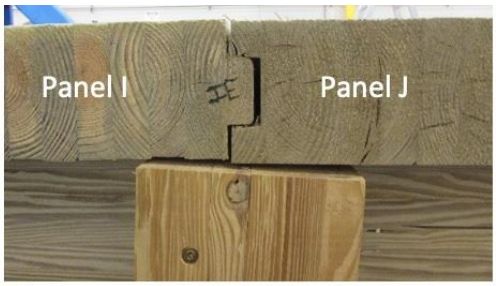

(c) Panel I-to-J Connection at 250,000 Cycles

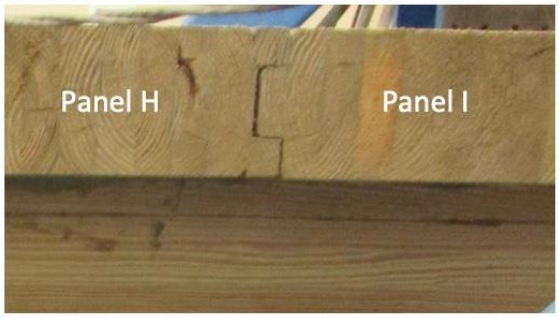

(d) Panel H-to-I Connection (West Side) at 0 Cycles

(e) Panel H-to-I Connection after 250,000 Cycles

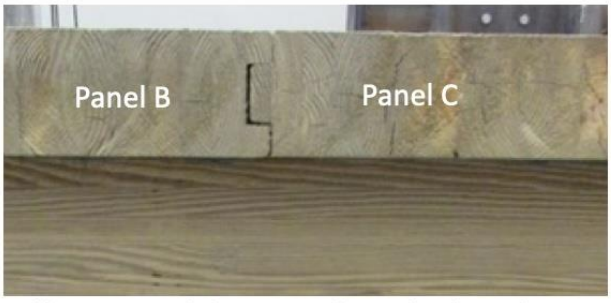

(f) Panel B-to-C Connection (West Side) at 0 Cycles

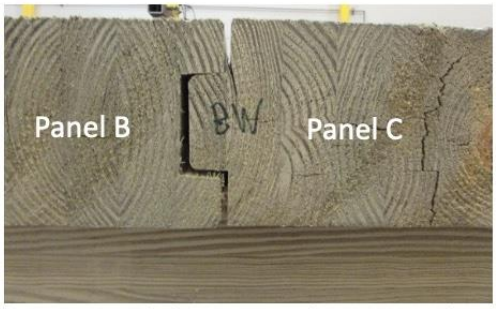

(g) Panel B-to-C Connection after 250,000 Cycles

Figure 6.54: Cracking of Deck-to-Deck Panel Connections for Glulam Timber Girder Bridge

6.2.3.1.2 Stiffness Degradation and Joint Integrity

Figure 6.55 shows the measured force-displacement relationship during the stiffness tests, which were performed every 50,000 load cycles. The bridge essentially remained linear-elastic during the fatigue testing with no stiffness degradation. The stiffness is the ratio of the actuator load to the average net mid-span deflection of the girders.

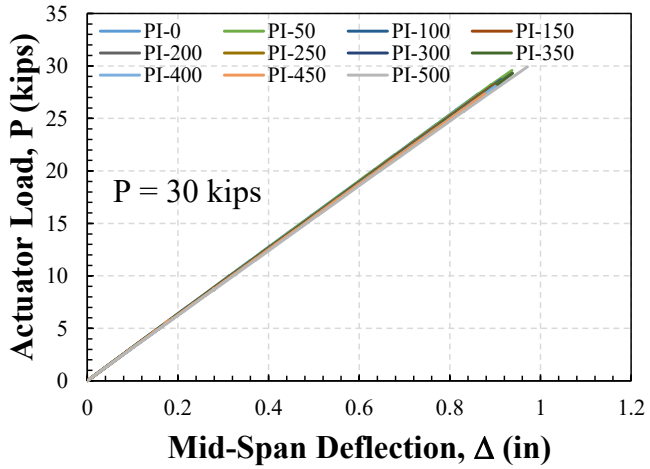

Figure 6.55: Measured Stiffness During Fatigue II Testing of the Glulam Timber Girder Bridge Specimen

Figure 6.56 shows the measured effective stiffness (*EI*) versus the number of load cycles. The overall bridge stiffness remained constant throughout the fatigue testing confirming that the proposed glulam girder bridge detailing is structurally viable for 75 years of service.

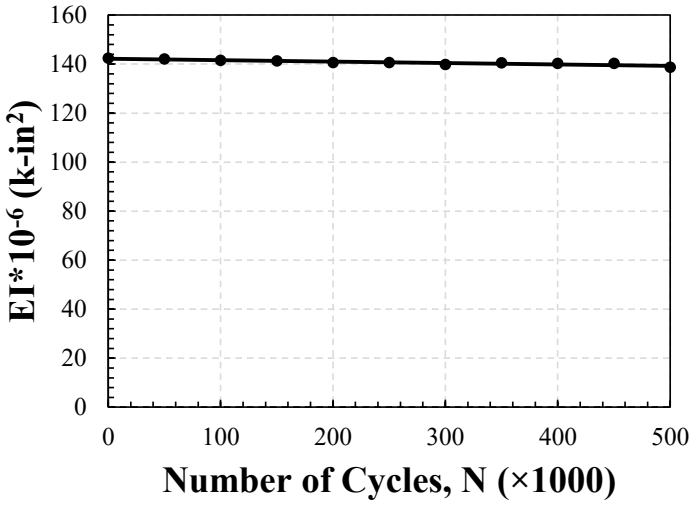

Figure 6.56: Stiffness Degradation during Fatigue II Testing of the Glulam Timber Girder Bridge Specimen

6.2.3.1.3 Measured Strains

The strain profiles of the timber bridge girders are shown in Figure 6.57. The strain profiles remained approximately the same through all 500,000 load cycles of the fatigue testing. “PI-X” in the graph refers

to the stiffness test at X-thousands of load cycles. Although there was some partial composite action, the graphs clearly show that the deck-to-girder connection did not act compositely since the strains of the deck were not compatible with the girder strains. Note that a partial composite action was considered during the design of the bridge. This assumption proved to be un-conservative since the composite action was minimal during the test. Therefore, the glulam girders should be designed as fully non-composite members.

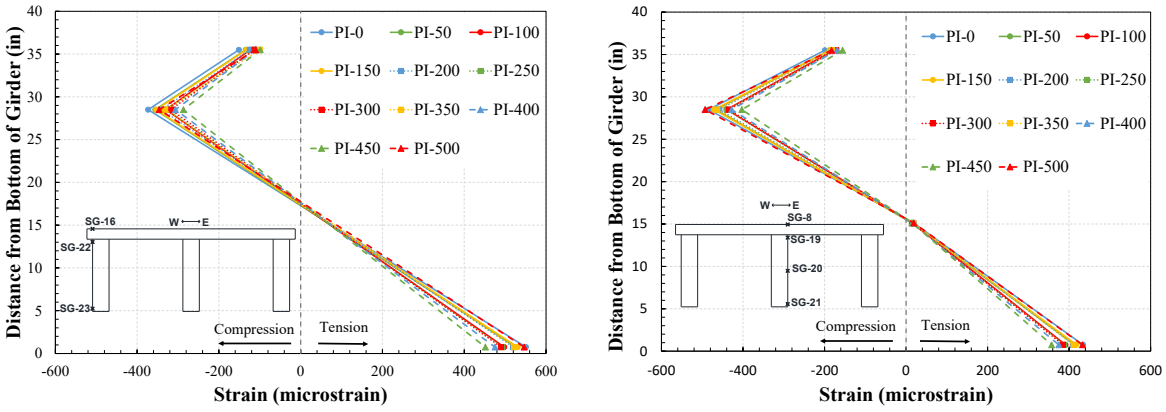

(a) West Girder (b) Interior Girder

Figure 6.57: Strain Profiles for Stingers of the Glulam Timber Girder Bridge Specimen

The strain profile of the deck is shown in Figure 6.58. Sixteen strain gauges were installed on the deck surface to determine the effective width of the deck in a composite behavior. However, the full composite behavior was not achieved using the proposed deck detailing.

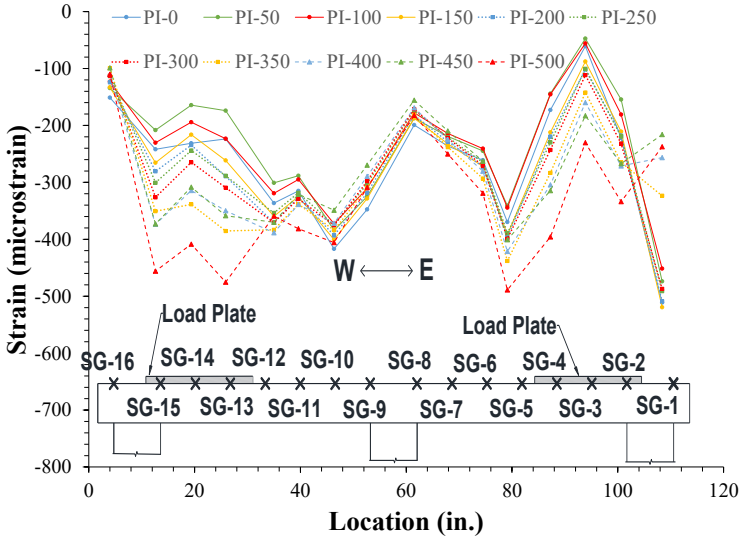

Figure 6.58: Deck Strain Profiles for the Glulam Timber Girder Bridge Specimen

6.2.3.1.4 Joint Rotations and Relative Displacements

The measured joint rotations versus the number of load cycles for one of the transverse joints is shown in Figure 6.59. The joint rotations were negligible throughout fatigue testing. The increase in the joint

rotations at the 250,000 cycles was because of the damage of the tongue-and-groove deck connections discussed in Sec. 6.2.3.1. Before the failure, the rotation was restrained by the panels while there was no such a restrain after the failure of the connection thus the rotations increased afterwards.

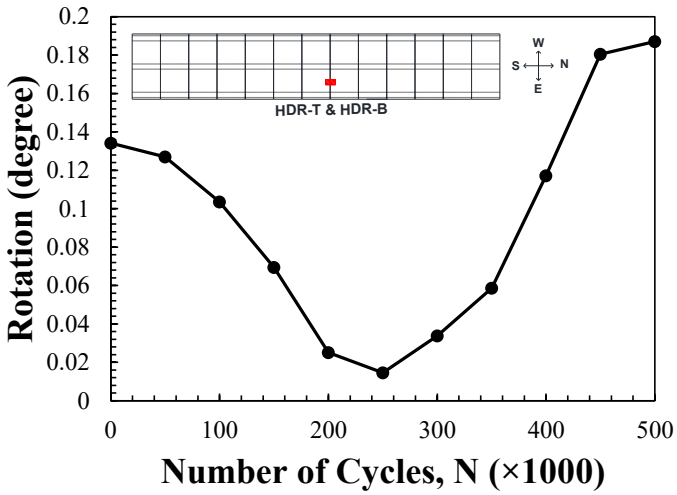

Figure 6.59: Transverse Joint Rotation during Fatigue Testing of the Glulam Timber Girder Bridge Specimen

The relative horizontal displacements between the girder and the deck (deck-to-girder slippage) was measured at different locations using six LVDTs during each stiffness test (Figure 6.60). The relative displacements were negligible throughout the fatigue testing indicating that the epoxy was able to hold the deck in-place and to prevent relative movement. Therefore, the proposed deck-to-girder connection using epoxy was adequate and may be used in the construction of new glulam girder bridges.

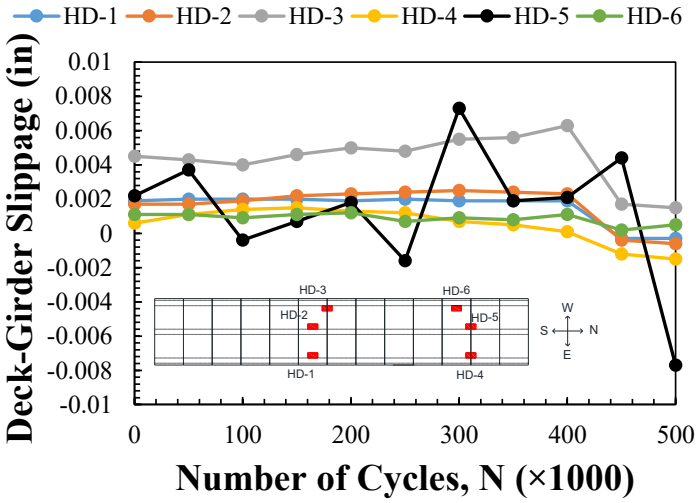

Figure 6.60: Deck-to-Girder Slippage during Fatigue Testing of the Glulam Timber Girder Bridge Specimen

6.2.3.1.5 Girder Load Distribution in Timber Girder Bridge

The load cell data was used to comment on the girder load distribution. The test setup was designed to produce the same loads in the three girders. Figure 6.61 shows the percentage of the load in each girder with respect to the total load during fatigue testing. The girder loads were 3% to 12% different from the target load (33% for each girder), and the overall distribution remained the same throughout the fatigue testing. The differences were attributed to the load cell accuracy, which was 0.5% of the load cell capacity (100 kips). At this low load level, 10% measurement error is expected for these load cells.

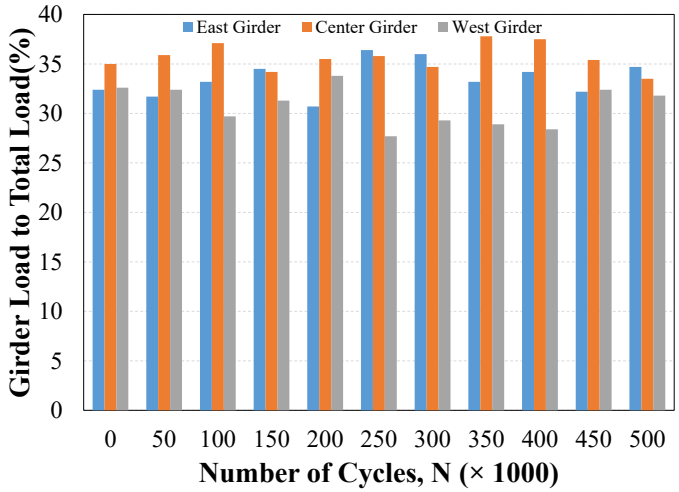

Figure 6.61: Girder Load Distribution During Fatigue Testing of the Glulam Timber Girder Bridge Specimen

6.2.3.2 Strength Testing of Timber Girder Bridge

The actuator load was equally spread to the three girders at the mid-span of the bridge. The bridge was loaded monotonically using a displacement-controlled loading to failure.

6.2.3.2.1 Observed Damage

The first crack in the form of delamination was observed in the west girder of the bridge (6 ft away from the bridge midspan, underneath Panel I shown in Fig. 6.54a) at 101 kips, followed by delamination of the center girder (at the midspan) at 113 kips. When the bridge farther displaced downward, the bridge deck significantly tilted. The specimen failed by simultaneous failure of the west and the interior girders at a peak load of 123 kips (Figure 6.62). There was no apparent damage in the east girder throughout the strength testing.

(a) Failure of West Girder

(b) Failure of West Girder

(c) Failure of Interior Girder

(d) Failure of Interior Girder

(e) Condition of East Girder at Mid-span

(f) Condition of East Girder at Mid-span

Figure 6.62: Glulam Girder Bridge Specimen Failure

6.2.3.2.2 Force-Displacement Relationship

Figure 6.63 shows the measured force-displacement relationship for the glulam girder bridge. The equivalent load level for each of the limit states is also shown in the figure with dashed lines. The bridge

remained linear up to the first cracking, which occurred in the west girder. Load carrying capacity was significantly reduced when the interior girder cracked. The bridge failed at 123 kips.

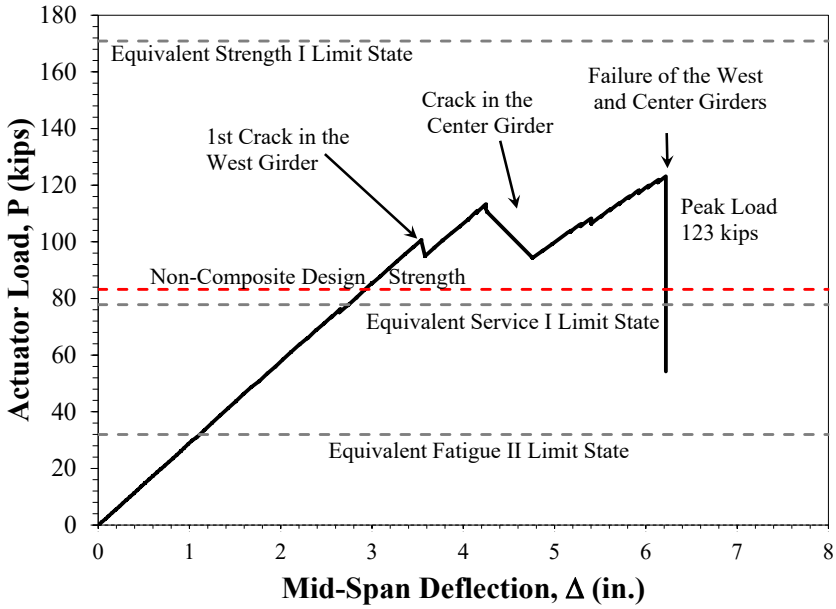

Figure 6.63: Force-Displacement Relationship During Strength Testing of the Glulam Timber Girder Bridge Specimen

Figure 6.63 clearly shows that the bridge did not meet the AASHTO strength limit state requirements because (1) the as-built girder constituent material was weaker than the specified material due to construction error, and (2) the bridge girders were designed assuming composite action. Review of the material datasheet provided by the manufacturer revealed that the girders were built with 24F-2.0E, while the design was based on 26F-1.9E. Furthermore, the strain profiles discussed in the previous section showed that the composite action was not achieved in this type of deck system.

Based on these findings, the bridge was redesigned with the as-built material properties and fully non-composite behavior, and the capacity was shown in Figure 6.63 with a dashed red line. The AASHTO specification requirements can be achieved using the proper design assumptions. Therefore, the AASHTO method for design of timber bridges is applicable for the proposed glulam girder bridges.

6.2.3.2.3 Measured Strains

Figure 6.64 shows the bridge girder strains during the strength testing. Tensile and compressive strains were identified in the graph. The strain distribution was linear for glulam girders up to the failure. The flexural strain capacity of the girder on the tension side was 1900 microstrain, which was 58% higher than the design strain capacity (F_b / E=1200 microstrain) for 24F-2.0E.

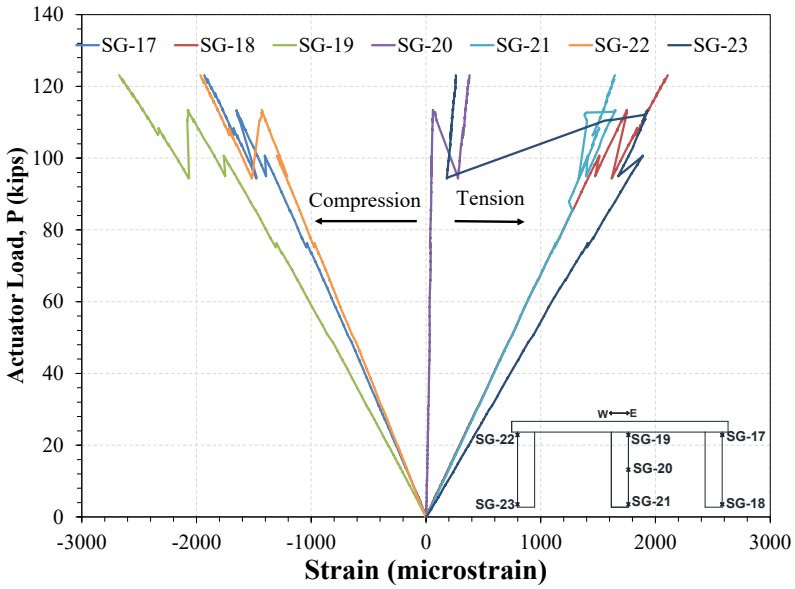

Figure 6.64: Measured Girder Strains During Strength Testing of the Glulam Timber Girder Bridge Specimen

Figure 6.65 shows the strain profile for the east girder of the bridge under the strength loading at various load levels. The glulam girder-deck sections were not composite since the strains were not linear over the depth of the section. However, the assumption of "plane section remains plane" was valid only for the glulam girders. Since the timber girders were laterally supported by panels and cross braces, torsional buckling was not a concern and was not observed.

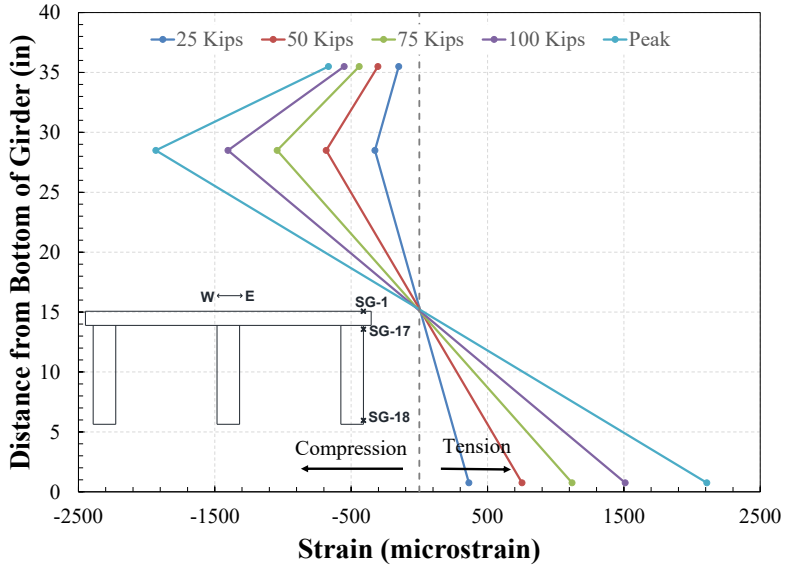

Figure 6.65: East Girder Strain Profile During Strength Testing of the Glulam Timber Girder Bridge Specimen

Figure 6.66 shows the deck strain profile during the ultimate testing at different load levels. Since the maximum strain was lower than the design strain capacities of the deck, the deck thickness was sufficient in the proposed bridge system.

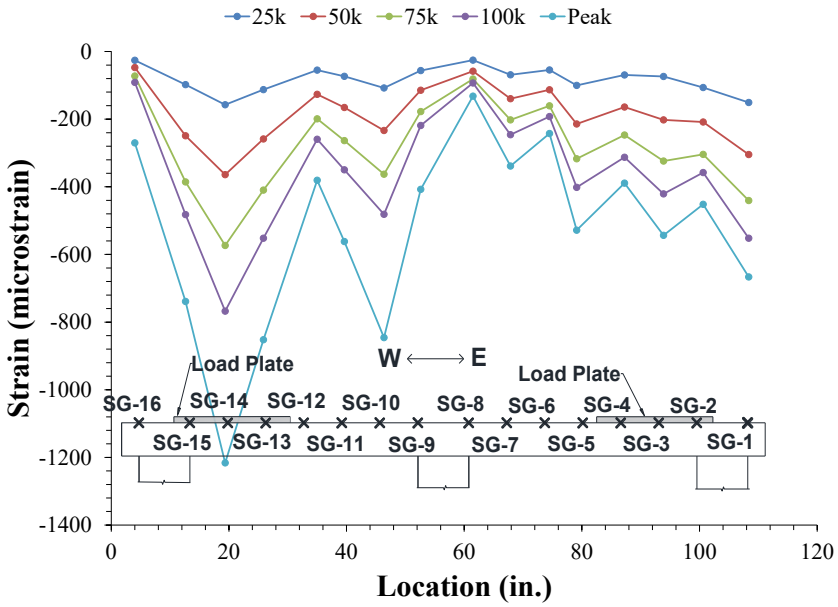

Figure 6.66: Deck Strain Profile During Strength Testing of the Glulam Timber Girder Bridge Specimen

6.2.3.2.4 Joint Rotations and Relative Displacements

LVDTs were placed at the top and the bottom of the bridge deck on the transverse joint closest to the mid-span to measure the joint rotation. Figure 6.67 shows the rotation during the ultimate testing. The

joint rotated monolithically, and rotation increased linearly under the applied load. The maximum rotation was negligible, however.

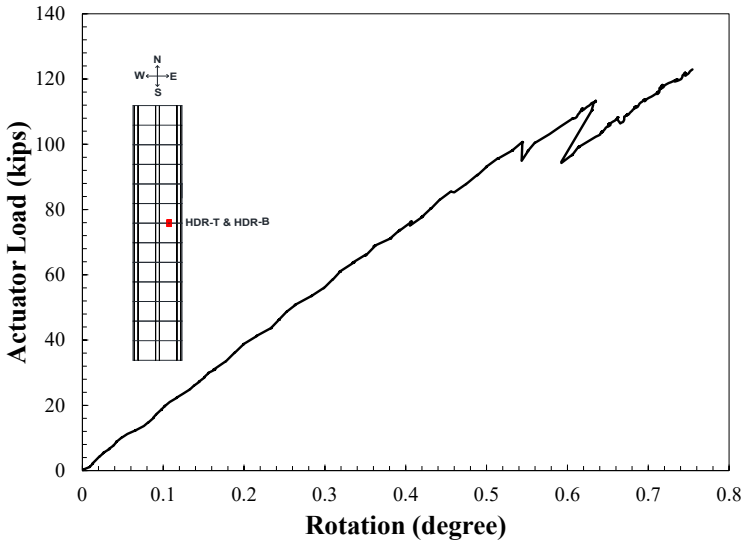

Figure 6.68:

Figure 6.67: Transverse Joint Rotation During Strength Testing of the Glulam Timber Girder Bridge Specimen

The deck-to-girder slippage for six different locations (HD-1 to HD-6) (Figure 6.68) indicates that all of the relative displacements were negligible. For the ultimate test, HD-7 was added to measure the opening of the deck transverse joint at the bottom of the deck. The deck-to-deck opening was higher for HD-7 compared to HD-1 through HD-6 measurements, and the girder failed beneath joint HD-7.

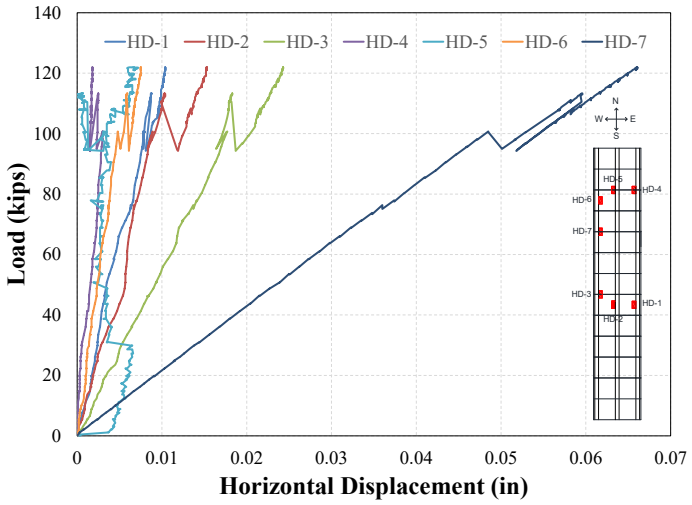

Figure 6.68: Deck-to-Girder Slippage During Strength Testing of the Glulam Timber Girder Bridge Specimen

6.3 Glulam Slab Bridge Specimen

Two types of glulam timber bridges (Figure 5.17) were introduced in the previous chapter: (1) bridges built with transverse glulam decks supported on glulam stringers (referred to as the "girder bridges"),

and (2) longitudinal glulam deck bridges (referred to as “slab bridges”). The structural performance of a glulam slab bridge was evaluated through full-scale experimentation. This section includes a summary of the design, construction, instrumentation, test setup, loading protocols, and test results for the full-scale timber slab bridge test specimen.

6.3.1 Glulam Timber Slab Bridge Test Specimen

6.3.1.1 Design of Test Specimen

Slab bridges can span up to 30 ft. and can cover several lanes of traffic. The prototype glulam timber slab bridge selected in this study was assumed to be 16.5 ft long and 34.5 ft wide (Figure 6.69a). The length was selected based on the manufacturer’s limitations in producing deeper slabs, and the width is typical for two lanes of traffic sufficient for local roads. A full-scale bridge model was selected for testing but with a width approximately equal to the width of one lane of traffic. The bridge test specimen (Figure 6.69b) consisted of (1) two 20-ft long longitudinal deck panels with a depth of 10.75 in. and a width of 48.125 in., and (2) three stiffeners each 7.5 ft long (in the transverse direction of the bridge), 5 in. wide (in the longitudinal direction of the bridge), and 5.5 in. thick. The panels were connected to the stiffeners using two 0.75-in. diameter lag bolts per panel.

(a) Prototype Bridge

(b) Test Model

Figure 6.69: Glulam Timber Slab Bridge

AASHTO (2013) standards and specifications were used in the design of the bridge components. The bridge was designed for HL-93 loading, which consists of a design truck or tandem accompanied by the design lane load.

6.3.1.1.1 Design of Deck Panels

The deck panels were analyzed and designed according to AASHTO (2013). Wheel load fractions were used to calculate the moment demand for each deck panel. The deck panels were designed using mechanical properties for 24F-2.0E Southern Yellow Pine. The final design resulted in 10.75 in. deep, 48.125 in. wide, and 16.5 ft long panels.

To further aid the designers, a spreadsheet was developed to find the capacity to demand ratio of the slab bridge in flexure, shear, compression, and tension. The spreadsheet allows checking the deflection of the bridge for different scenarios.

6.3.1.1.2 Design of Transverse Stiffeners

The transverse stiffeners were also designed according to AASHTO (2013). One stiffener must be placed at the mid-span, and the spacing of the stiffeners cannot exceed 8 feet. According to AASHTO specifications, the strength of a stiffener based on the adjusted modulus of elasticity (*E'*) times the moment of inertia (*I*) must be greater than 80,000 kip-in^2. The stiffeners were designed using 24F-2.0E Southern Yellow Pine. The final design resulted in 5.5 in. deep, 5 in. wide, and 7.5 ft long stiffeners.

6.3.1.1.3 Design of Deck-to-Stiffener Connections

The deck panels were attached to the stiffeners using 0.75-in. diameter lag bolts, each 12 in. long. Two bolts were used per panel. Initially epoxy was considered to be used along the length of the stiffener in addition to the bolts, but the epoxy was deemed unnecessary for this connection since the bolt was connected from the bridge underneath with minimal durability issues.

6.3.1.2 Fabrication and Assembly of Glulam Timber Slab Bridge Test Specimen

The entire test bridge was fabricated in Tea, SD, then shipped as one piece to the Lohr Structures Laboratory. The following sections discuss the fabrication, assembly, and transportation of the test specimen.

6.3.1.2.1 Fabrication of Deck Panels

The glulam deck panels were built from 24F-2.0E Southern Yellow Pine. Thirty-five 1.375-in thick laminations were glued together to form one 48-in. deck panel. The laminations were clamped together to apply pressure and to activate the epoxy between the laminations. This type of epoxy does not activate until a minimum pressure of 150 psi is applied. The panels were stored in the construction facility with ambient room temperature to allow the epoxy to dry and harden.

6.3.1.2.2 Fabrication of Stiffeners

The stiffeners were also made from 24F-2.0E Southern Yellow Pine. Four 1.375-in. thick laminations were glued together to form each stiffener. After the epoxy was placed between the laminations, the panel was clamped to apply pressure. The stiffeners were then stored in ambient room temperature until the epoxy dried and hardened.

6.3.1.2.3 Transportation of Test Specimen

The test specimen was transported from the manufacture site in Tea, SD, to the Lohr Structures Laboratory on a trailer pulled by a pickup truck. In Tea, the deck panels were loaded onto the trailer using a fork lift, and the stiffeners were placed in the truck bed. Upon arrival at the lab, the trailer backed as far into the lab as possible. Two straps were placed around the panels to lift them. The straps were hooked to a 15-ton crane. The panels were then lifted and placed on the reaction blocks.

6.3.1.2.4 Assembly of Test Specimen

The test specimen was assembled in the Lohr Structures Laboratory. First the deck panels were placed beside one another on the reaction blocks, then shimmed to have continuous support. Subsequently, the stiffeners were installed from the underside of the deck. The center stiffener was installed first;

then the other two were bolted to the deck. A pilot hole was initially drilled in the stiffener, and then the lag bolts were screwed 6.5 in. into the underside of the deck.

6.3.1.3 Test Setup for Glulam Timber Slab Bridge

The slab bridge test specimen was tested under two different loading scenarios: fatigue loading, and ultimate (strength) loading. The test setup for the two test procedures were slightly different and are discussed.

6.3.1.3.1 Fatigue Test Setup

The bridge test specimen was continuously supported on two reaction blocks at each end (Figure 6.70). A continuous neoprene bearing pad was used at each end, between the panel and the abutment, to allow the specimen to rotate freely. Two 22-kip actuators were used to apply the load at the center of the panel at the mid-span.

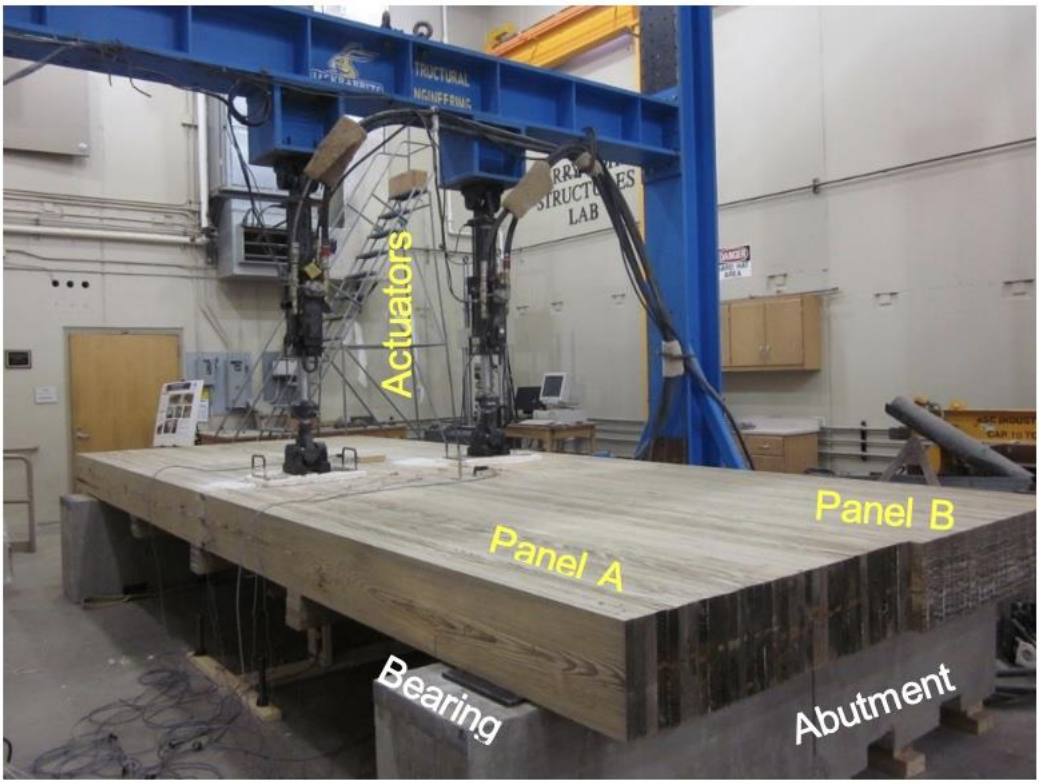

Figure 6.70: Fatigue Test Setup for Glulam Timber Slab Bridge

6.3.1.3.2 Ultimate (Strength) Test Setup

For the ultimate test, a 328-kip actuator was used to monotonically apply the load at the mid-span of the bridge. The load was equally distributed to the two panels using a spreader beam (Figure 6.71).

Figure 6.71: Strength Test Setup for Glulam Timber Slab Bridge

6.3.1.4 Instrumentation Plan for the Glulam Timber Slab Bridge Specimen

The glulam timber slab bridge test specimen was instrumented with strain gauges, LVDTs, load cells, and string potentiometers (string pots) to measure the response of the bridge at different load levels. This section presents the bridge instrumentation detailing.

6.3.1.4.1 Strain Gauges

Each panel was instrumented with three strain gauges on the side surface to measure the strains at different depths of the panel (Figure 6.72). Two additional strain gauges were installed on the top and bottom of the deck 6 in. away from the bridge longitudinal centerline. All deck panel strain gauges were offset 6 in. from the bridge transverse centerline to avoid interfering with the stiffener. The center stiffener was instrumented with five strain gauges measuring the strain in the transverse direction (Figure 6.72c). Wood strain gauges (PFL-30-11-5L), each with a length of 30 mm (1.18 in.), were used in this project.

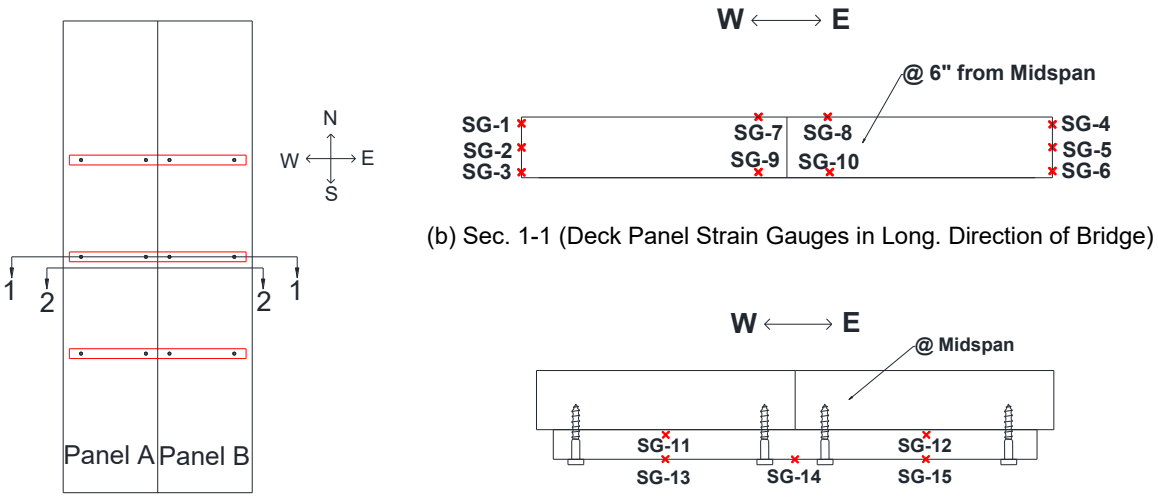

(a) Bridge Plan View

(b) Sec. 1-1 (Deck Panel Strain Gauges in Long. Direction of Bridge)

(c) Sec. 2-2 (Stiffener Strain Gauges in Trans. Direction of Bridge)

Figure 6.72: Strain Gauge Plan for the Glulam Timber Slab Bridge Specimen

6.3.1.4.2 Linear Variable Differential Transformers

Fourteen LVDTs were used to record displacements and rotations at various locations of the glulam timber slab bridge specimen (Figure 6.73). Since the panels were placed on bearing pads that compress under applied load, vertical LVDTs were installed at the end of each panel to measure the deformation of the pads and to calculate the net mid-span deflection. Two additional vertical LVDTs were placed at the mid-span under the stiffener to measure deflection. Two more vertical LVDTs were placed 4.5 in. away from the mid-span on the deck panels. Six horizontal LVDTs were used to measure the slippage, relative displacements, and rotations. The HD-1 was installed to measure the slippage between the deck panels in the longitudinal direction. The HD-2 was used to measure the relative transverse displacement of the deck panels. The HD-3 was installed to measure the slippage between the deck panels and the stiffener. Two rotational LVDTs were installed above and below the longitudinal joint to measure the joint rotation.

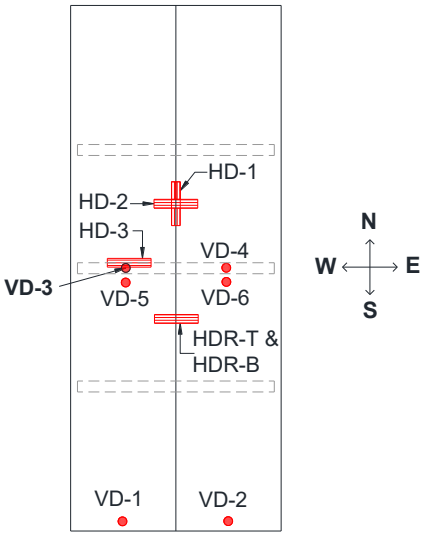

Figure 6.73: LVDT Installation Plan for the Glulam Timber Slab Bridge Specimen

6.3.1.4.3 String Potentiometers (String POTs)

Since string potentiometers have a larger measuring range than LVDTs, they were used at the mid-span of the bridge during the ultimate test to measure deflections. The string pots were installed at the centerline of the girders at their bottom face.

6.3.1.4.4 Data Acquisition System

All of the instrumentation was connected to a 128-channel data acquisition system by Vishay. A scan rate of 10 readings per second was used for the monotonic loading and a scan rate of 100 readings per second was used for cyclic loading.

6.3.1.5 Test Procedure for the Glulam Timber Slab Bridge Specimen

The bridge specimen was tested under two loading scenarios: fatigue and ultimate. Fatigue testing was performed to investigate the performance of the bridge under 50 years of service, and the ultimate testing was carried out to determine the capacities of the bridge. The test procedures are described in detail.

6.3.1.5.1 Fatigue Testing

Phase I of slab bridge testing was fatigue loading. Two 11-kip point loads were cyclically applied at the mid-span of the bridge (Figure 6.70). The fatigue loading protocol was determined using the AASHTO (2013) Fatigue II Limit State specifications. Since the slab bridge specimen is shorter than 40 ft, every truck passing the bridge applies two load cycles. This is because there are two 32-kip axles per truck, each has a significant contribution to the maximum moment. Therefore, applying two load cycles on the test bridge was equivalent to one truck load in field. The fatigue test was performed with 550,000 cycles of loading, which is equivalent to 50.2 years of the service life based on the expected average daily truck traffic of 15. The load was applied at a frequency of 1.3 Hz and a magnitude of 22 kips. Stiffness tests were performed at an interval of 50,000-load cycles including an initial stiffness test.

The stiffness load amplitude was 30 kips. The load was applied under a displacement-based control condition at a displacement rate of 0.007 in/sec.

6.3.1.5.2 Ultimate Testing

After completion of the fatigue testing, an ultimate test was carried out to determine the capacity of the bridge and to investigate the failure mode. A point load was applied at the mid-span of the bridge. The specimen was loaded under a monotonic displacement-controlled protocol to failure with a displacement rate of 0.007 in/sec. The data was recorded after completion of each displacement step, which was 0.02 in.

6.3.2 Material Properties for the Glulam Timber Slab Bridge Specimen

Grade 24F-2.0E glulam was used for the construction of the test specimen. Table 6.7 presents the mechanical properties of the material. Correction factors were applied to these values for the design.

Table 6.7: Mechanical Properties of Glulam Timber Used in Slab Bridge

Properties	Notation	Unit	24F-2.0E
Tension Zone Stressed in Tension	F_{bxo}^{+}	ksi	2.4
Compression Zone Stressed in Tension	F_{bxo}^{-}	ksi	1.45
Shear Parallel to Grain	F_{vxo}	ksi	0.265
Modulus of Elasticity	E_{xo}	ksi	2000

6.3.3 Test Results of Timber Slab Bridge Specimen

The slab bridge specimen was first tested under 550,000 cycles of the AASHTO (2013) Fatigue II loading using two 22-kip actuators at the mid-span. Then, it was loaded monotonically to failure using a 328-kip actuator applying point loads at the mid-span. Results of each testing are presented.

6.3.3.1 Fatigue Testing of the Glulam Timber Slab Bridge Specimen

6.3.3.1.1 Observed Damage

The only apparent damage during the fatigue test was the widening and extending of existing natural or manufacturing cracks at higher load cycles

(

(a) Crack Growth after 550k Cycles – Elevation View

(b) Crack Growth after 550k Cycles – Slab at North Support

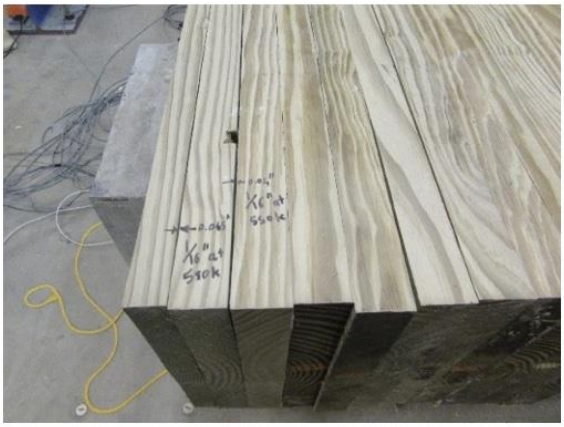

(c) Separation of Lamination after 550k Cycles at Southwest Support

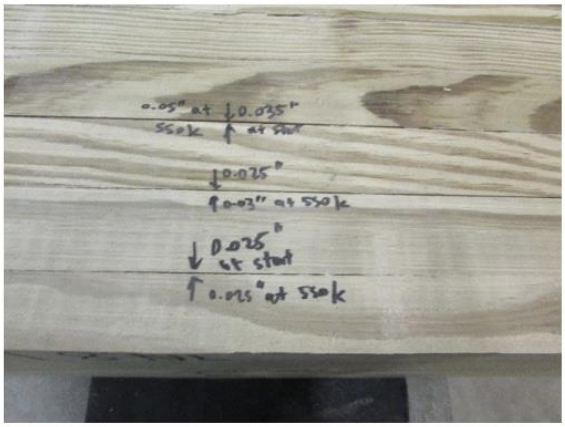

(d) Separation of Lamination after 550k Cycles at Southeast Support

Figure 6.74). For example, the crack between the two laminations at the south end of the bridge was increased from 0.06 in. to 0.0625 in. before and after 550,000 load cycles. In field applications, the bridge deck will be flooded with epoxy; thus, the damage observed during testing should not occur. No other damage was observed in the fatigue testing of the slab bridge.

(a) Crack Growth after 550k Cycles – Elevation View

(b) Crack Growth after 550k Cycles – Slab at North Support

(c) Separation of Lamination after 550k Cycles at Southwest Support

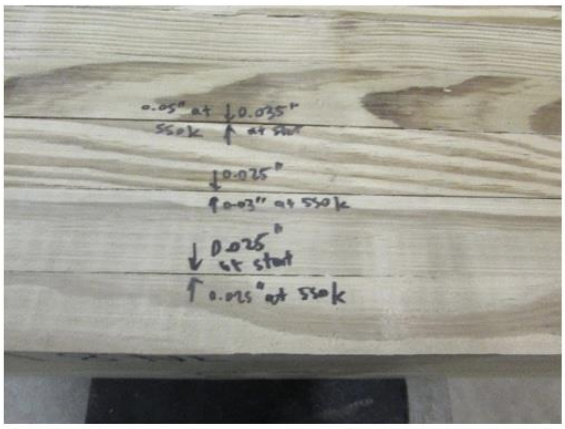

(d) Separation of Lamination after 550k Cycles at Southeast Support

Figure 6.74: Observed Damage during Fatigue II Testing of the Glulam Timber Slab Bridge Specimen

6.3.3.1.2 Stiffness Degradation

Figure **6.75** shows the measured force-displacement relationships for the glulam slab bridge during the stiffness tests that were performed after every 50,000 load cycles. The bridge essentially remained linear-elastic during the fatigue testing with no stiffness degradation. The stiffness is the ratio of the actuator load to the average net mid-span deflection of the deck panels.

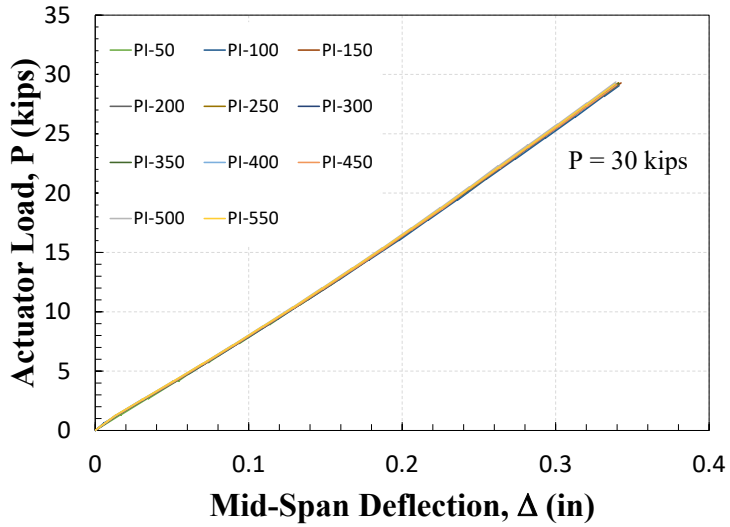

Figure 6.75: Measured Stiffness During Fatigue II Testing of the Glulam Timber Slab Bridge Specimen

Figure 6.76 shows the measured effective stiffness (*EI*) versus the number of load cycles. The overall bridge stiffness remained constant throughout the fatigue testing confirming that the proposed glulam slab bridge detailing is structurally viable for the design service life.

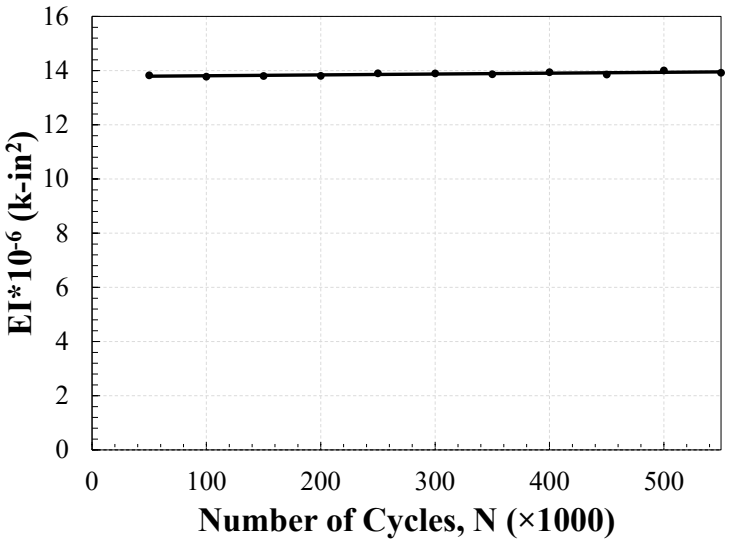

Figure 6.76: Stiffness Degradation During Fatigue II Testing of the Glulam Timber Slab Bridge Specimen

6.3.3.1.3 Measured Strain

Strain profiles of the deck panels throughout fatigue testing did not change (Figure 6.77), indicating minimal damage and degradation of the bridge. The strain distribution was almost linear showing that the "plane section remains plane" assumption is valid for the design of timber slab bridges. The strain profile might not be completely linear due to a slight misalignment of the strain gauges.

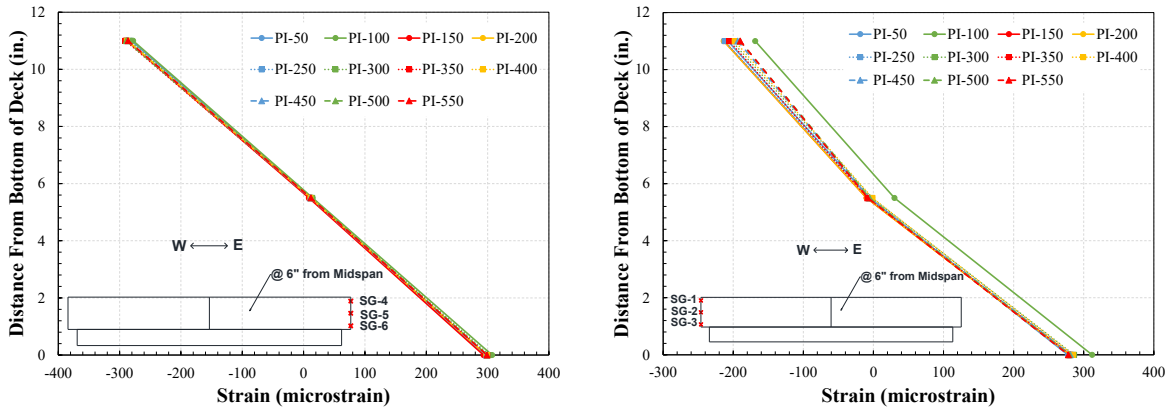

(a) East Face of Deck Panel

(a) West Face of Deck Panel

Figure 6.77: Deck Panel Strain Profiles under Fatigue II Testing of the Glulam Timber Slab Bridge Specimen

6.3.3.1.4 Joint Rotations and Relative Displacements

The measured joint rotations in the transverse direction of the bridge versus the number of load cycles for one of the transverse joints indicates that joint rotations were very small and remained relatively constant through all 550,000 load cycles of the fatigue II testing (Figure 6.78).

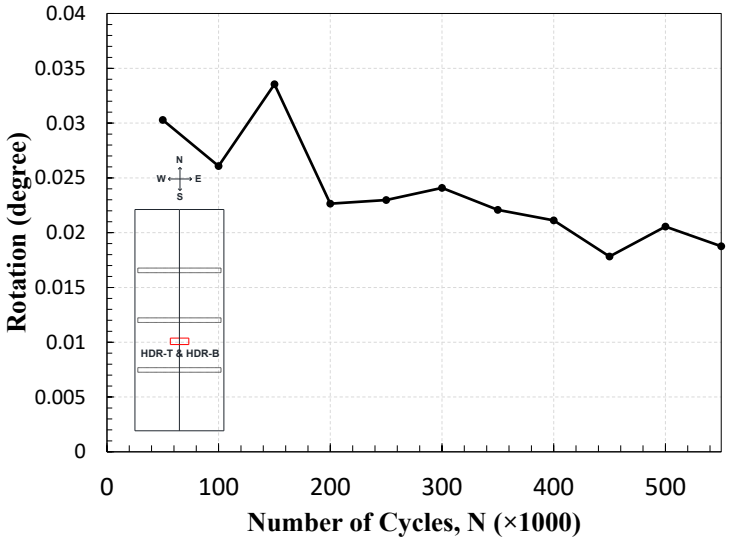

Figure 6.78: Joint Transverse Rotation During Fatigue II Testing of the Glulam Timber Slab Bridge Specimen

Shown in Figure 6.79 are the (1) slippage between the two slabs (LVDT HD-1) in the longitudinal direction of the bridge, (2) opening of the joint at the bottom of the specimen (LVDT HD-2) in the transverse direction of the bridge, and (3) slippage between the deck and the stiffener (LVDT HD-3) in the transverse direction of the bridge during each stiffness test. All of these values were negligible, indicating adequate performance.

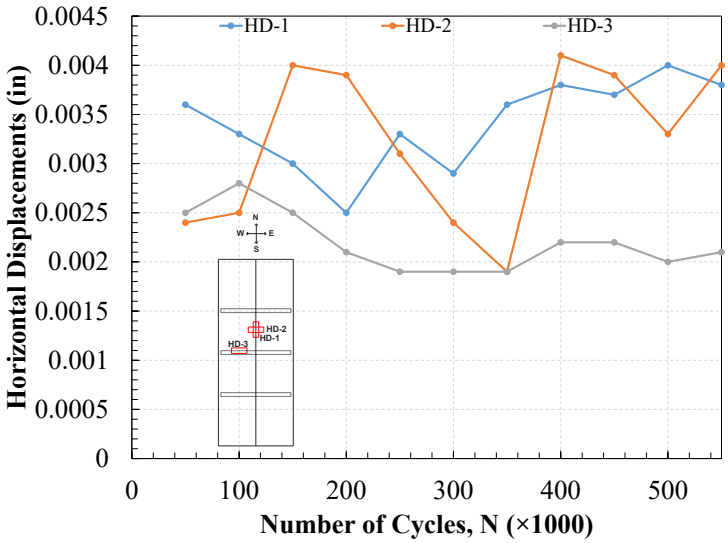

Figure 6.79: Horizontal Joint Displacements During Fatigue II Testing of the Glulam Timber Slab Bridge Specimen

6.3.3.2 Ultimate (Strength) Testing of the Glulam Timber Slab Bridge Specimen

The actuator load was equally spread to the two panels at the mid-span of the bridge at the centerline of each panel. The deck panels were loaded monotonically under a displacement-controlled loading protocol until 270 kips, when the test was stopped due to setup limitations.

6.3.3.2.1 Observed Damage

There was no major damage throughout the entire strength testing of the glulam timber slab bridge specimen (**Error! Reference source not found.**). The only apparent damage was the widening and e xtending of the existing wood cracks and minor separation of the stiffeners from the deck panels (**Error! Reference source not found.**b). This problem could be easily fixed be retightening the bolts, if n eeded.

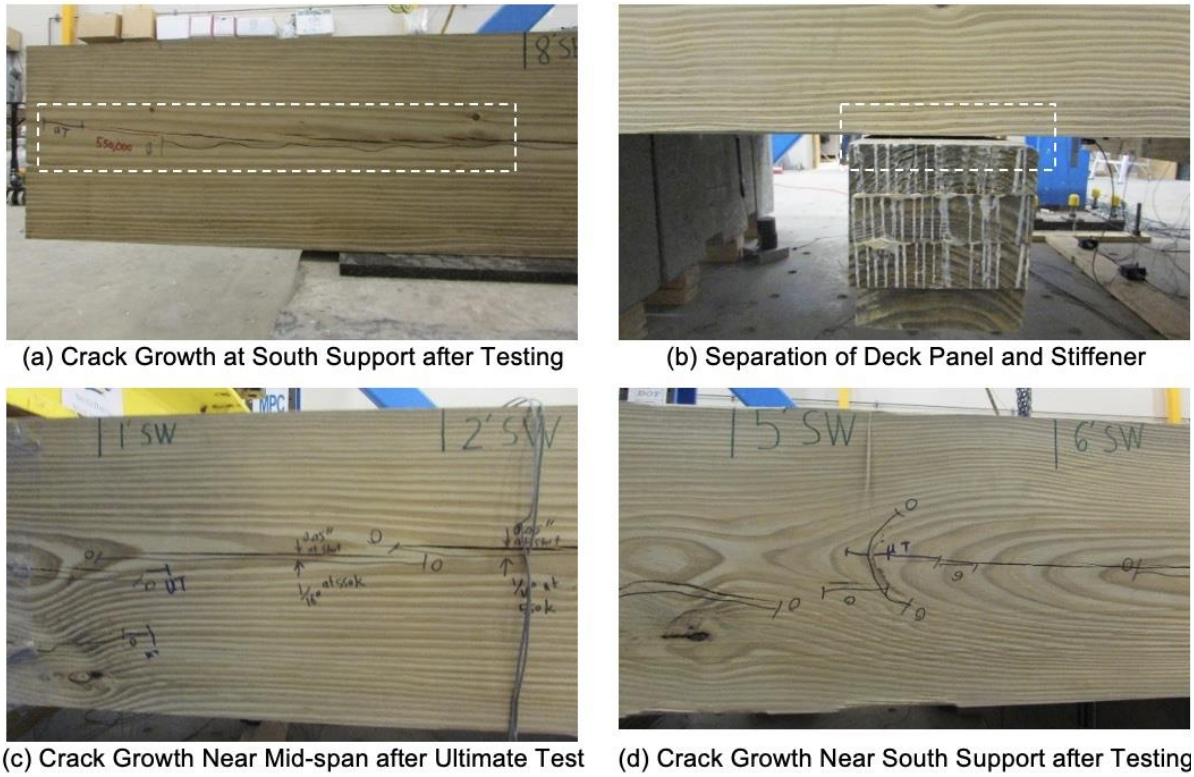

(a) Crack Growth at South Support after Testing

(b) Separation of Deck Panel and Stiffener

(c) Crack Growth Near Mid-span after Ultimate Test

(d) Crack Growth Near South Support after Testing

Figure 6.80: Damage of Glulam Slab Timber Bridge Specimen under Ultimate Loading

6.3.3.2.2 Force-Displacement Relationship

Figure 6.81 shows the measured force-displacement relationship of the timber slab bridge during the strength testing. The equivalent loads for each of the AASHTO (2013) limit states are also shown in Figure 6.81 with dashed lines. The test was stopped at a peak load of 270 kips due to the setup limitations. Based on AASHTO (2013) specifications, the allowable displacement for the service limit state is 0.466 in for this bridge. The measured service level displacement was 0.29 in., which is lower than the AASHTO (2013) requirement indicating that the design was adequate. Note these limit state values are not the same for different bridges due to their geometry. Overall, since there was no significant damage, and the bridge surpassed all the AASHTO (2013) limit states, it can be concluded that this bridge is a viable short-span option for local roads.

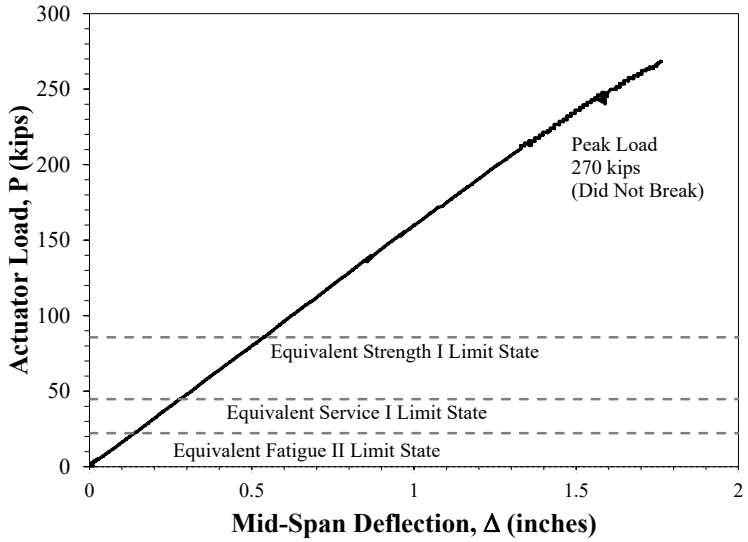

Figure 6.81: Force-Displacement Relationship During Strength Testing of the Glulam Timber Slab Bridge Specimen

6.3.3.2.3 Measured Strains

Figure 6.82 shows the strains in the deck in the longitudinal direction of the bridge during the strength testing. Negative numbers correspond to compression, and positive numbers correspond to tension. The strain distribution is linear for the panels. The lower bound flexural strain capacity of the panels on the tension side was 4,000 microstrain, which was 3.33 times higher than the design strain capacity (F_b / E=1200 microstrain) for 24F-2.0E glulam timber.

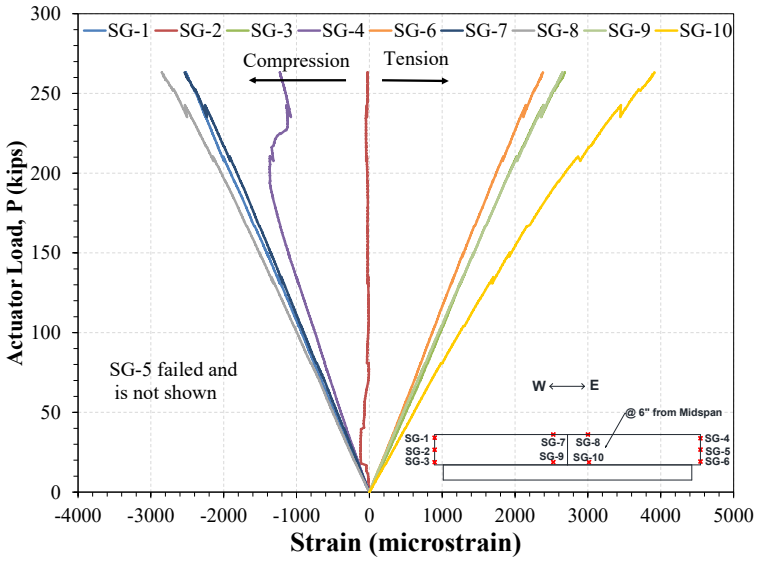

Figure 6.82: Measured Deck Strains During Strength Testing of the Glulam Timber Slab Bridge Specimen

Figure 6.83 shows the strains in the middle stiffener in the transverse direction of the bridge during strength testing. The strains were not completely linear since there was some slight slippage between the deck panels and the stiffeners, changing the load transfer between the members. Overall, it can

be concluded that the stiffeners were engaged at different load levels; thus, they should be used in the design and construction of this type of bridges to unify the deck system.

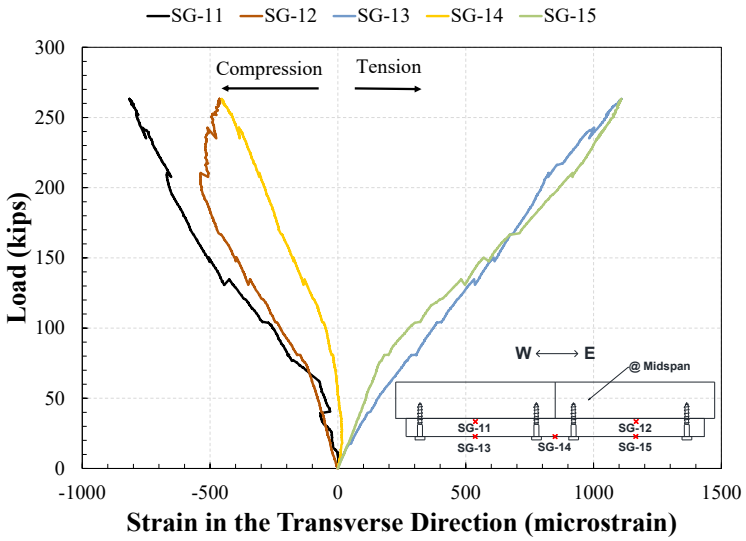

Figure 6.83: Measured Stiffener Strains During Strength Testing of the Glulam Timber Slab Bridge Specimen

6.3.3.2.4 Joint Rotations and Relative Displacements

LVDTs were installed at the top and bottom of the specimen on the longitudinal joint in the bridge transverse direction to measure the joint rotations. During the ultimate testing, the joint rotation increased approximately linearly under the applied increasing load (Figure 6.84). However, the maximum rotation was negligible.

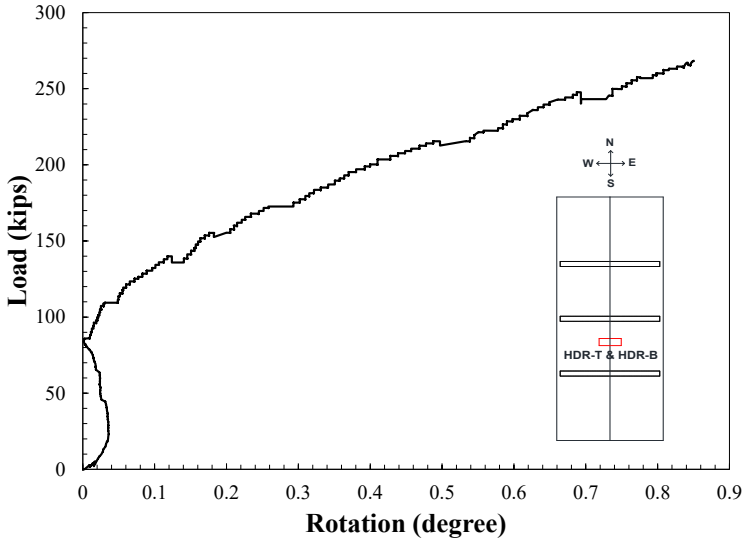

Figure 6.84: Joint Transverse Rotation During Strength Testing of the Glulam Timber Slab Bridge Specimen

During ultimate testing, Figure 6.85 shows: (1) slippage between the two panels (using LVDT HD-1) in the longitudinal direction of the bridge, (2) opening of the joint at the bottom of the specimen (HD-2)

in the transverse direction of the bridge, and (3) slippage between the deck and the stiffener (HD-3) in the transverse direction of the bridge. The deck panel's relative movement was negligible in the longitudinal direction of the bridge. All relative displacements were negligible at the AASHTO (2013) service limit state (less than 0.01 in.), as well as the AASHTO strength limit state (approximately 0.015 in.). However, the longitudinal joint opened in the transverse direction of the bridge, and the stiffener slipped with respect to the panels at higher loads.

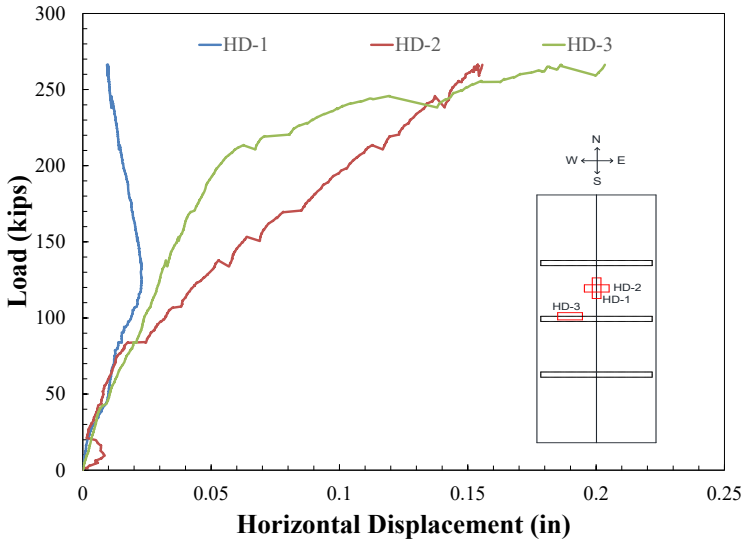

Figure 6.85: Relative Horizontal Joint Displacements During Strength Testing of the Glulam Timber Slab Bridge Specimen

7 EVALUATION OF PROPOSED BRIDGE SYSTEMS

This chapter presents an evaluation of the three proposed bridge systems including: (1) structural performance, (2) comparison with the inverted tee bridges (for the precast bridge only), (3) constructability, and (4) superstructure costs.

7.1 Full-Depth Deck Panels Supported on Inverted Tee Girders

7.1.1 Performance under Service, Fatigue II, and Strength Limit States

The number of trucks passing the prototype bridge over a 75-year design life is 411,000 based on the average daily truck traffic (ADTT) of 15 for local roads in South Dakota. The full-scale single-lane test bridge was subjected to 500,000 load cycles at the mid-span and an additional 150,000 load cycles adjacent to the mid-span panel transverse joints to maximize the shear transfer. The load at the mid-span corresponded to the moment experienced by the interior girders of the prototype bridge based on the Fatigue II limit state loading specified by AASHTO (2013).

The test bridge stiffness did not degrade, and the joints remained water-tight through 650,000 fatigue load cycles (Figure 7.1). The 650,000 fatigue load cycles are equivalent to 119 years of service for this bridge on South Dakota local roads. The stiffness change during the entire fatigue test was less than 3% with respect to the bridge's initial stiffness. Narrow or shallow shrinkage cracks were observed in the haunch region and the deck full-depth pockets, as well as the transverse joints filled with either conventional grout or latex modified concrete. However, no crack was observed on the hidden pockets. No other significant damage was observed during the entire fatigue testing for decks, joints, and girders.

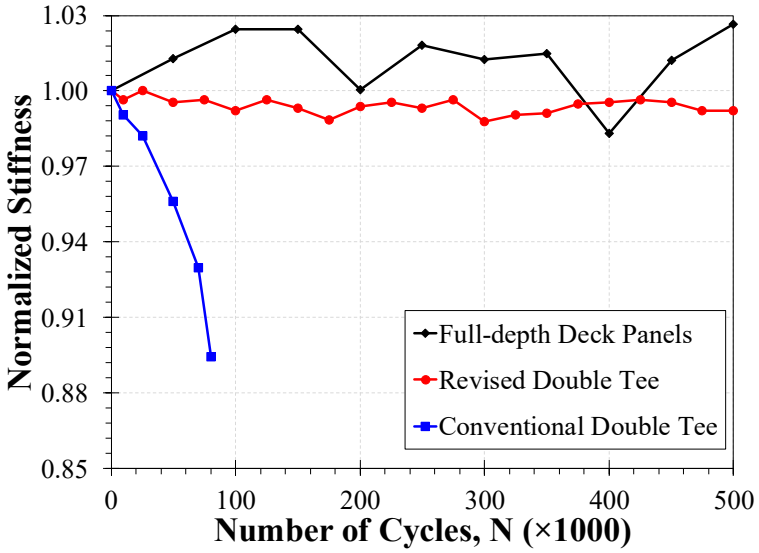

Figure 7.1: Comparison of Stiffness Degradation for Precast Bridges

Double-tee bridges consist of precast prestressed girders commonly used for superstructure bridges on South Dakota local roads. A previous experimental study by Wehbe et al. (2016) was performed to revise the longitudinal joint detail to improve serviceability and strength performance of double-tee bridges. They showed that the stiffness of the revised double-tee girders did not deteriorate under

500,000 fatigue load cycles, while original double-tee girders were not structurally sufficient for long-term performance (Figure 7.1). This experimental study confirmed that the stiffness of the full-depth deck panels supported on inverted tee girders can be expected to remain essentially the same for 75 years of service.

The equivalent AASHTO (2013) Service I limit state load was 76.7 kips, and the Strength I limit state load was 131.4 kips for the proposed precast bridge. The test bridge girders did not crack at these limit states. The test bridge girder's first flexural crack occurred at a load of 149 kips, which indicates that the bridge has adequate capacity (Figure 7.2). More cracks formed on the girders at higher loads. The test was stopped at 263 kips due to setup limitations. The load corresponding to the flexural failure of the test bridge was 402 kips based on a moment-curvature analysis. No significant damage was observed in the deck panels, joints, and haunch region under the entire ultimate testing.

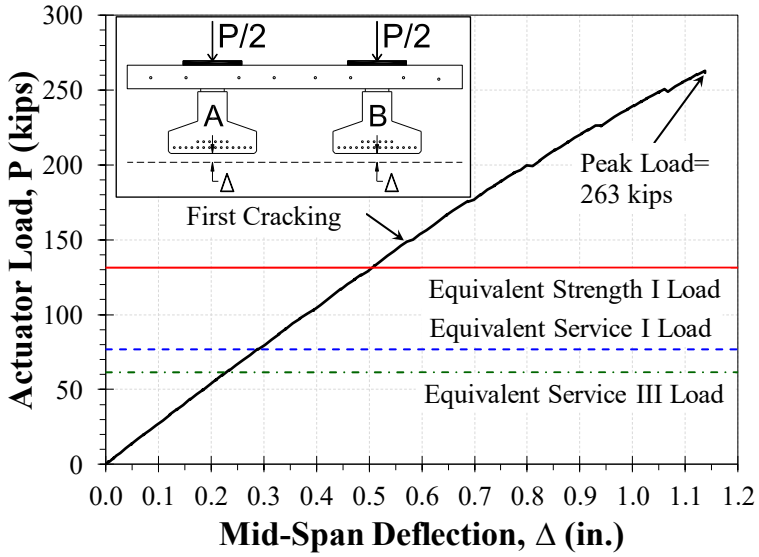

Figure 7.2: Measured Force-Displacement Relationship for Proposed Precast Bridge

7.1.2 Constructability

The constructability of the main components of the precast full-depth deck panels supported on inverted tee girders is evaluated.

7.1.2.1 Precast Inverted Tee Girders

The precast inverted tee girders were cast using partial-depth I-girder forms. Overall, the proposed girder design and construction are similar to current practice.

An actual bridge on a local road will typically consist of seven inverted tee girders; whereas, local road bridges built with double-tee girders consist of nine girders. Onsite construction is expected to be rapid for each system but more involved for the proposed inverted tee girder bridges since there are more joints to be filled.

7.1.2.2 Full-Depth Deck Panels

The formwork for full-depth deck panels were made of 2 by 4-in. lumber and 1-in. plywood. Overall, current practice can be applied for the design and construction of the proposed deck panels.

The full-depth deck panels were quickly installed in the laboratory. In terms of onsite activities, special care should be taken on the adjustment of the panel grades, which can be easily done by adjusting the leveling bolts. Double-tee bridges will be easier to install onsite since the deck is integrated with the webs.

7.1.2.3 Shear Pockets

The hidden pocket detail was formed using plywood for the pocket and PVC pipes for the grout and vent ports. Fabrication of the hidden shear pockets was relatively easy and efficient. Pockets should be cleaned before installation of the panel.

7.1.2.4 Horizontal Shear Studs

Both the double headed and inverted U-shape shear studs were found to be viable options for use in inverted tee girders. The studs are installed prior to girder casting.

7.1.2.5 Transverse Joints

The transverse joint groove-to-groove shear key geometry was formed with plywood. The Hollow Structural Steel (HSS) sections were secured to the transverse joint formwork using threaded rods, nuts, and steel plates inside the HSS. Transverse joints can be easily prepared, sealed, and filled with grout from the top of the bridge during onsite construction.

7.1.2.6 Leveling Bolts

A leveling bolt device was formed using a threaded rod welded to a steel plate at the bottom and a nut at the top, a vertical steel pipe embedded in concrete to encase the rod, and a 2 in. by 4-in. lumber piece for the blockout at the top of the deck (Figure 7.3).

Figure 7.3: Leveling Bolt Construction Detail

7.1.2.7 Grouted Haunch

It is expected that forming and sealing the grouted haunch of the proposed system from the top of the bridge will be the most challenging onsite activity. In the laboratory, the grouted haunch was formed by securing 2 in. by 4 in. lumber between the girders to hold ¾ in. thick plywood against the girder sides (Figure 7.4). Placing the forms inside the girders was easier than placing forms outside the girders, which required clamping reaction lumber to the bridge deck to secure 2 in. by 4 in. struts and to hold the plywood.

Figure 7.4: Grouted Haunch Region Formwork Installed between Girders

7.1.3 Precast Bridge Cost Estimate

Table 7.1 presents a comparison of superstructure materials and fabrication cost for the proposed precast bridge system and the inverted tee (new detailing based on Wehbe et al., 2016) systems for a 50-ft long by 34.5-ft wide bridge. Materials and fabrication cost for 46 in. wide by 23 in. deep precast double-tee girders is approximately $247 per linear foot, based on data provided by SDDOT. The nine double-tee girders are used in a 50-ft long by 34.5-ft wide bridge would cost approximately $111,000 for the superstructure materials and fabrication.

Table 7.1: Proposed Precast Bridge and Inverted Tee Superstructure Material and Fabrication Cost Comparison

Bridge System	Precast Full-Depth Deck Panels on Inverted Tee Girders	Inverted Tee Girders
Materials/Fabrication ($)	123,000	111,000
Materials/Fabrication ($/sq. ft.)	71	64

The 21 in. deep precast inverted tee girders were estimated to cost $130 per linear foot, and the precast 8 in. thick full-depth deck panels were estimated to cost $45 per square ft. The 50 ft long by 34.5 ft wide actual bridge materials and fabrication cost estimate in Table 6.1 was calculated based on seven 50 ft long by 21 in. deep precast inverted tee girders with a total cost of $45,500, and five 34.5 ft wide by 10 ft long by 8 in. deep precast full-depth deck panels with a total cost of $77,625. The total materials and fabrication cost estimated by the manufacturer for precast full-depth deck panels supported on inverted tee girders is approximately $123,000 for the actual bridge. Therefore, the materials and fabrication cost of this type of bridges is approximately 11% more than that for double-tee bridges.

Note that other costs such as mobilization, onsite activities, and substructure fabrication and construction are not included in Table 7.1. The total superstructure cost including mobilization and onsite activities for the proposed precast bridge is estimated to be from $99 to $108 per square foot. This data was not available for double-tee bridges at the time of this writing.

Overall, the cost of the proposed bridge system is slightly more than the double-tee bridge system, which is the most common type of bridge on South Dakota local roads. It is expected that the proposed precast bridge system will be more competitive with the double-tee bridges when spans are more than 40 ft.

7.2 Glulam Timber Girder Bridges

7.2.1 Performance under Service, Fatigue II and Strength I Limit States

Based on the Average Daily Truck Traffic (ADTT) of 15 for local roads in South Dakota, approximately 411,000 trucks will cross a bridge in 75 years. The full-scale 50-ft long test bridge was subjected to 500,000 load cycles at the mid-span to simulate the traffic loading for 75 years. The load at the mid-span corresponded to the maximum moment experienced by the interior girders of the prototype bridge based on the Fatigue II limit state loading specified in AASHTO (2013).

The bridge specimen's stiffness did not degrade throughout the 500,000 cycles (Figure 7.5). The change in the stiffness throughout the fatigue test was less than 3% compared to the initial bridge stiffness. The only damage observed during the fatigue testing was at the deck-to-deck connections in which the tongue-and-groove connection cracked. This type of connection shall be avoided in field applications. One possible solution is to place the two deck panel faces directly against one another and to fill the joint with wood adhesive epoxy.

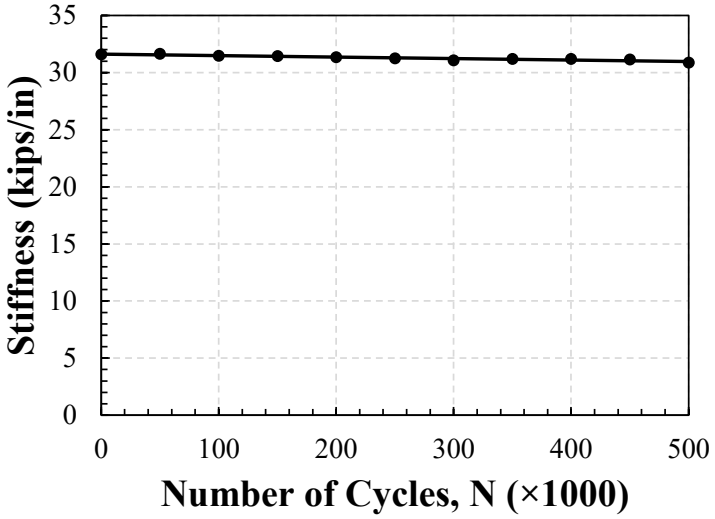

Figure 7.5: Stiffness of Glulam Timber Girder Bridge under Fatigue II Loading

Figure 7.6 shows the measured load-deflection for the glulam timber girder bridge specimen. Shown in the figure are the equivalent AASHTO (2013) service I limit state load (77.8 kips) and the Strength I Limit State load (170.9 kips). The first crack in the glulam timber bridge girders occurred at a load of 101 kips, 30% higher than the Service I Limit State load. However, the specimen's load carrying capacity of 123 kips was lower than estimated and the girders failed before reaching the Strength I Limit State load. Overestimation of the specimen's load carrying capacity was due to (1) a construction error which resulted from using weaker than specified wood grade, and (2) the incorrect design assumption that composite action would develop between the girders and the deck panels. The design capacity of a non-composite timber girder bridge with the same geometry and materials as those used in the bridge test specimen would be 83.21 kips, which is less than the measured load carrying capacity of 123 kips. Thus, glulam girder bridge design should be conservatively based on non-composite section. No significant damage was observed on the deck panels throughout the ultimate testing.

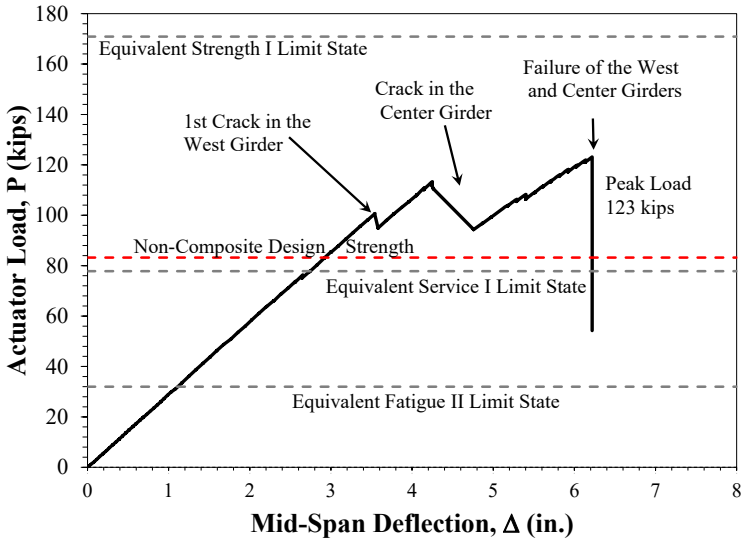

Figure 7.6: Force-Displacement Relationship during Strength Testing of the Glulam Timber Girder Bridge Specimen

Overall, the AASHTO (2013) method of design for glulam girder bridges was found to be adequate assuming non-composite behavior.

7.2.2 Constructability

The constructability of the main components of a glulam timber girder bridge is evaluated. The construction of this bridge system is generally fast and does not require skilled labor.

7.2.2.1 Glulam Girders

The glulam girders will be prefabricated in a controlled environment at the manufacturer's plant. A 34.5-ft wide bridge will consist of nine glulam girders. Onsite activities regarding the girders would be minimal since they would be prebuilt and ready to be put in place.

The construction of a glulam timber girder bridge can be further accelerated if the bridge is prefabricated. The timber bridge construction can be in line with the Accelerated Bridge Construction (ABC) paradigm if the bridge is prefabricated in one or more segments and shipped to the bridge site. This is especially favorable since wood is a relatively light weight material.

7.2.2.2 Glulam Deck Panels

The glulam deck panels will be prefabricated in a controlled environment at the manufacturer's plant. Field installation of the deck panels can be relatively fast and requires minimal training and skills. The construction workers will place adhesive epoxy between the girders and the deck to complete the deck-to-girder connections. The amount and placement of epoxy, and surface preparation should follow the epoxy manufacturer's requirements. As was discussed in the previous section, a fully prefabricated bridge in line with ABC does not need this step.

7.2.2.3 Glulam Cross Braces

The glulam cross-bracing will be prefabricated in a controlled environment at the manufacturer's plant. The field installation of glulam diaphragms is more involved than the other members, since diaphragms have to be placed perfectly between the girders. After alignment, the workers will drill lag bolts through the diaphragms into the girders. If the system is prefabricated, this process will be eliminated in the field.

7.2.3 Costs of Glulam Timber Girder Bridges

Table 7.2 presents material and fabrication costs for the superstructures of 50-ft span, two-lane, glulam timber girder bridge and a inverted tee bridge (new detailing based on Wehbe et al., 2016). The materials and fabrication cost for 46-in. wide by 23-in. deep precast double-tee girders is approximately $247 per linear foot based on data provided by SDDOT. Nine double-tee girders are used in a 34.5-ft wide bridge. Therefore, the total superstructure materials and fabrication cost for this bridge is approximately $111,000.

Table 7.2: Material and Fabrication Cost for Glulam Timber Girder Bridge and Inverted Tee Bridge Superstructures

Bridge System	Glulam Timber Girder Bridge	Inverted Tee Bridge
Materials/Fabrication ($)	78,000	111,000
Materials/Fabrication ($/sq. ft.)	45	64

The total material and fabrication cost estimated by the manufacturer for a 50-ft long and 34.5-ft wide glulam timber girder bridge is approximately $78,000, which was also verified by the research team. Therefore, the materials and fabrication cost of this type of bridge is approximately 30% less than that for double-tee bridges. The transportation cost for glulam girder bridges is $2.65 per mile at the time of this writing. Additional costs such as assembly, onsite activities, life cycle costs, and substructure fabrication and construction should be added to the total bridge cost. Including the additional costs, glulam timber girder bridges are estimated to be 15%-20% less costly to construct and install than the inverted tee bridges.

7.3 Glulam Timber Slab Bridge Prototype

7.3.1 Performance under Service, Fatigue II and Strength I Limit States

Based on the average daily truck traffic (ADTT) of 15 for local roads in South Dakota, approximately 411,000 trucks will cross a bridge in 75 years. Since these types of bridges are very short span, each truck will count as two load cycles (the maximum moment will occur when each of the rear axles crosses the mid-span). The full-scale 16.5-ft long test bridge was subjected to 550,000 load cycles at the mid-span, which is equivalent to 50 years of traffic loading. Note each truck in field would load the slab timber bridge twice due its short span length thus every two-load-cycle in the lab was equivalent to one truck load. The fatigue test was stopped at this load cycle since there was no damage to the bridge, and the stiffness did not degrade. The load at the mid-span corresponds to the maximum moment experienced by an interior deck panel of the prototype bridge based on the Fatigue II limit state loading specified in AASHTO (2013).

The test bridge stiffness remained constant throughout the 550,000 fatigue II loading (Figure 7.7). The change in stiffness throughout the fatigue test was less than 1% with respect to the initial bridge stiffness. There was no apparent damage from the fatigue testing. Therefore, it can be concluded that this bridge system is adequate for the entire service life.

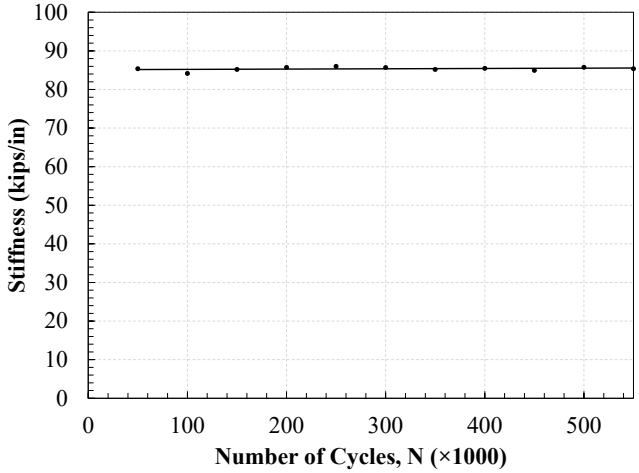

Figure 7.7: Stiffness of Glulam Timber Slab Bridge under Fatigue II Loading

The equivalent AASHTO (2013) service I limit state load was 44.8 kips and the strength I limit state load was 85.7 kips (Figure 7.8). Note these limit state values are not the same for different bridges due to their geometry. The test bridge did not crack up to 270 kips where the test was stopped due to setup limitations. This indicates that the bridge design was adequate. No significant damage was observed in the deck panels and stiffeners under the ultimate loading. The glulam slab timber bridge was found to be a viable option for short spans on local roads.

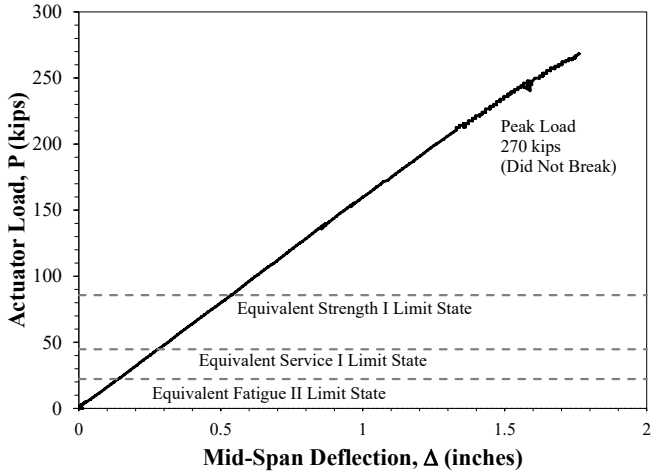

Figure 7.8: Measured Force-Displacement Relationship – Strength Testing of Glulam Timber Slab Bridge

7.3.2 Constructability

The constructability of the main components of a glulam timber slab bridge is evaluated. The construction of this bridge system is relatively fast and does not require highly skilled labor.

7.3.2.1 Glulam Deck Panels

The glulam deck panels will be prefabricated in a controlled environment at the manufacturer's plant. A two-lane bridge with shoulders on both sides will consist of eight glulam deck panels. Onsite construction will be minimal since the only onsite work will be to place the panels and to anchor them at the ends. The construction can be further accelerated if the entire bridge is prefabricated.

7.3.2.2 Glulam Stiffeners

The glulam stiffeners will also be constructed in a controlled environment at the manufacturer's plant. Glulam stiffeners can be installed very rapidly in the field. The construction workers need to clamp the stiffeners to the deck panels, and then install stiffener-to-deck lag bolts from the underside of the bridge. The onsite installation of stiffeners can be eliminated if the bridge is prefabricated in line with ABC.

7.3.3 Costs of Glulam Timber Slab Bridges

Table 7.3 presents a comparison of superstructure materials and fabrication costs for a timber slab bridge to a inverted tee bridge with a length of 16.5 ft and a width of 34.5 ft. The materials and fabrication cost for double-tee girder bridges is approximately $64 per square foot. Note that the estimated cost of the double-tee bridge was the cost per square foot for a bridge with a length of 50-ft and a width of 34.5 ft.

Table 7.3: Material and Fabrication Cost for Glulam Timber Slab Bridge and Inverted Tee Bridge Superstructures

Bridge System	Glulam Timber Slab Bridge	Inverted Tee Girders Bridge
Materials/Fabrication ($)	17,000 (for 16.5-ft long 34.5-ft wide bridge)	111,000 (for 50-ft long 34.5-ft wide bridge)
Materials/Fabrication ($/sq. ft.)	30	64

The total material and fabrication cost estimated by the manufacturer for a 16.5-ft long by 34.5-ft wide glulam timber slab bridge is approximately $17,000, which was verified by the research team. Therefore, the materials and fabrication cost of a glulam timber slab bridge superstructure is approximately one-half of that of inverted tee girders bridge superstructure.

Transportation costs for glulam timber slab bridges is $2.65 per mile at the time of this writing. Additional costs such as assembly, onsite activities, and substructure fabrication and construction should be included in the total bridge cost. In summary, the cost of glulam slab bridges is expected to be 50% of that of double-tee bridges. However, direct comparison could not be made due to span length differences.

7.4 Application of Proposed Bridge Systems

The three proposed bridge systems can span a wide range of terrains. Figure 7.9 shows the recommended span length for each tested system based on the structural performance of the bridge test models, material availability in South Dakota, and the constructability. The depth of each system should be calculated based on the load combinations and span length. The overall precast bridge depth is comparable to current double-tee bridge depths. The overall depth of glulam timber girder bridges

will be 50% more than that for current double-tee bridges. The overall depth of glulam timber slab bridges is less than that for double-tee bridges.

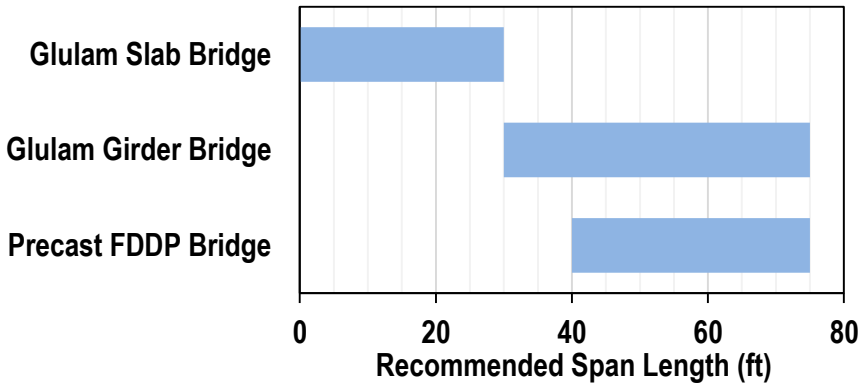

Figure 7.9: Recommended Span Length for Three Proposed Bridge Systems

Table 7.4 presents a summary of the cost estimate for the three bridges. It can be concluded that the proposed timber bridges are the most cost-effective options compared to double-tee bridges.

Table 7.4: Material and Fabrication Costs for Three Proposed Bridge Systems

Bridge System	Cost/sq. ft	Inverted Tee Girders Bridge
Precast FDDP Bridge	$74 / sq. ft	$64 / sq. ft
Glulam Girder Bridge	$45 / sq. ft	
Glulam Slab Bridge	$30 / sq. ft	

8 CONCLUSIONS

Based on design, construction, full-scale testing, and cost estimation for the three proposed bridge systems, the following conclusions can be drawn.

8.1 Fully Precast Full-Depth Deck Panel Bridge

- The proposed construction process does not require advanced technology and was relatively simple.
- The proposed bridge system did not exhibit any sign of deterioration or water leakage through 500,000 Fatigue II load cycles (91 service years assuming ADTT = 15) and an additional 150,000 Fatigue II load cycles adjacent to the interior panel transverse joints (27 service years). The bridge's overall stiffness essentially remained the same throughout the fatigue testing.
- Shrinkage cracks were observed in almost all full-depth shear pockets, all transverse joints, and grouted haunch regions at 125,000 load cycles. Shrinkage cracks in the haunch can be minimized by using two longitudinal reinforcing steel bars placed in the haunch region.
- The first horizontal shear cracks in the grouted haunch region were observed at an actuator load of 200 kips, which was higher than the equivalent AASHTO (2013) Strength I limit state load of 131.4 kips.
- Both inverted U-shape shear studs and double headed shear studs performed adequately throughout the entire fatigue testing, as well as the ultimate testing.
- The hidden pocket detail was found to be a better alternative than the full-depth pockets since they provide better durability. Shrinkage cracks were observed in almost all full-depth pockets, but none for hidden pockets.
- The test bridge girders did not crack until the applied load exceeded the equivalent Strength I limit state load, indicating adequate design and performance.
- No significant damage in addition to the shrinkage cracks was observed throughout the entire fatigue testing, and the overall bridge stiffness remained the same.
- The superstructure materials and fabrication cost of the proposed system for a 50-ft long by 34.5-ft wide bridge is 11% higher than that for a double tee bridge with the same bridge geometry.

Overall, it can be concluded that the proposed bridge system, full-depth deck panels supported on inverted tee girders, is a viable alternative to the precast double-tee girder bridges.

8.2 Glulam Girder Bridge

- Construction of a glulam girder bridge is fast and does not require advanced technology or skilled labor.
- The girder bridge did not exhibit any signs of deterioration throughout the 500,000 AASHTO (2013) Fatigue II load cycles (equivalent to 91 years of service life) and the bridge's overall stiffness essentially remained constant throughout the fatigue testing.

- Damage of tongue-and-groove deck-to-deck connections was observed at 250,000 load cycles (equivalent to 45 years of service life). The damage can be eliminated by connecting flat deck panels with epoxy instead of using a tongue-and-groove connection.
- Although there was partial composite action, it was not sufficient to warrant composite design. The girders should be designed fully non-composite.
- The epoxy connection for the deck-to-girder connection in the girder bridge performed adequately throughout all testing phases.
- The girder bridge did not meet the AASHTO (2013) service and strength limit state requirements under strength testing because a wrong grade of wood was used in the fabrication by mistake.
- A calculation of the bridge capacity assuming non-composite behavior and as-built material properties and bridge geometry led to accurate estimation of the bridge test model's capacities. Therefore, current AASHTO (2013) design method for this type of bridge is valid.
- The superstructure cost for a 50-ft long by 34.5-ft wide glulam girder bridge is 70% of that for a double-tee bridge with the same bridge geometry.

Overall, it can be concluded that glulam girder bridges are viable alternatives to the precast double-tee girder bridges, the type most commonly used in South Dakota.

8.3 Glulam Slab Bridge

- Construction of a glulam slab bridge is fast and does not require advanced technology or skilled labor.
- The glulam slab bridge stiffness did not degrade through the 550,000 AASHTO (2013) Fatigue II load cycles (equivalent to 50 years of service life).
- No damage was observed at an actuator load of 270 kips, which was three times higher than the AASHTO (2013) Strength I limit state load of 85.7 kips. The test was stopped due to setup limitations.
- The superstructure cost per square foot for a 16.5 ft long by 34.5 ft wide glulam slab bridge is only 50% of that for a typical double-tee bridge with the same geometry.

Overall, it can be concluded that glulam slab bridges are viable alternative to the precast double-tee girder bridge, the type most commonly used in South Dakota.

9 RECOMMENDATIONS

Based on the findings of this study, the research team offers the following recommendations.

9.1 Recommendation 1: Precast Full-Depth Deck Panel Bridges

The guidelines as detailed in Section A.1 of Appendix A should be adopted for the construction of "precast full-depth deck panel bridges". A span length of 40 ft to 70 ft is recommended for this bridge type.

Precast full-depth deck panel bridges generally consist of precast inverted tee girders and precast full-depth deck panels. The test results of a full-scale 50-ft long precast full-depth deck panel bridge showed that this bridge type is a viable alternative to double-tee girder bridges, which are common in South Dakota. To minimize durability issues due to cold joints: (1) only hidden pocket detailing was allowed, (2) all bridge deck reinforcement was recommended to be epoxy coated, and (3) hollow structural steel sections, which are used to reduce the splice length, was recommended to be galvanized. These precast bridges with the recommended span lengths are constructible in South Dakota and may cost slightly more than double-tee bridges.

9.2 Recommendation 2: Glulam Timber Girder Bridges

The guidelines as detailed in Section A.2 of Appendix A should be adopted for the construction of "glulam timber girder bridges". A span length of 30 ft to 70 ft is recommended for this bridge type.

Glulam timber girder bridges generally consist of glulam girders, glulam deck panels, and diaphragms. The test results of a full-scale 50-ft long glulam girder bridge showed that this bridge type is a viable alternative to double-tee girder bridges. Glulam timber bridges with the recommended span lengths can be fabricated in South Dakota and will be more cost-effective than double-tee bridges.

9.3 Recommendation 3: Glulam Timber Slab Bridges

The guidelines as detailed in Section A.3 of Appendix A should be adopted for the construction of "glulam timber slab bridges". A span length of 30 ft or less is recommended for this bridge type.

Glulam timber slab bridges generally consist of glulam deck panels and glulam stiffeners. The test results of a full-scale 16.5-ft long glulam slab bridge showed that this bridge type is a viable alternative to double-tee girder bridges. Currently, glulam slab bridges with a span length of 20 ft can be fabricated in South Dakota and will be more cost-effective than double-tee or glulam timber bridges.

10 RESEARCH BENEFITS

Numerous bridges in South Dakota need replacement due to deterioration. The expected design life of these existing bridges was 75 years, but some built less than 40 years ago already need replacement. The double-tee precast girder bridge is the standard bridge system used on local roads in South Dakota. The most common problem in double-tee bridges is that longitudinal joints deteriorate over time, most likely due to inadequate shear transfer between girders, allowing water and debris to enter the joints. It is only a matter of time before the joint begins to spall, creating a path for moisture to reach the prestressing steel, initiate corrosion, and degrade the structural capacity of the bridge.

Facing limited budgets, local governments in South Dakota need a durable and inexpensive bridge system that is easy to construct and will last for at least 75 years. Three new bridge systems were proposed and tested through full-scale experiments. Those systems included a fully precast bridge, a glulam timber girder bridge, and a glulam timber slab bridge. It was found that all three bridge systems are viable alternatives to the currently used double-tee bridges.

Each proposed system is suitable for a certain range of span length as discussed under Sec. 7.4. The cost of the new bridge systems is comparable to or lower than the cost of double-tee bridges as discussed under Section 7.4 Application of Proposed Bridge Systems. However, the proposed timber bridges offer the highest cost saving compared to double-tee and the precast bridges. The overall precast bridge depth is comparable to current double-tee bridge depths especially for long spans (e.g. more than 50 ft). The overall depth of glulam timber girder bridges will be 50% more than that for current double-tee bridges. However, the overall depth of glulam timber slab bridges with a shorter span is less than that for double-tee bridges.

Local governments will now have a total of four options (three proposed systems in the present study and the inverted tee girder bridge proposed by Wehbe et al., 2016) when planning to construct a new bridge or to replace an old one on local roads in South Dakota.

11 REFERENCES

Aaleti, S., and Sritharan, S. (2014). "Design of Ultrahigh-Performance Concrete Waffle Deck for Accelerated Bridge Construction." *Transportation Research Record: Journal of the Transportation Research Board, No. 2406*. Transportation Research Board of the National Academies, Washington, D.C., pp. 12-22, DOI: 10.3141/2406-02.

Aktan, H., and Attanayake, U. (2013). "Improving Bridges with Prefabricated Precast Concrete Systems." Report No. RC-1602. Western Michigan University. , Kalamazoo, MI. Retrieved from https://www.michigan.gov/documents/mdot/RC-1602_Part_1_444145_7.pdf.

AASHTO (2013). "AASHTO-LRFD Bridge Design Specifications, Sixth Edition." American Association of State Highway and Transportation Officials, Washington, DC.

ASTM A370 (2011). "Standard Test Methods and Definitions for Mechanical Testing of Steel Products." American Society for Testing Materials, West Conshohocken, PA.

ASTM C39 (2010). "Standard Test Method for Compressive Strength of Cylindrical Concrete Specimens." American Society for Testing Materials, West Conshohocken, PA.

ASTM C109 (2010). "Standard Test Method for Compressive Strength of Hydraulic Cement Mortars (Using 2-in. Cube Specimens)." American Society for Testing Materials, West Conshohocken, PA.

ASTM C143 (2010). "Standard Test Method for Slump of Hydraulic-Cement Concrete." American Society for Testing Materials, West Conshohocken, PA

ASTM C231 (2010). "Standard Test Method for Air Content of Freshly Mixed Concrete by the Pressure Method." American Society for Testing Materials, West Conshohocken, PA.

Badie, S., Baishya, M., and Tadros, M. (1998). "NUDECK – An Efficient and Economical Precast Prestressed Bridge Deck System." *PCI Journal*, *43*(5), pp. 56-74. DOI: 10.15554/pcij.09011998.56.74.

Badie, S., Tadros, M, and Girgis, A. (2006). "Full-Depth, Precast-concrete Bridge Deck Panel Systems." NCHRP Report No. 12-65, TRB. National Research Council, Washington, D.C. Retrieved from www.trb.org/notesdocs/nchrp12-65_fr.pdf.

Badie, S., and Tadros, M. (2008). "Full-Depth Precast Concrete Bridge Deck Panel Systems." NCHRP Report No. 584, TRB. National Research Council, Washington, D.C., Retrieved from https://www.scribd.com/document/220593817/nchrp-rpt-584

Badie, S., and Tadros, M. (2008). "Full-Depth Precast Concrete Bridge Deck Panel Systems." NCHRP Report No. 584 Appendix, TRB. National Research Council, Washington, D.C., Retrieved from https://www.scribd.com/document/220593817/nchrp-rpt-584

Baer, C. (2013). "Investigation of Longitudinal Joints between Precast Prestressed Deck Bulb Tee Girders Using Latex Modified Concrete." M.S. Thesis. Columbia, SC: University of South Carolina. Retrieved from http://scholarcommons.sc.edu/etd/2452.

BASF Corporation (2011). "Placement of Latex Modified Concrete." Charlotte, NC: BASF Corporation.

Brashaw, B., Wacker, J., and Jalinoos, F. (2013). "Field Performance of Timber Bridges: A National Study." International Conference on Timber Bridges, Las Vegas, NV. pp. 1-12. Retrieved from http://www.woodcenter.org/docs/ICTB2013/technical/papers/ID_132_BRASHAW.pdf

California Department of Transportation (2012). “Bridge Design Manual.” Sacramento, CA: Caltrans.

Carnahan, Z.C. (2017). “Glulam Timber Bridges for Local Roads,” MS Thesis, South Dakota State University, 182 pp., Available at: https://openprairie.sdstate.edu/etd/1173/.

Computers and Structures, Inc. (2016). “CSi Bridge, Version 18.” Berkeley, CA.

Computers and Structures, Inc. (2016). “SAP2000, Version 18.” Berkeley, CA.

Chandra, V. and Kim, J. (2012). “World's First Recycled Plastic Bridges.” *Proc., Integrating Sustainable Practices in the Construction Industry*, Kansas City, MO, pp. 585-593. Retrieved from ascelibrary.org/doi/abs/10.1061/41204%28426%2972.

Ekholm, K. (2013). “Performance of Stress-Laminated-Timber Bridge Decks.” Chalmers University of Technology, Gothenburg, Sweden. Retrieved from publications.lib.chalmers.se/records/fulltext/183986/183986.pdf.

Erie Canal Bridge. (2014). Retrieved from http://laminatedconcepts.com/.

Erikkson Technologies, Inc. (2011), “PSBEAM, Version 4.27.” Temple Terrace, FL.

Federal Highway Administration. (2012a). “Bridge Inspector’s Reference Manual.” Retrieved from https://www.fhwa.dot.gov/bridge/nbis/pubs/nhi12049.pdf.

Federal Highway Administration. (2012b). “Deficient Bridges by State and Highway System.” Retrieved from https://www.fhwa.dot.gov/bridge/nbi/no10/defbr12.cfm.

Franke, S., Franke, B., and Harte, A. (2015). “Failure Modes and Reinforcement Techniques for Timber Beams - State of the Art.” *Construction and Building Materials,* Vol. 97, pp. 2-13. Retrieved from https://doi.org/10.1016/j.conbuildmat.2015.06.021.

Grace, N., Enomoto, T., Baah, P., Bebawy, M. (2012). “Innovative CFCC Prestressed Decked Bulb T Beam Bridge System.” *Proc., Innovative Infrastructures- Toward Human Urbanism*, IABSE, Seoul, Korea, pp. 1-8, DOI: 10.2749/222137912805110394.

Graybeal, B. (2010). “Behavior of Field-Cast Ultra-High Performance Concrete Bridge Deck Connections under Cyclic and Static Structural Loading.” Report No. FHWA-HRT-11-023, Federal Highway Administration, McLean, VA. Retrieved from https://ntl.bts.gov/lib/35000/35400/35413/FHWA-HRT-11-023.pdf.

Hoadley, R.B. (1980). “*Understanding Wood: A Craftsman’s Guide to Wood Technology.”* Newton, CT.: Taunton Press.

Hosteng, T. (2013). “Advances in Timber Bridge Design.” 2013 Annual Conference, National Association of County Engineers, Des Moines, IA.

Idaho Transportation Department (IDT) (2015). “Idaho Manual for Bridge Evaluation.” ITD, Boise, ID Retrieved from apps.itd.idaho.gov/apps/bridge/manual/IMBE2016.pdf.

Ji, H.S., Son, B.J., and Chang, S.Y. (2007). “Field testing and capacity-ratings of advanced composite materials short-span bridge superstructures.” *Composite Structures*, 78(2), pp. 299-307, Retrieved from https://doi.org/10.1016/j.compstruct.2005.10.014.

Jones, A., and Oppong, K. (2015). “Structure Alternatives for Local Roads.” Report No. SD2013-06, South Dakota State University, Brookings, SD.

Joyce, P. (2014). “Development of Improved Connection Details for Voided Slab Bridges.” MS thesis, Civil Engineering. Virginia Polytechnic Institute and State University, Blacksburg, VA.

Retrieved from https://vtechworks.lib.vt.edu/bitstream/handle/10919/49108/Joyce_PC_T_2014.pdf?sequence=1.

Konrad, M. (2014). "Precast Bridge Girder Details for Improved Performance." M.Sc. Thesis, South Dakota State University, Brookings, SD.

Mingo, M.J. (2016), "Precast Full-Depth Deck Panels Supported on Inverted Tee Bridge Girders," MS Thesis, South Dakota State University, 208 pp., Available at: https://openprairie.sdstate.edu/etd/1093/.

Pirayeh Gar, S., Head, M., Hurlebaus, S., and Mander, J. (2013). "Comparative Experimental Performance of Bridge Deck Slabs with AFRP and Steel Precast Panels." *J. Compos. Constr.*, 17(6), 04013014. Retrieved from https://doi.org/10.1061/(ASCE)CC.1943-5614.0000380#sthash.w7ngAdsc.dpuf.

Ritter, M.A. (1990). "Timber Bridges: Design, Construction, Inspection, and Maintenance." Washington, D.C., 944 p. Retrieved from https://www.fpl.fs.fed.us/documnts/misc/em7700_8--entire-publication.pdf.

Ritter, M.A., Faller, R.K., Lee*, P.D.H., Rosson, B.T., and Duwadi, S.R. (1995). "Plans for Crash-Tested Bridge Railings for Longitudinal Wood Decks," United State Department of Agriculture, Forest Service, General Technical Report FPL-GTR-87, http://www.woodcenter.org/docs/fplgtr87.pdf.*

Ritter, M.A., Faller, R.K., Lee, P.D.H., Rosson, B.T., and Duwadi, S.R. (1998). "Plans for Crash-Tested Wood Bridge Railings for Concrete Decks," United State Department of Agriculture, Forest Service, General Technical Report FPL-GTR-108, http://www.woodcenter.org/toolkit/guardrails/documents/FPL%20Files/fplgtr108.pdf.

Smith, M. (2014). "Timber Bridge Blog." *Laminated Concepts Inc*. retrieved from laminatedconcepts.com/timber-bridge-blog/.

Scholz, D., Wallenfelsz, J., Lijeron, C., and Roberts-Wollmann, C. (2007). "Recommendations for the Connection between Full-Depth Precast Bridge Deck Panel Systems and Precast I-Beams." Report No. FHWA/VTRC 07-CR17, Virginia Polytechnic Institute & State University, Charlottesville, Virginia. Retrieved from www.virginiadot.org/vtrc/main/online_reports/pdf/07-cr17.pdf.

Stenko, M.S. and Chawalwala, A.J. (2001). "Thin Polysulfide Epoxy Bridge Deck Overlays." *Transportation Research Record 1749*. 01(0154), pp. 64-67, Retrieved from https://doi.org/10.3141/1749-10.

Virginia Department of Transportation. (2005). "Prestressed Concrete Voided Slabs Preliminary Design Tables." Volume 5, Part 2, File 12.05-3. Retrieved from http://www.virginiadot.org/business/resources/pc-voidedslabs-12.pdf.

Wacker, J.P. and Smith, M.S. (2001). "Standard Plans for Timber Bridge Superstructures." U.S. Department of Agriculture, Forest Service, and Forest Products Laboratory, General Technical Report No. FPL-GTR-125, Madison, WI, 53 pp. Retrieved from https://www.fpl.fs.fed.us/documnts/fplgtr/fplgtr125.pdf.

Wehbe, N., Konrad, M., and Breyfogle, A. (2016). "Joint Detailing Between Double Tee Bridge Girders for Improved Serviceability and Strength." *Transportation Research Record: Journal of the*

Transportation Research Board, No. 2592, Transportation Research Board of the National Academies, Washington, D.C. Retrieved from https://trid.trb.org/view.aspx?id=1393072.

Wenzlick, J.D. (May 2006). "Evaluation of Very High Early Strength Latex Modified Concrete Overlays." Organizational Results Research Report. Report No. OR06-004, Missouri Department of Transportation, Jefferson City, MO. Retrieved from https://library.modot.mo.gov/RDT/reports/Ri04005/or06004.pdf.

APPENDIX A: DESIGN AND CONSTRUCTION GUIDELINES

Based on the findings, the research team proposes the following design and construction guidelines for each of the three proposed bridge systems: fully precast full-depth panel bridge, glulam timber girder bridge, and glulam timber slab bridge.

A.1 Precast Full-Depth Deck Panel Bridges

The proposed design recommendations are based on the experimental data of the full-scale bridge test model with the proposed detailing. The construction recommendations are based on a literature review, fabricating and assembling of the test girders, and engineering judgment.

A.1.1 Inverted Tee Girders

Inverted tee girders should be designed and constructed using current codes and practices (e.g., AASHTO, 2013).

Note that the installation of shear studs in the inverted tee girders require tight construction tolerances to allow for proper embedment into the shear stud pockets in the deck.

A.1.2 Full-Depth Deck Panels

Full-depth deck panels should have a minimum thickness of 7 in. according to AASHTO (2013). The width of the full-depth deck panels is recommended to be the same as the bridge width (in the transverse direction) resulting in a single-grade for the bridge deck (Fig. A.1). Single-grade decks do not need longitudinal joints to connect precast panels resulting in lower cost, faster construction, and improved durability. The length of each full-depth precast panel (in the longitudinal direction of the bridge) should not exceed 12-ft.

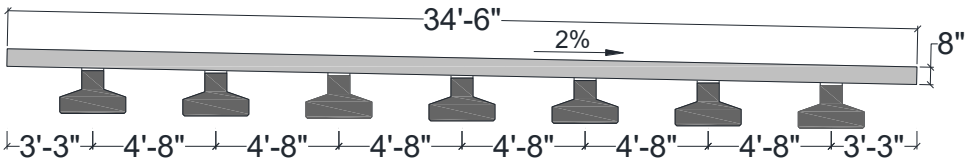

Figure A.1: Cross-Section of Precast Bridge System with Single-Unit Panel

If a crown along the longitudinal centerline is desired (deck with two grades), the precast panels should be connected with a longitudinal joint along the center of the bridge (Fig. A.2). Previous studies developed detailing for longitudinal joints (e.g., Baer, 2013; Aaleti and Sritharan, 2014). One of the proof tested longitudinal joint details is shown in Fig. A.3, which uses U-shape bars extending from two adjacent panels into the longitudinal joint to transfer shear and moment, and headed bars in the longitudinal direction of the bridge, to aid in developing the U-shape reinforcing steel bars.

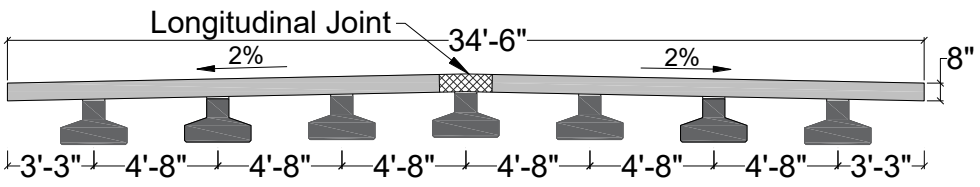

Figure A.2: Cross-Section of Fully Precast Bridge with Two-Unit Panels

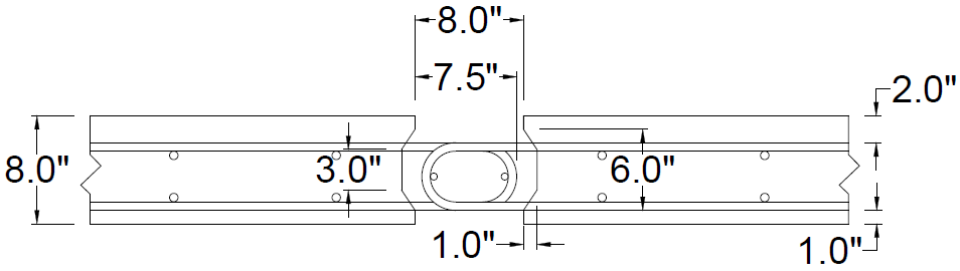

(a) Section View

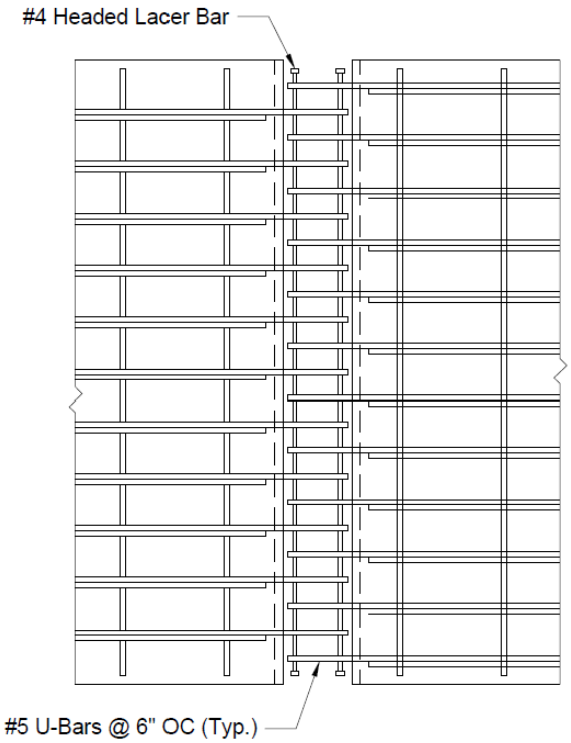

(b) Plan View

Figure A.3: Longitudinal Deck-to-Deck Joint Detailing in Fully Precast Bridge
(after Baer, 2013)

The deck reinforcement should be designed according to a current code such as AASHTO (2013). All deck reinforcing steel bars should be epoxy coated to increase the durability of the deck against shrinkage cracks that may develop in the pockets, grouted haunch, and at the transverse joints.

A.1.2.1 Shear Pockets

The center-to-center spacing of the shear pockets should not exceed 24 in. according to Article 5.8.4.2 of AASHTO (2013). Only hidden pockets shall be used (Fig. A.4) since they provide better durability. Furthermore, the shear pockets should be designed to allow a minimum of 0.75-in. clear spacing between the shear studs and all side surfaces of the shear pockets. The hidden-pocket grout port diameter should be at least 2 in. to allow grout to be easily poured. Two 0.75-in. diameter vent ports should be provided on the opposite sides of the grout ports to avoid air pockets. The shear studs should be designed according to Section 5.8.4 of AASHTO (2013). The embedment length of shear studs into the pocket should not be less than six times the stud diameter ($6d_b$). AASHTO (2013) minimum concrete cover requirements should be followed for the studs in hidden pockets. Two types of shear studs, double-headed and inverted U-shape bars, are allowed to be inserted in hidden pockets (Fig. A.4). Full-depth pockets shall not be used since shrinkage cracks may develop at the edge of these pocket. The hidden pocket can be filled with conventional non-shrink grout. All pockets should be free of debris, oil, or any other foreign materials to ensure good bond.

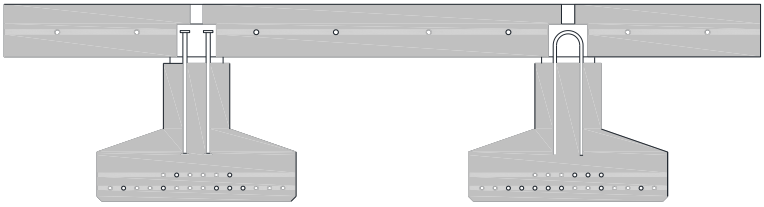

(a) Hidden Pockets – Transverse Section View

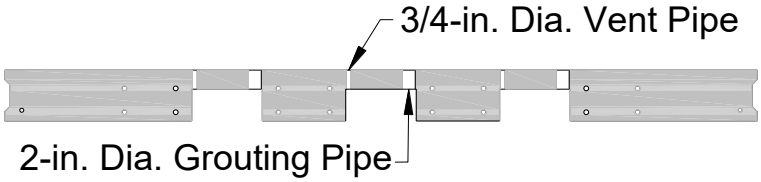

(b) Hidden Pockets – Longitudinal Section View

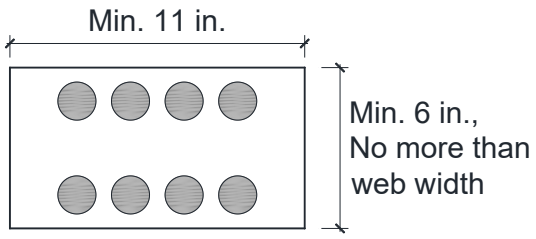

(c) Double Headed Studs Footprint

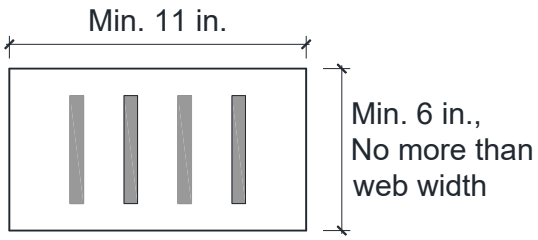

(d) Inverted U-Shape Bar Studs Footprint

Figure A.4: Proposed Detailing for Studs and Shear Pockets

A.1.2.2 Transverse Joints

Figure A.5 shows proposed groove-to-groove transverse joint detailing. A minimum gap of 2.75 in. in the longitudinal direction of the bridge should be provided between the precast panels. A reinforcing steel bar with the same type, grade, and size as those of the largest deck transverse reinforcement should be placed in the transverse joints. Steel dowels with the same type, grade, and size as those of the deck's largest longitudinal reinforcement should be spliced with the deck reinforcement (Fig. A.6). Hollow structural steel sections, which are used to reduce the splice length, should be galvanized to avoid corrosion and to increase the bridge's overall durability. All transverse joints should be clean and free of debris or any foreign contaminant to ensure good bond.

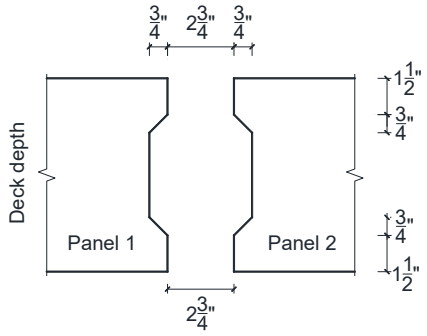

Figure A.5: Groove-to-Groove Transverse Joint Detailing for Fully Precast Bridge

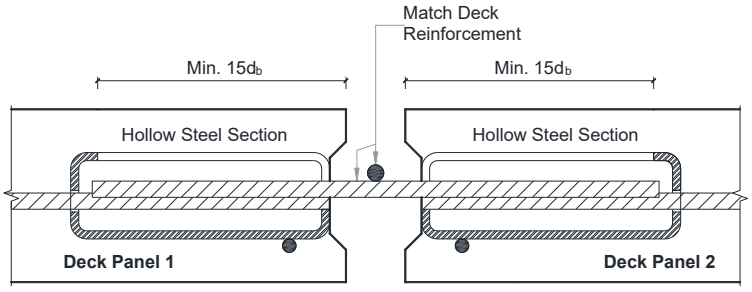

(a) Detailing of Transverse Joint

(b) Hollow Structural Steel Section

Figure A.6: Transverse Joint Detailing for Fully Precast Bridge

A.1.2.3 Leveling Bolts

A minimum of four leveling bolts should be incorporated into each precast full-depth deck panel to adjust the grades (Fig. A.7). The bolts should be located above the centerline of the supporting girders. Each bolt should be designed to carry at least 25% of the weight of the precast panel. The use of long bolts in lieu of threaded rods with welded nuts is recommended.

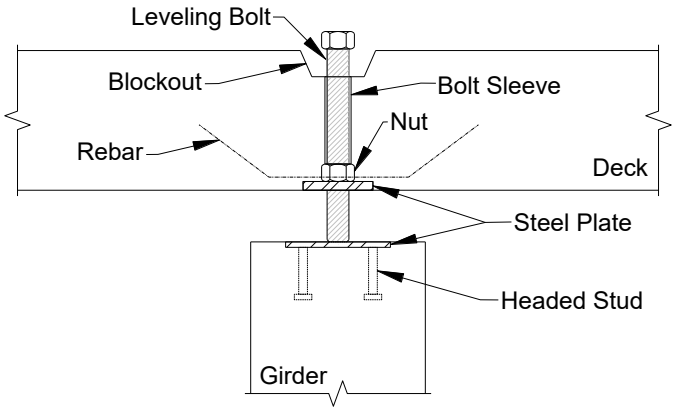

Figure A.7: Leveling Bolt Detailing for Fully Precast Bridge

A.1.3 Grouted Haunch

The haunch depth at the bridge mid-span should not be less than 0.75 in. to allow the grout to easily flow through the haunch and to avoid air pockets (Fig. A.8). A minimum of two longitudinal reinforcing steel bars should be placed in the haunch region and sized according to AASHTO Section 5.10.8 (2013) to eliminate shrinkage cracking (Fig. A.8). The size and location of the bars should allow a free flow of the grout specially at the girder midspan. Clear cover requirements should be met for the additional bars from the sides of the haunch region. These additional bars should be placed at the mid-depth of the haunch region by tying them to the shear studs.

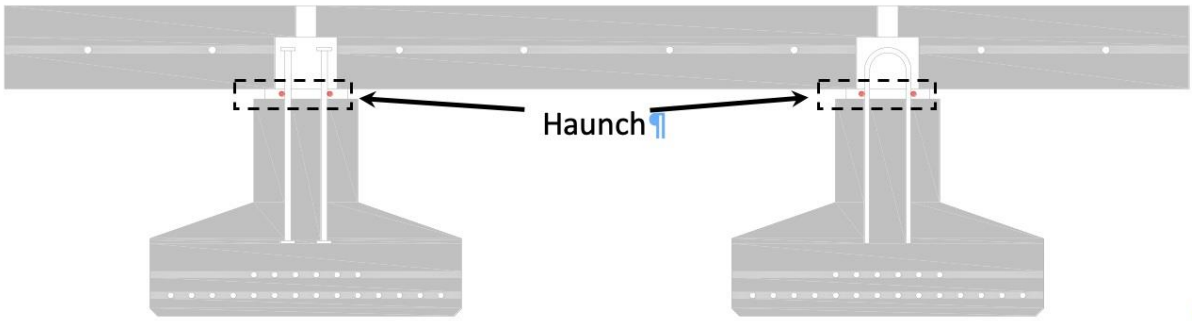

(a) Haunch Longitudinal Reinforcing Steel Bars Detailing

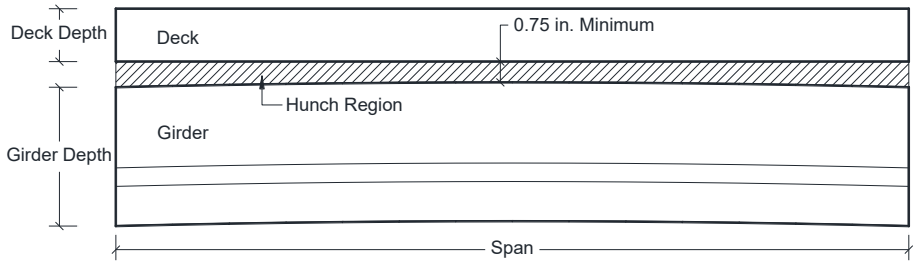

(b) Girder Elevation View

Figure A.8: Haunch Detailing for Precast Bridge

Several methods can be used to form the haunch from the top of the bridge. One example is shown in Fig. A.9, in which the form was made using threaded rods and anchorage plates to clamp plywood to the girder top flange. Compressible foam was glued to the top of the plywood to seal the haunch area after the panel placement.

Figure A.9: Grouted Haunch Formwork
(after Aktan and Attanayake, 2013)

A.2 Glulam Timber Girder Bridges

Design and construction guidelines are proposed for different components of glulam timber girder bridges (Fig. A.10) including: (1) glulam girders, (2) glulam deck panels, (3) diaphragms, (4) wearing surface, (5) railing system, and (6) abutments. Those components and inspection and maintenance recommendations are discussed herein.

Figure A.10: Typical Glulam Timber Girder Bridge

A.2.1 Glulam Girders

Glulam girders shall be designed fully non-composite meeting the requirements of current AASHTO (2013) bridge design standards. The base material type and properties shall be according to AASHTO (2013). The AASHTO does not specify the spacing between glulam girders. Nevertheless, a girder spacing of 3 to 6 ft generally results in the most cost effective design.

The type, rating, treatment, and geometry of the wood shall be verified and approved by the designer before fabrication of the girders. The girders shall be precision milled to allow the deck panels to form the crown and to meet the minimum camber required by AASHTO (2013).

A.2.2 Glulam Deck Panels

Glulam deck panels shall be at least 6 in. deep as required by AASHTO (2013). The width of the deck panels can cover either the full width of the bridge with one cross slope, or can cover one-half of the bridge width with two cross slopes (Fig. A.11).

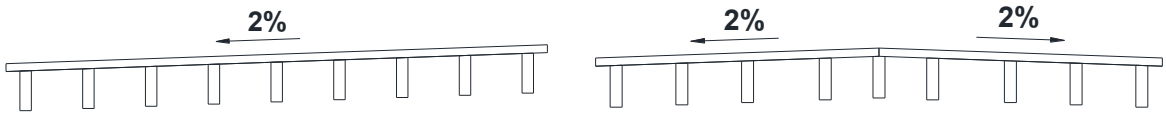

(a) Glulam Timber Girder Bridge with Single Cross Slope

(b) Glulam Timber Girder Bridge with Two Cross Slopes

Figure A.11: Cross-Section of Glulam Timber Girder Bridges

There would be a longitudinal joint directly above the middle girder when installing the bridge with two grades. The panel edges should be cut and prepared to minimize the gap at the joint. The gap should be filled with wood adhesive epoxy.

Compared to the wood used for glulam girders that is often Southern Pine, a weaker wood is often used for deck panels to minimize costs. The edge of each deck panel shall be straight then covered with epoxy to complete deck-to-deck connections in the longitudinal direction of the bridge, as shown in Fig. A.12.

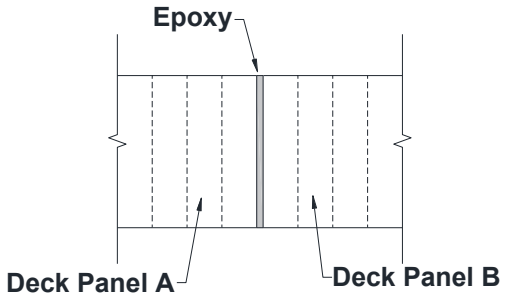

Figure A.12: Recommended Deck-to-Deck Connections for Glulam Girder Bridges

The deck panels can be connected to the girders using adhesive epoxy at the interface. Two rows of screws spaced no more than 18-in. apart along the length of the girder shall be incorporated to hold the panels and to activate the epoxy (Fig. A.13).

Figure A.13: Deck-to-Girder Connections for Glulam Timber Girder Bridges

A.2.3 Diaphragms

AASHTO (2013) allows the use of two types of diaphragms to be installed between the girders to improve the stability of the bridge: (1) solid glulam diaphragms (Fig. A.14a) and (2) steel cross braces (Fig. A.14b). Another type of diaphragm, glulam cross braces (Fig. A.14c), was used in the full-scale bridge test model of the present study and was found to be a viable alternative. All three options are recommended for field applications.

(a) Solid Glulam Diaphragm, (after Hosteng, 2013)

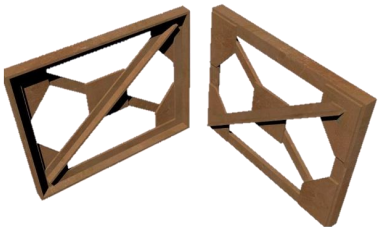

(b) Steel Cross Braces, (after etraxx.com)

(c) Glulam Cross Braces

Figure A.14: Three Types of Diaphragms for Glulam Timber Girder Bridges

A.2.4 Wearing Surface

The use of four types of wearing surfaces shall be allowed for glulam timber bridges: (1) asphalt overlay, (2) asphalt chip seal, (3) aggregate overlay, or (4) epoxy with embedded grit. Figure A.15 shows an example of each wearing type. Option (4) may be preferred to other methods since the wood natural cracks and joints will be filled with adhesive epoxy, which is compatible with glulam. Long term performance of the first three options confirmed that they are adequate, as long as they are well maintained.

(a) Asphalt Overlay

(b) Asphalt Chip Seal (after Gruen-Wald 2011)

(c) Aggregate Overlay

(d) Epoxy with Embedded Grit

Figure A.15: Different Types of Wearing Surfaces for Glulam Girder Bridges

A.2.5 Railing System

According to AASHTO (2013), a bridge railing system must be positioned to safely contain an impacting vehicle without allowing it to pass over, under, or through the rail elements. Furthermore, a proper railing system must be free of features that may catch on the vehicle or cause it to overturn or decelerate rapidly.

Any crash-tested railing configuration (details can be found in Ritter et al., 1995; and Ritter et al., 1998) or those designed according to AASHTO (2013) Section 13.7 can be used for timber bridges. Timber bridge components connected to rails shall be designed to resist the railing design loads. The rail material can be timber, metal, or concrete. Timber railings (Fig. A.16) are recommended for aesthetic reasons.

Figure A.16: Timber Railing for Timber Bridges

A.2.6 Abutments

Timber bridge abutments are typically constructed using either timber or concrete, as shown in Figure A.17. The connections should be designed to resist appropriate design loads (AASHTO, 2013). It is recommended that the existing abutments, if any, be modified for reuse to potentially save time and money. Bearing pads designed according to AASHTO (2013) shall be used to allow the girder to freely rotate.

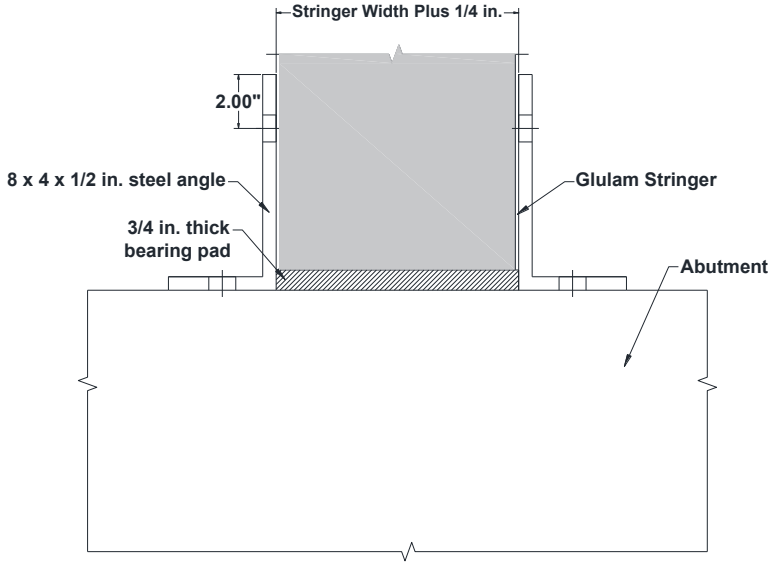

Figure A.17: Glulam Timber Bridge Girder-to-Abutment Sample Connection

A.2.7 Inspection and Maintenance

It is necessary to perform routine maintenance to keep the wearing surface and other exposed areas of the glulam timber girder bridge in good condition. It is also highly recommended that timber bridges be inspected every two years and any wood that is exposed be retreated every six years (Ritter, 1990). Retreatment can be done by spreading the preservative on the wood using a brush.

A.3 Glulam Timber Slab Bridges

Design and construction guidelines are proposed for different components of glulam timber slab bridges (Fig. A.18) including: (1) glulam deck panels, (2) glulam stiffeners, (3) wearing surface, (4) railing system, and (5) abutments. Those components, as well as the inspection and maintenance recommendations, are discussed herein.

Figure A.18: Typical Glulam Timber Slab Bridge

A.3.1 Glulam Deck Panels

Glulam deck panels shall be at least 6-in. deep as required by AASHTO (2013). The panel thickness shall be determined according to the AASHTO (2013) strength I limit state. The deck can be either sloped in one direction or crowned in the middle (Fig. A.19). The strong Southern Pine is recommended to be used for the deck panels due to high shear demand. All four edges of deck panels shall be cut and prepared with high precision to minimize the number and the width of fabrication joints.

(a) Slab Bridge with Single Cross Slope (b) Slab Bridge with Two Cross Slopes

Figure A.19: Cross-Section of Glulam Timber Slab Bridges

There would be a longitudinal joint directly at the center of the bridge when installing the bridge with two grades. The panel edges should be cut and prepared to minimize the gap at the joint. The gap should be filled with epoxy.

A.3.2 Glulam Stiffeners

According to current AASHTO (2013) standards, the product of the wood adjusted modulus of elasticity (E') and the moment of inertia (I) of a stiffener must be greater than 80,000 k-in^2. The minimum width of the stiffener is recommended to be 5 in. Each stiffener shall be made with the same material used in the deck panels.

Zinc-coated lag bolts shall be installed from the underside of the bridge to connect stiffeners to deck panels (Fig. A.20). The lag bolts shall not penetrate beyond 75% of the depth of the deck panels (Fig. A.20b) from underneath the deck. The lag bolts shall be at least 12 in. long with a diameter of 0.75 in. Two lag bolts shall be placed per panel on the stiffener.

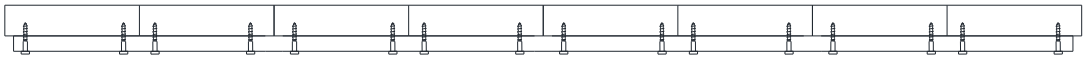

(a) Glulam Slab Timber Bridge Cross-Section

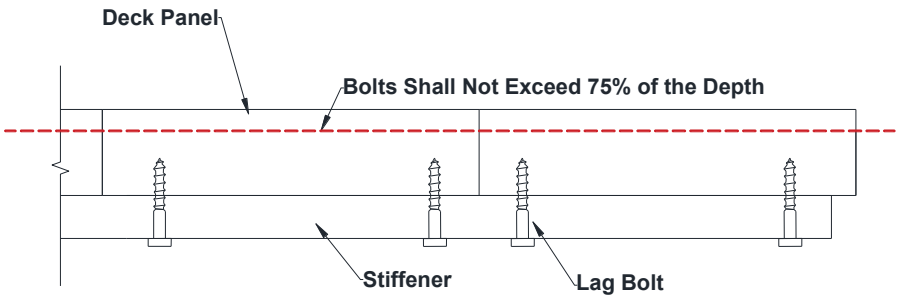

(b) Close-up of Two Panels

Figure A.20: Lag Bolt Requirements for Glulam Timber Slab Bridges

A.3.3 Wearing Surface

Refer to Sec. A.2.4 of the present report regarding the recommended wearing surfaces for timber bridges.

A.3.4 Railing System

Refer to Sec. A.2.5 of the present report regarding the recommended railing systems for timber bridges.

A.3.5 Abutments

Timber bridge abutments are typically constructed using either timber or concrete. The connections should be designed to resist appropriate design loads as required by AASHTO (2013). It is recommended that the existing abutments, if any, be modified for reuse to potentially save time and money. It is important that the abutment be completely flush with the deck panels to prevent point loads at the ends of the panels. Continuous bearing pads designed according to AASHTO (2013) shall be used for glulam timber slab bridges. The bridge panels shall be connected to the abutment using no more than two anchor bolts per panel, each with a minimum diameter of 0.75 in.

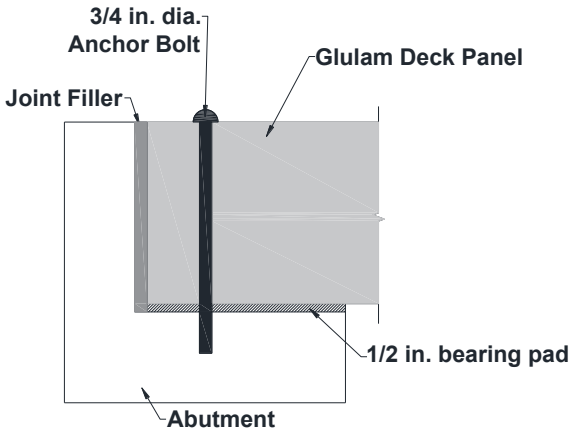

Figure A.21: Glulam Slab-to-Abutment Sample Connection

A.3.6 Inspection and Maintenance

Refer to Sec. A.2.7 of the present report regarding inspection and maintenance for timber bridges.